Synthesis of (*S*)-pindolol with Lipase B from *Candida antarctica* as catalyst

Oskar Dale*

17. June, 2019, Realfagsbygget D2-144

*oskard@stud.ntnu.no

Preface

This thesis, "Synthesis of (*S*)-pindolol with Lipase B from *Candida antarctica* as catalyst" has been written at the Department of Chemistry at The Norwegian Norwegian University of Science and Technology (NTNU) under the supervision of associate professor Elisabeth Egholm Jacobsen. All work has been done from January 2019 to June 2019, as a part of my education in the five year study program Industrial Chemistry and Biotechnology.

I would like to thank my supervisor Elisabth Egholm Jacobsen for fantastic guidance and for being available at all times. I would also like to thank Julie Asmussen for teaching me HPLC and GC and Roger Aarvik for supplying chemicals and everything else needed. Thanks to Mari Bergan Hansen for sharing your knowledge and helping me through my Master's.

Finally, I would like to thank friends and family for support and motivation throughout this period. A special thanks to Nora Iman Hagesæther for sticking with me through all these five years and always being there with a smile no matter how many reactions failed that day.

Abstract

The goal of this thesis is to synthesize enantiopure (*R*)-1-((1H-indol-4-yl)oxy)-3-chloropropan-2-ol ((*R*)-**2**) and synthesize (*S*)-pindolol ((*S*)-**5**) from it.

A chemoenzymatic synthesis of the β-blocker (*S*)-pindolol ((*S*)-**5**) was performed from 1H-indol-4-ol (**1**). This synthesis was performed by first doing an organic synthesis to synthesise 1-((1H-indol-4-yl)oxy)-3-chloropropan-2-ol (**2**) from 1H-indol-4-ol (**1**). This gave a 76 % yield of pure **2** over two reaction steps after purification by flash column. The enzyme *Candida antarctica* Lipase B (CALB) was used as a stereoselective catalyst to produce (*R*)-1-((1H-indol-4-yl)oxy)-3-chloropropan-2-ol ((*R*)-**2**) and (*S*)-1-((1H-indol-4-yl)oxy)-3-chloropropan-2-yl butyrate ((*S*)-**4**) from the racemic mixture of **2**. The last step was to synthesize (*S*)-pindolol ((S)-**5**) from (*R*)-1-((1H-indol-4-yl)oxy)-3-chloropropan-2-ol ((*R*)-**2**).

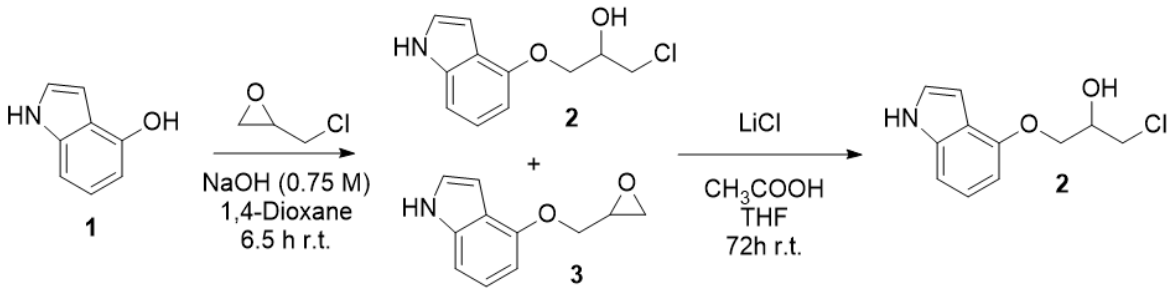

Scheme 1: Synthesis of 1-((1H-indol-4-yl)oxy)-3-chloropropan-2-ol (**2**) from 1H-Indol-4-ol (**1**).

The enzyme reaction was performed by reacting 1-((1H-indol-4-yl)oxy)-3-chloropropan-2-ol (**2**) with vinyl butyrate using the enzyme CALB as a catalyst in dichloromethane (Scheme 5) to make (*R*)-1-((1H-indol-4-yl)oxy)-3-chloropropan-2-ol ((*R*)-**2**) and (*S*)-1-((1H-indol-4-yl)oxy)-3-chloropropan-2-yl butyrate ((*R*)-**4**). The kinetic resolution gave an E-value of 46 and at 50.2% conversion, the ee_s and ee_p values were 96 % and 99 %, respectively. The E-value and ee_s were calculated with an R_s of 1.08 and are therefore imprecise. The specific rotation of (*R*)-**2** was $[\alpha^{20}_{379}]$=-10.4° (MeOH, c=1.00g/100cm^3) and $[\alpha^{20}_{379}]$= 5.8° for (*R*)-**4** (MeOH, c=1.00g/100cm^3).

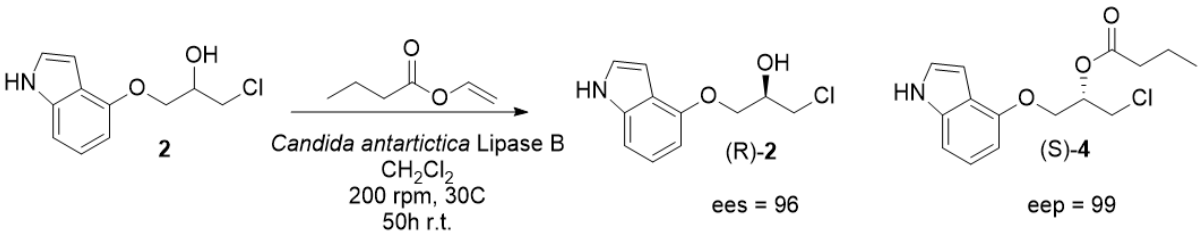

Scheme 2: Reaction of **2** catalyzed by CALB using vinyl butyrate as acyl donor and CH_2Cl_2 as solvent making (*R*)-**2** and (*S*)-**4**.

(R)-1-((1H-Indol-4-yl)oxy)-3-chloropropan-2-ol ((R)-**2**) reacted with isopropylamine over 24 h to synthesize (S)-pindolol ((S)-**5**). Due to small amounts of starting material the product was not purified. The product included impurities and the yield is therefore not given.

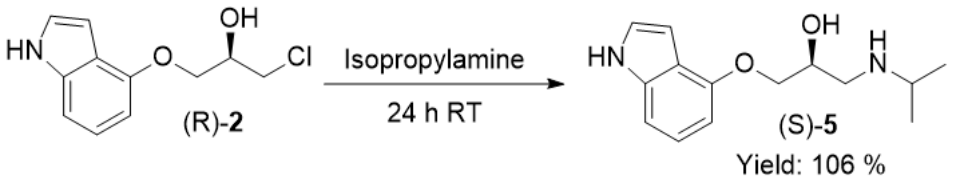

Scheme 3: Reaction of (R)-**2** to make (S)-pindolol ((S)-**5**) through a substitution reaction, substituting the chloride with isopropylamine.

Sammendrag

Målet med denne oppgaven er å syntetisere enantioren (*R*)-1-((1H-indol-4-yl)oxy)-3-chloropropan-2-ol ((*R*)-**2**) og å syntetisere (*S*)-pindolol ((*S*)-**5**) fra (*R*)-**2**.

En kjemoenzymatisk syntese av β-blokkeren (*S*)-pindolol ((*S*)-**5**) ble utført fra 1H-indol-4-ol (**1**). Syntesen ble utført ved å først gjøre en organisk syntese for å syntetiserere 1-((1H-indol-4-yl)oxy)-3-chloropropan-2-ol (**2**) fra 1H-indol-4-ol (**1**). Dette ga 76 % utbytte av ren **2** over to reaksjonssteg etter rensing med flash kolonne. Enzymet *Candida antarctica* Lipase B (CALB) ble brukt som en stereoselektiv katalysator for å lage (*R*)-1-((1H-indol-4-yl)oxy)-3-chloropropan-2-ol ((*R*)-**2**) og (*S*)-1-((1H-indol-4-yl)oxy)-3-chloropropan-2-yl butyrate ((*S*)-**4**)fra en rasemisk blanding av **2**. Det siste steget gikk ut på å syntetisere (*S*)-pindolol ((S)-**5**) fra (*R*)-1-((1H-indol-4-yl)oxy)-3-chloropropan-2-ol ((*R*)-**2**).

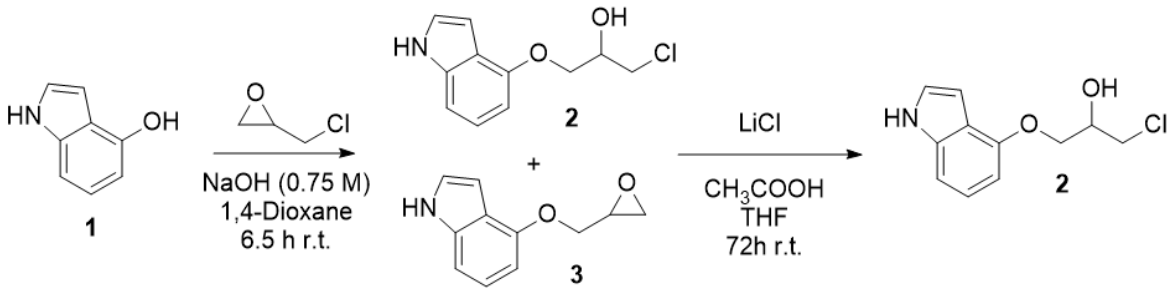

Scheme 4: Syntese av 1-((1H-indol-4-yl)oxy)-3-chloropropan-2-ol (**2**) fra 1H-Indol-4-ol (**1**).

Enzymreaksjonen ble utført ved å reagere 1-((1H-indol-4-yl)oxy)-3-chloropropan-2-ol (**2**) med vinylbutyrate ved å bruke enzymet CALB som en katalysator i diklormetane (Skjema 5) for å lage (*R*)-1-((1H-indol-4-yl)oxy)-3-chloropropan-2-ol ((*R*)-**2**) og (*S*)-1-((1H-indol-4-yl)oxy)-3-chloropropan-2-yl butyrate ((*R*)-**4**). Den kinetiske oppløsningen gav en E-verdi på 46 og ved 50.2% omdannelse var ee_s og ee_p verdiene 96 % og 99 %, respektivt. E-verdien og ee_s ble beregnet med en R_s på 1.08 og er derfor upresis. Den spesifikke rotasjonen av (*R*)-**2** var $[\alpha^{20}_{379}]$=-10.4° (MeOH, c=1.00 g/100cm^3) og $[\alpha^{20}_{379}]$= 5.8° for (*R*)-**4** (MeOH, c=1.00 g/100cm^3).

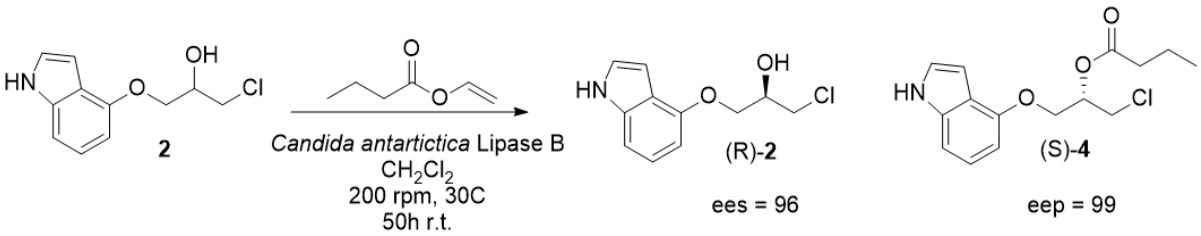

Scheme 5: Reaksjonen av **2** katalyser av CALB med vinyl butyrate som acyl donor og CH_2Cl_2 som løsningsmiddel som blir (*R*)-**2** og (*S*)-**4**.

(*R*)-1-((1H-Indol-4-yl)oxy)-3-chloropropan-2-ol ((*R*)-**2**) reagerte med isopropylamine over 24 t for å syntetisere (*S*)-pindolol ((*S*)-**5**). Grunnet små mengder startmateriale, ble ikke produktet renset. Produktet inneholdt urenheter og utbytte er derfor ikke gitt.

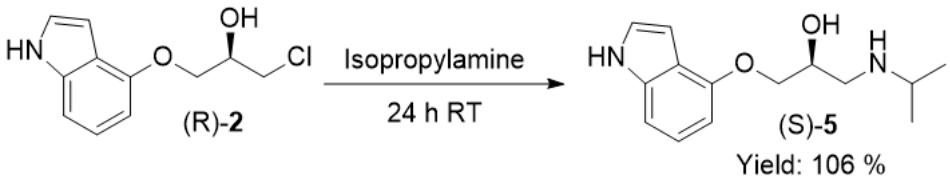

Scheme 6: Reaksjon av (*R*)-**2** for å lage (*S*)-pindolol ((*S*)-**5**) gjennom en substitusjonsreaksjon ved å substituere klorid med isopropylamine.

Compounds featured in this thesis

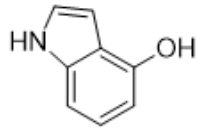

1

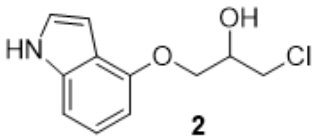

2

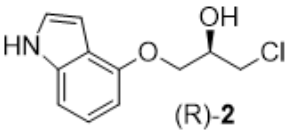

(R)-**2**

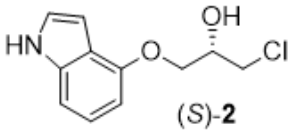

(*S*)-**2**

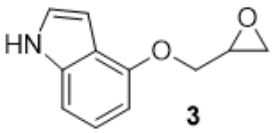

3

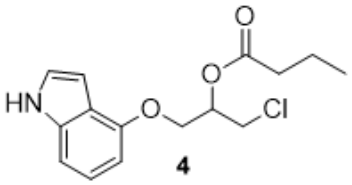

4

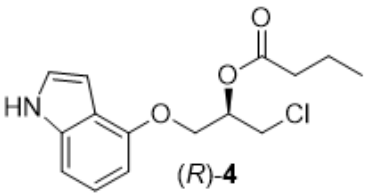

(*R*)-**4**

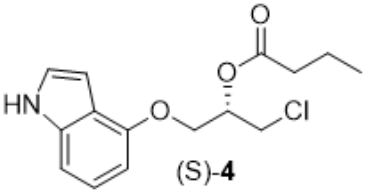

(S)-**4**

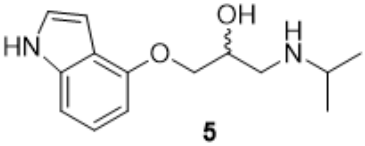

5

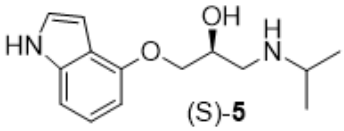

(S)-**5**

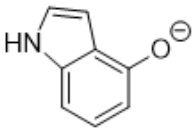

6

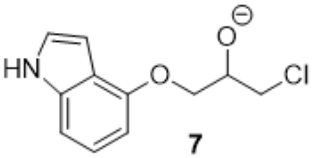

7

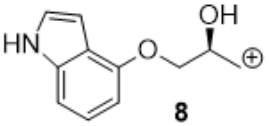

8

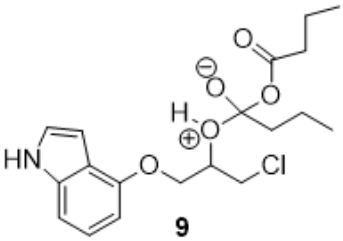

9

Contents

1 Introduction

1.1 Background for the project

In recent times the focus on stereoisomeric drugs has increased. One of the reasons for this is the fact that USA's Food and Drug Administration (FDA) issued a new policy in 1992 regarding future drugs [1]. Among other parts in this policy, there are two important points on stereoisomeric drugs. The first is to ensure correct stereoisomeric composition of a product and that good procedures should be implemented in manufacturing. The second point is that for all drugs that have stereoisomers, the isomers should be studied individually. The goal of this Master's is therefore in line with USA's FDA policy.

In 1998 a definition of green chemistry was proposed by Paul Anitas and John Warner;"Green chemistry is the utilization of a set of principles that reduces or eliminates the use or generation of hazardous substances in the design, manufacture and application of chemical products."[2]. Using enzymes in organic synthesis is an example of green chemistry. This is due to enzymes being reusable and biodegradable. When this is compared to energy-intensive metal processing, the environmetal advantages of enzymes becomes clear [3]. Due to the the increasing importance of environmentally friendly alternatives, the use of enzymes as catalysts is of importance.

1.2 Importance of enantiopure drugs

An enantiopure drug is a drug where only (<96 % ee) one of the enantiomers are present in the drug. Drugs are made enantiopure due to the fact that only one enantiomer act as the active pharmaceutical ingredient (API), and therefore the other enantiomer is either redundant, or in some cases, damaging. Since the body consists of many chiral molecules, the enantiomers often display different effects when entering the body. An example of these chiral molecules are signal receptors - a protein made out of amino acids that transmits a signaling cascade, a chemical or physical signal, through a cell. Amino acids only exist as one of the enantiomers, the *S*-form, and receptors can display 3 different 3D structures. This means that the drug will have a different affinity depending on the spatial arrangement of the receptors. As a result of this, the effects of the enantiomers can vary greatly [4].

The most known example of this is the drug called Thalidomide (See figure 1). This drug was used in the late 1950s and 1960s for treatment of nausea in pregnant women. However, it was withdrawn from the market due to severe birth defects in thousands of children [5]. This led to new studies on the drug and it was shown in mice and rats that the *S*-(-)-enantiomer had the undesired teratogenic effects, while the *R*-(+)-enantiomer

did not show the undesired effects [6]. Later testing showed that Thalidomide racemizes *in vivo* and that therefore both the enantiomers caused the undesired effects [7]. However, even though Thalidomide led to a lot of defects, it also sparked a revolution in toxicity testing of drugs, as it prompted international regulatory agencies to develop a systematic testing protocol for toxicity in drugs. As a consequence of this, both the creation of the Society of Toxicology and the withdrawal of Thalidomide happened in 1961 [7].

Even though the enantiomers of Thalidomide ended up not being relevant because it racemizes *in vivo*, there are many examples where the enantiomers greatly affect the medicinal effect of the drug. An example of this is the calcium channel antagonists drug called Verapamil (See figure 1). *S*-(-)-Verapamil has 10-20 times more pharmalogical potency than *R*-(+)-Verapamil in terms of negative chromatropic effect on atrioventricular conduction, and as vasodilators [8, 9]. Verapamil also has an application in chemotherapy as a modifier of multidrug resistance. The problem is that it has to be used with a high concentration leading to too high carditoxicity. However, *R*-(+)-Verapamil has a lower cardiotoxicity than *S*-(−)-Verapamil. This leads to *S*-(-)-Verapamil being the best choice for use as a calcium channel blocker for cardiovascular therapy, while *R*-(+)-Verapamil is the best choice as a modifier of multidrug resistance in cancer chemotherapy [10]. Since different enantiomers can have different effects as drugs, it is important to synthesize enantiopure molecules to better research their effect. It is also important to find new and effective ways to synthesize enantiopure drugs.

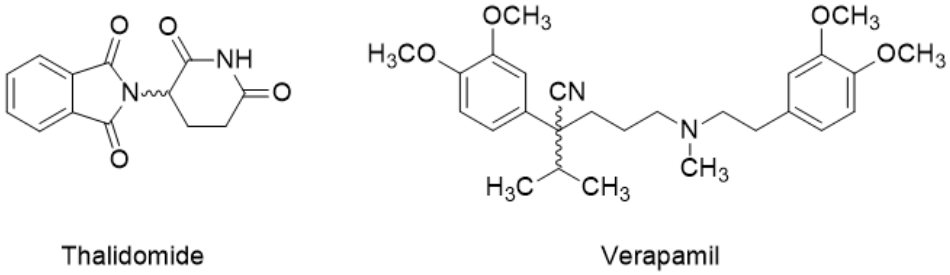

Figure 1: The molecular structure of racemic Thalidomide and Verapamil.

1.3 Effects and use of pindolol

Pindolol (see Figure 2) is a β-blocker that reduces high blood pressure. The drug is used in treatment of angina pectoris and hypertension [11]. It has also been researched to be used in treatment of depression as an add-on therapy to selective serotonin re-uptake inhibitors (SSRIs) [12, 13].

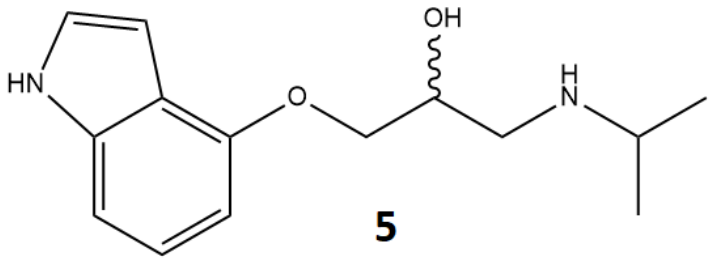

Figure 2: The molecular structure of racemic pindolol.

Racemic pindolol was patented in 1966 [14] and the first clinical use in USA took place in 1982 [15]. The compound is lipophilic and quickly absorbed into the body and is therefore quickly absorbed by the nervous system. It has a plasma half-time of 3-4 hours in patients with normal renal functions. Side effects of pindolol include unwanted changes in respiratory system and reduced hearth function. These side effects are expected because they are related to the β-adrenergetic blocking activity of pindolol. Other reported side effects are nausea, dizziness, feeling of weakness or fatigue, vivid dreams and muscle cramps [16].

1.4 β-Adrenoceptor

(S)-pindolol ((S)-**5**)) is a β-adrenoceptor antagonist. β-adrenoceptors antagonists, more commonly know as β-blockers, are a group of drugs that are used in the treatment of many cardiovascular disorders by blocking the β-receptors. This blocks the the stimulation of these receptors from neurotransmitters, like dopamine, epinephrine and norepinephrine, that normally stimulate these receptors. The heart will beat slower which leads to reduced blood pressure [17, 18].

β-Adrenoreceptors are classified in two groups; β_1-receptors and β_2-receptors. β_1-receptors are primarily found in the heart, but also the kidneys, while β_2-receptors are found in visceral organs such as the heart, liver and kidneys. It is also found in the bronchioles and in the smooth muscle of arteries and arterioles. Stimulating β_1-receptors increases heart rate, renin secretion in the kidneys, and the heart's ability to contract. The arteries and the bronchi are dilated if β_2-receptors are stimulated, which increases airflow to the lungs and blood flow.

β-Blockers are either called β_1-blockers or β_2-blockers depending on their selectivity for either β_1-receptors or β_2-receptors [17, 18]. Figure 3 shows the two main types of adreno receptors, α- and β-receptors, and their effects.

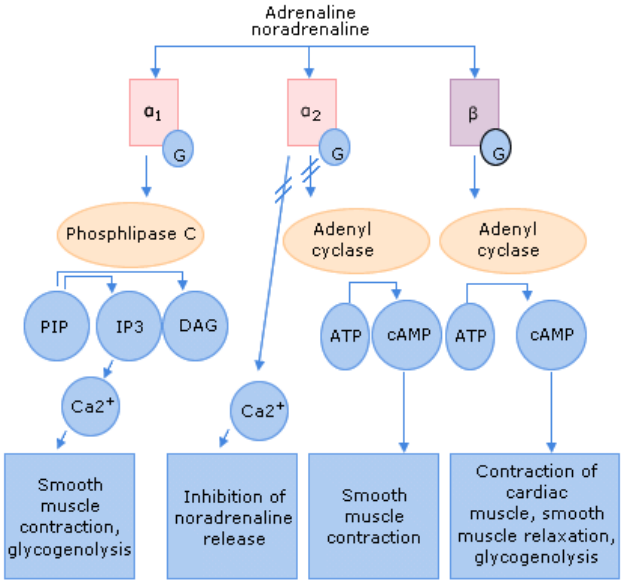

Figure 3: The two main types of adreno receptors, α- and β-receptors and their effects [19].

β-blockers are also categorized as either antagonists or agonists. If the β-blockers promote the process stimulated by a neurotransmitter it is an agonist and if it blocks the process functions as an antagonist [20].

1.5 Biocatalysis

Biocatalysis is the use of enzymes in chemical synthesis in order to convert a molecular substrate to a product. Enzymes are proteins that consist of chiral (S)-amino acids and will therefore interact with enantiomers differently. They also work as catalysts, accelerating chemical reactions. The first example of modern biocatalysis was performed by Louis Pasteur [3]. He used racemic tartaric acid and demonstrated its resolution through fermentation with a variety of microorganisms, including the common mold *Penicillium glaucum* [21]. This enantioselective microbial metabolism of tartaric acid lead to the discovery of enantioselectivity in a biochemical reaction[22].

Biocatalysis has many uses in industrial chemical processes. An example of this is its use in the bleaching processes in the textile industry. Previously, dichloride or sodium hypochlorite was used, while now H_2O_2 is used. Initially this swap was hampered by the residual peroxide that was detrimental to subsequent dying processes, but this was solved with the use of the enzyme peroxidases [23]. There are many factors that have led to the growth in use of biocatalyst in industry and/or organic synthesis. Unlike energy intensive processing metal-based alternatives, biocatalysts can be considered as renewable catalysts that are biodegradable and can be replaced easily, inexpensively using environ-

mentally benign fermentation processes [3]. Other important advantages are the low mole percentage required of the enzyme and the faster reaction rates. Enzymes-catalyzed processes can react at rates 10^8-10^{10} times faster than the non-catalyzed alternatives. The mole percentage can be as low as 10^{-4}-10^{-3}%, while its chemical catalyst counterpart is often needed at 0.1-1% [24]. Enzymes can also display different types of selectivity. In this project the most important selectivity is the enantioselectivity. One of the enantiomers will fit the active site of the enzyme better and convert the substrate to one of the enantiomers at a higher rate. A reaction with this effect is called kinetic resolution [24].

1.5.1 Kinetic resolution

A kinetic resolution is a chemical reaction where a racemic substrate is converted to the enantiomers at different rates, leading to different rations of the enantiomers in both the substrate and the product. The enantiomers react at different rates due to different activation energies. The Gibbs free energy level is, by definition, the same for the enantiomers of both the substrate and the product. The transition state energy, $\Delta G^{\ddagger}$, can differ. This is shown in Figure 4, where the R-enantiomer has a lower $\Delta G^{\ddagger}$ and would therefore react faster than the S-enantiomer [25].

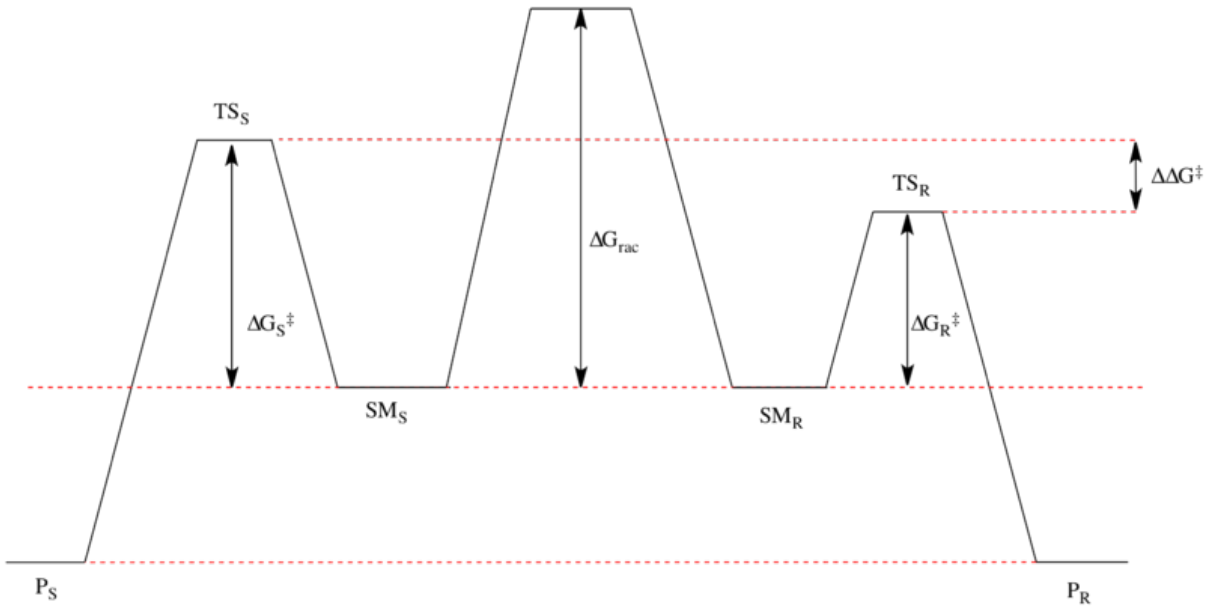

Figure 4: The figure shows Gibbs free energy of the different transition state in a theoretical reaction with two enantiomers. TS_S and TS_R are the transition states of the S and R enantiomers, $\Delta G_S^{\ddagger}$, $\Delta G_R^{\ddagger}$ and $\Delta G_{rac}^{\ddagger}$ are the transition state energy of the S and R enantiomers and the racemic mixture. The R enantiomer has a lower $\Delta G^{\ddagger}$ and would thus react faster than the S enantiomer [26].

To measure the different ratios of the enantiomers present, the entiomeric excess (%ee) is used. Equation 1 was used to calculate %ee.

$$\%ee = \frac{P - Q}{P + Q} * 100\% \tag{1}$$

P is the area of the major peak in a chromatogram and Q is the area of the minor peak of the other enantiomer. %ee is calculated for both the substrate and the product. ee_s is the ee for the substrate and ee_p is the ee for the product. There are examples of specific enzymes that only convert one of the enantiomers. This will lead to one enantiopure product and one enantiopure substrate with none of their counterparts present. This is called enantiospecificity and would give 100% ee_s and ee_p [24]. If the enzyme has more affinity for one of the enantiomers, it is called enantioselectivity.

The enantiomeric ratio, E, can be used to further quantify the selectivity towards one substrate of the enzyme. The higher the E-value, the higher selectivity of the enzyme is towards one enantiomer, and vica versa. The enantiomeric ratio can be calculated using $\%ee_s$ and $\%ee_p$, as seen in Equation 2.

$$E = \frac{ln[1 - c(1 + ee_p)]}{ln[1 - c(1 - ee_p)]} = \frac{ln[1 - c(1 - ee_s)]}{ln[1 - c(1 + ee_s)]} \tag{2}$$

In equation 2 c is the conversion. The conversion can be calculated using enantiomeric excess of the substrate and product as seen in equation 3.

$$C = \frac{ee_s}{ee_s + ee_p)} \tag{3}$$

Equation 2 is unreliable if the conversion is either very high or very low, due to the possibility of parsing errors. Therefore equation 4 is used since it uses relative values.

$$E = \frac{ln(\frac{[\%ee_p(1-\%ee_s)]}{\%ee_p+\%ee_s})}{ln(\frac{[\%ee_p(1+\%ee_s)]}{\%ee_p+\%ee_s})} \tag{4}$$

This equation works best for reaction where there is only one substrate and one product; a uni-uni reaction. However, the kinetic resolution performed in this thesis uses two substrates, 1-((1H-indol-4-yl)oxy)-3-chloropropan-2-ol (**2**) and vinyl butyrate, to make two products, (*R*)-1-((1H-indol-4-yl)oxy)-3-chloropropan-2-ol ((*R*)-**2**) and (*S*)-1-((1H-indol-4-yl)oxy)-3-chloropropan-2-yl butyrate ((*R*)-**4**). This is bi-bi reaction and follows a ping-pong mechanism shown in Figure 5 [27].

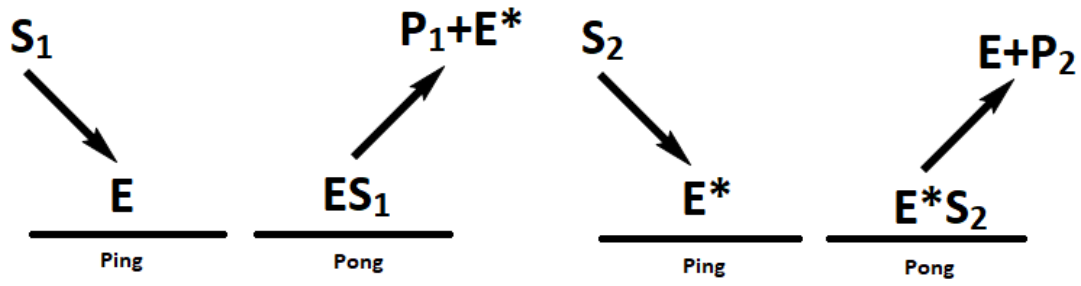

Figure 5: A bi-bi reaction following a ping-pong mechanism where two products are formed, P_1 and P_2, without consuming the enzyme used, E [28].

Figure 5 shows the first substrate (S_1) bind to the enzyme (E) and the enzyme-substrate (ES_1) is formed. The first product (P_1) is formed and released from the intermediate state (E*) forms. The other substrate (S_2) then binds to the intermediate state (E*) and is converted to the second product (P_2), while the intermediate state (E*) returns to the original enzyme (E).

Even though equation 2, 3 and 4 apply to uni-uni reaction, it is assumed to work well for CALB - an assumed ping-pong bi-bi reaction [29]. To calculate the E-value of a ping-pong bi-bi reaction the software *E & K Calculator* was used. In *E & K Calculator* the E-value is calculated by using ee_s and ee_p from HPLC or GC [30].

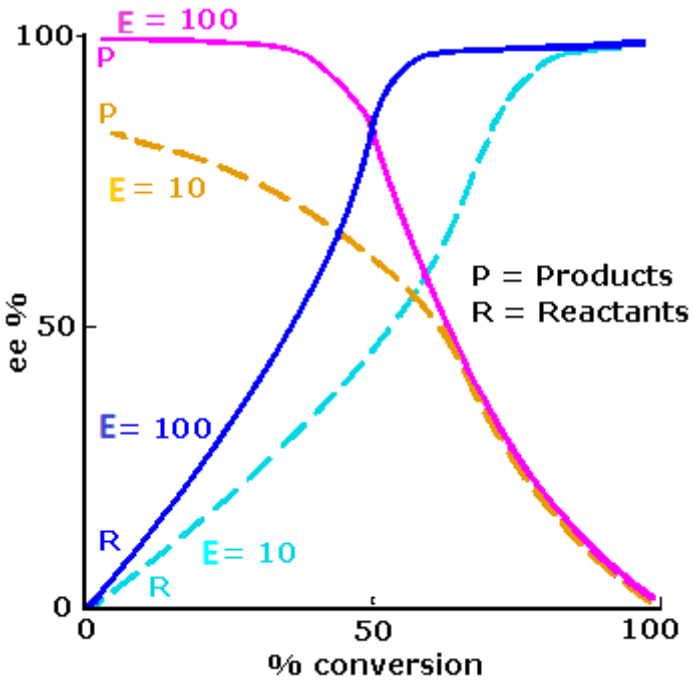

Figure 6: This figure shows %ee as a function of conversion. The pink and blue lines represent a reaction giving an E-value of 100. The yellow and cyan represents an E-value of 10. The pink and yellow lines show the ee_p and the blue and cyan lines show the ee_s [31].

Since enzymes catalyze equilibrium in both directions it is important to try to optimize for an irreversible reaction. One way to do this is by using an acyl donor. In this thesis vinyl butyrate was used. The enantiomers will be aclyated at different rates depending on the selectivity of the enzyme, and the remaining acetaldehyde will evaporate, due to volatility. This hampers the reverse reaction, making the reaction irreversible. When a kinetic resolution is irreversible the ee_s will start at zero and increase depending on the E-value while the ee_p will decrease equally. Figure 6 shows the enatiomeric excess as a function of conversion with two different E-values in an irreversible kinetic resolution [24].

1.5.2 Important factors in biocatalysis

When using enzymes in organic synthesis nit is important to be aware of factors that can influence the reactions in the synthesis. Water is the natural environment for enzymes. Enzymes therefore show a higher conversion rate when water is used as a solvent. It can still be used in other solvents (see section 1.5.3), but it is important to control the water activity [32]. This can be achieved either by using salt hydrates or by mixing different solvents [24]. Another factor is pH. Enzymes are often found in natural environments in nature and therefore the conversion rates are often higher with pH 7. This can be done by using a buffer or adding base/acid to change the pH to 7. As stated in section 1.5, enzymes are selective. An example of this selectivity is chemoselectivity and regioselectivity. Chemoselectivity is the ability to differentiate different functional groups and regioselectivity is the ability to differentiate identical functional groups that hold different positions on a molecule. This means that small changes in molecules can greatly affect the conversion rate [22, 24].

1.5.3 Effects of solvent and acyl-donor

Solvent is an important factor when affecting the activity of an enzyme. Generally speaking, enzymes have the highest activity in non-polar solvents, like hexane, and lower activity in polar solvents [33]. While lower activity is not desired in itself, it will lead to a higher enantimeric ratio and will therefore often be desired when making enantiopure compounds [34]. The solvent can also, in some cases, change the substrate preference of the enzyme [35].

The water content in the solvent is also an important factor for both the activity of the enzyme and the reaction rate. Higher water content will lead to lower reaction rate, without necessarily affecting the enantioselectivity. For polar solvents, a higher water activity will lead to low reaction rate or it can even stop the reaction. This is because it lets reaction that was irreversible in the first place, become reversible (See scheme 7).

This will lead to the formation of esters and hydrolysis of the acyl donors. In dry solvents reaction 2 and 3 in scheme 7 will not happen, unless water is added, in which case the reaction would stop. Polar solvents need a higher water content for the water activity to increase the same as in a non-polar solvent due to the solubility of water in polar and non-polar solvents [36].

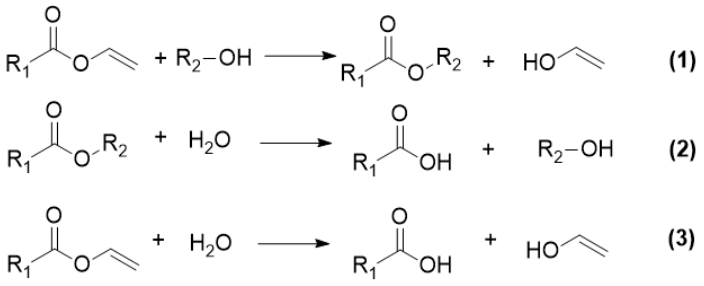

Scheme 7: Equilibrium of esterification reaction [36].

Karl Fischer titration uses coloumetric or volumetric titration to measure the water content in the solvent [36]. In this thesis the water content in the solvent was not measured because dry solvents with molecular sieves were used, so there was no water content.

Simulation were done with CALB, measuring the effect of different solvents. It concluded that CALB has a stable conformation in both polar and non-polar solvents. However, the solvent affects the active site. Some polar solvents can influence the conformation of the active site and hamper the interactions for Ser^{105} and His^{224} in the catalytic triad [37].

The choice of acyl donor can also affect the activity of the enzyme. As seen in scheme 7, the reaction will be irreversible if vinlyesters are used as acyl donors with no water present. If other esters are used, the reversible reactions can happen. Even so, Jacobsen *et al.* found high E-values by using halogenated acyl donors, but the reactions were really slow [38]. Another advantage of vinyl esters is the tautomerization of the leaving vinylalcohol. The tautomerization forms an acetalaldehyde which will evaporate in room temperature making the workup easier.

1.5.4 *Candida antartica* lipase B

Candida antartica lipase B (see Figure 7) is a serine hydrolase from the antarctic yeast *Candida antartica*. Hydrolases is one of 7 groups of enzymes and they are used for reactions such as hydrolysis and esterification, as well as in kinetic resolutions of alcohols and amines [39]. CALB has been reported to work as a catalyst for synthesis of peroxy acid [40], esterification [41] and depolymerization [42]. CALB is easy to use and handle

since the enzyme does not require co-factors. It has high stability in organic solvent and has high enantio- and regioselectivity [43]. The selectivity of CALB in kinetic resolutions of secondary alcohols tend to be towards the *R*-configuration unless the smallest group of the alcohol, is a halogen because then the ranking of the groups change, according to the IUPAC rules change [24].

CALB consists of 317 amino acids where the catalytic activity is decided by the catalytic triad consisting of serine, histidine and aspartate [44]. For esterification reactions it follows the ping-pong bi-bi reaction shown in figure 5 [27]. Structural studies of CALB shows a small α-helix lid at the entrance of the active site, but the lipase shows no sign of interfacial actication. The small entrance and lid are possibly the reason for the high selectivity of CALB [45, 46].

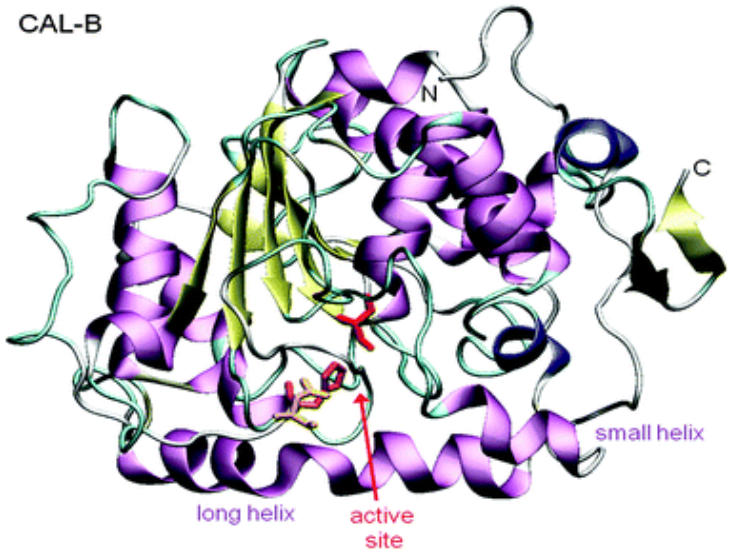

Figure 7: Cartoon representation of the structure of *Candida antartica* lipase B (CALB) [47].

1.5.5 Classification of enzymes

There are 7 classes of enzymes depending on which reactions it catalysis. The different classes are shown in table 1 with the reaction it catalysis [48]. Classically there has been 6 classes of enzymes, but as of 2018 a seventh enzyme class was added [48]. The Enzyme Commission has devised a system for classification of enzymes. All enzymes are prefixed with EC and contain up to four numbers after EC separated by points. The first number indicates the class of the enzyme, the second number indicates the subclass, the third indicates the sub-subclass and the last indicates the serial number of the enzyme in its sub-subclass [49].

Table 1: This table shows the 7 classes of enzymes and the type of reaction they catalyze.

Enzymeclass	**Reaction**
Oxidoreductases	Oxidation-reduction reactions with transfer of electrons.
Isomerases	Reactions that transfer functional groups within a molecule, producing isomeric forms
Hydrolases	Hydrolysis reactions.
Transferases	Group transfer reactions.
Lyases	Reactions were double bonds are formed or broken through adding/removing functional groups
Ligases	Reactions where two substrates are ligated and the formation of C-C, C-S, C-N, and C-O bonds due to condensation reactions
Translocases	Enzymes that catalyze the movement of molecules/ions across membranes or their separation within membranes

The most used of all the enzymes are the hydrolases [50]. CALB, used in this thesis, is also a hydrolase. Hydrolases are classified as EC 3 and have 12 sub-classes that act on different bonds. Hydrolases are often used in the industry because, among other reasons, you don't have to use cofactors, which are often expensive. Hydrolases are also not selective towards a specific substrate, but rather to a functional group. This makes them coefficient and easy to use.

1.6 Chiral high-performance liquid chromatography

High-performance liquid chromatography (HPLC) is a tool to separate, quantify and/or identify the different components in a mixture. The sample is added to a pressurized solvent that passes through a column consisting of a solid adsorbant material. The different components of the sample will interact differently with the solid material in the column and therefore exit the column at different times. Chiral compounds are only different in their spacial orientation and consequently difficult to separate. To separate them by HPLC, chiral selectors have to be added to either the stationary phase or the mobile phase. Common additives to both phases are cyclodextrins, metal chelates and proteins [39]. There are many types of HPLC. In this thesis a normal-phase chiral HPLC apparatus was used. In normal-phase HPLC, the analytes are separated based on their affinity for the polar stationary surface. It is therefore based on the analytes ability to engage in polar interactions, such as dipole-dipole and hydrogen bonding, with the surface of the sorbent. In normal-phase HPLC non-aqueous and non-polar mobile phases such as hexane are used, and therefore requires analytes that are readily soluble in these non-polar solvents. The stationary phase is usually achiral, but if the goal is to separate a chiral compound the stationary phase needs to consist of a single enantiomer of a chiral

compound. This will lead to different affinity for the different enantiomers of the analytes and the enantiomers of the same compound will therefore exit the column at different times.

A good indicator for how good the separation is in chiral HPLC is the resolution, R_s. R_s can be calculated using Equation 5.

$$R_s = 1.177 * \frac{t_R(2) - t_R(1)}{b_{0.5}(1) + b_{0.5}(2)} \tag{5}$$

In the equation $t_R(1)$ and $t_R(2)$ are the retention times of the enantiomers and $b_{0.5}(1)$ and $b_{0.5}(2)$ are the peak widths at half height. Two enantiomers that are base-line separated should have a R_s value of 1.5 or more. Figure 8 visualizes how to find $t_R(1)$, $t_R(2)$, $b_{0.5}(1)$ and $b_{0.5}(2)$.

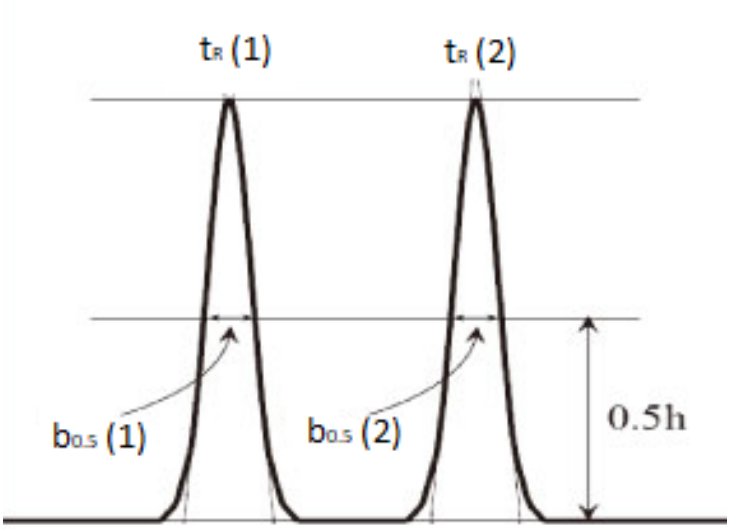

Figure 8: This figure visualizes what $t_R(1)$, $t_R(2)$, $b_{0.5}(1)$ and $b_{0.5}(2)$ are in a HPLC chromatogram [51].

1.7 Gas chromatography

Gas chromatography (GC) is a tool used to analyze volatile substances in gas phase. The sample is dissolved in a solvent that is vaporized in order to separate the analytes by splitting the sample between the stationary phase and mobile phase. The sample being analyzed will interact differently with the stationary phase coated on the walls of the column. This leads to different retention times because the compounds, being analytes, will elute at different times [52].

In GC, the mobile phase is a carrier gas such as helium (inert) or nitrogen (unreactive). The mobile phase carries the sample through the column. The most used mobile phase is helium at 90 % use, but for improved separation hydrogen is preferred [53]. The

stationary phase a microscopic layer of polymer or liquid on an inert solid support inside the column. There are two types of columns; wall-coated open tabular (WCOT) column and supported-coated open tabular (SCOT) column. In SCOT-columns, the walls are coated with a thin later of adsorbent solid which is then treated with a liquid stationary phase. WCOT columns are capillary tubes coated with a thin layer of stationary phase on the column walls. The advantage of SCOT columns is the possibility of holding a greater volume of stationary phase, while the advantage of WCOT is a greater column deficiencies. The choice of detector is also an important part of using GC. The detector is at the end of the column and measures the components of the eluting mixture in combination with the carrier gas. Any properties that are different from the carrier gas can be used as a detection method. The GC detector should, ideally, be able to have high sensitivity, the quantity of sample must be reproducible, it should be chemically inert, withstand temperatures in the range of -200 °C to 400 °C and it should be reliable, predictable and easy to use. Different detectors will have different characteristics and should therefore be used with care. Table 2 shows some typical detectors and their detection limits [52].

Table 2: This table shows some typical detectors, what samples they can be used in and their detection limits [52].

Type of Detector	**Applicable Samples**	**Detection Limit**
Mass Spectrometer (MS)	Tunable for any sample	0.25 to 100 pg
Flame Ionization (FID)	Hydrocarbons	1 pg/s
Thermal Conductivity (TCD)	Universal	500 pg/ml
Electron-Capture (ECD)	Halogenated hydrocarbons	5 fg/s
Atomic Emission (AED)	Element-selective	1 pg
Photoionization (PID)	Vapor and gaseous Compounds	0.002 to 0.02 µg/L

1.8 Polarimetry

Polarimetry is a measuring technique used to measure optical activity. It is sensitive and non-destructive. Different physical properties and concentration of the solution influence the plane of polarized light. This is detected by a polarimeter as the angle of optical rotation. These measurements can be used to define different parameters. Polarimetry is used to understand chiral molecules, because they can be characterized based on the property to rotate the plane of polarized light and are therefore optically active. The measured effect of this property is called optical rotation. The optical rotation can be used to measure the enantimeric properties of a sample. If the sample is racemic (equal amount of both enantiomers) the sample is optically inactive as the clockwise and counterclockwise optical rotations cancel each other out. From the optical rotation, the

specific rotation, a material constant of a substance can be derived. It is the optical rotation for a given concentration, sample cell length, temperature, and wavelength. The relation between optical rotation and specific rotation is given as Biot's law shown in equation 6.

$$\alpha = \frac{[\alpha]_\lambda^T * l * c}{100} \tag{6}$$

α is the optical rotation, $[\alpha]_\lambda^T$ is the specific rotation at a given temperature and wavelength, l is the length of the cell and c is the concentration in the sample. Solving equation 6 for α can be used to find the specific rotation by measuring the optical rotation as seen in equation 7.

$$[\alpha]_\lambda^T = \frac{\alpha * 100}{l * c} \tag{7}$$

1.9 Relevant reaction theory

This section presents the theoretical basis for the organic reactions performed, and their mechanisms.

1.9.1 Base-catalyzed S_N2 addition opening epichlorohydrin to form secondary alcohols

The first step is synthesizing **2** from **1**. This is an S_N2 reaction with sodium hydroxide as the base catalyzing the reaction. The ionized **1** (**6**) reacts with epichlorohydrin to form both the desired alcohol (**2**) and an epoxide intermediate product.

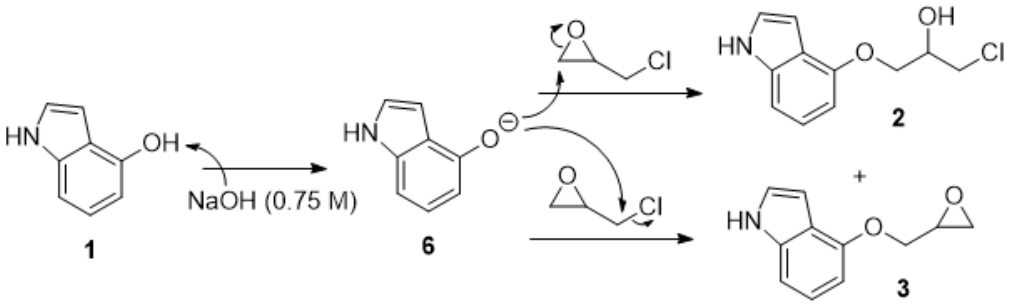

Scheme 8: Reaction mechanisms of the base-catalyzed S_N2 addition of epichlorohydrin.

After sodium hydroxide has deprotonated **1**, the resulting anion (**6**) undergoes a nucleophilic attack of epichlorohydrin. The anion can attack multiple carbons on epichlorohydrin. As shown in Scheme 8, depending on the carbon attack, the product can either

be **2** or **3**. To avoid an internal reaction where the desired product (**2**) turns into the epoxide (**3**), it is important to keep the reaction time short, while still giving the reaction enough time to produce **2**. Previous research reported using both potassium carbonate and sodium hydroxide, where sodium hydroxide gave the highest purity of the desired halohydrin. Previous research also reported a dimer by-product that, possibly, was formed with a reaction between the deprotonated starting material (**6**) and the alcohol (**2**) [54].

1.9.2 Acid-catalyzed opening of epoxide using a halogen donor

In order to increase the yield of the desired product (**2**) an acid-catalyzed opening of the epoxide (**3**) was performed using a halogen donor. The lithium chloride opens the epoxide group and the anion (**7**) reacts with acetic acid forming **2**.

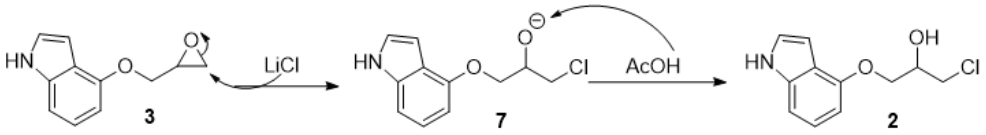

Scheme 9: Reaction mechanism for acid-catalyzed opening of epoxide using a halogen donor

First the lithium chloride coordinates with the epoxide group , opens it and leaves an anion that is protonated by acetic acid giving the desired product (**2**). Lithium chloride is not the only halogen donor that can be used. Similar work in our research group was performed using lithium bromide [55] and dilithium tetrachlorocuprate(II) [56].

1.9.3 S_N1 addition of isopropylamine

After the kinetic resolution, (*R*)-**2** reacts with isopropylamine forming (*S*)-pindolol ((*S*)-**5**).

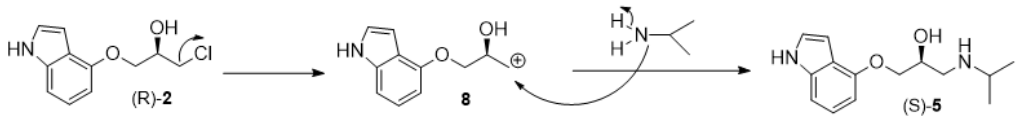

Scheme 10: Reaction mechanism of the S_N1 reaction of (*R*)-**2** forming (*S*)-pindolol ((*S*)-**5**)

First chloride leaves, forming a carbocation intermediate (**9**). Isopropylamine reacts with the carbocation forming (*S*)-pindolol ((*S*)-**5**) in a S_N1 reaction.

1.9.4 Esterification of alcohol with butyric anhydride.

Racemic **2** attacks butyric anhydride to form racemic **4**. Racemic **2** was derivitized into racemic **4** to find the retention time of (*R*)-**4** and (*S*)-**4** in HPLC. It was also synthesized to be used to develod a HPLC method for compound **4**.

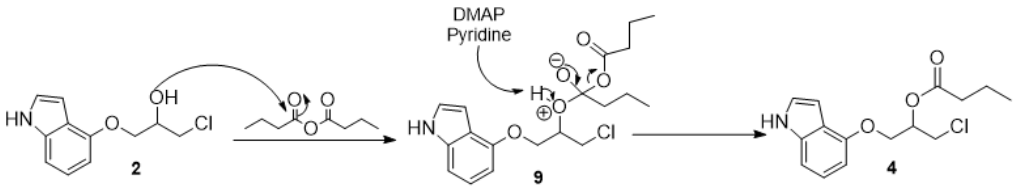

Scheme 11: Reaction mechanism for esterification of **2** to form **4**

First **2** attacks butyric anhydride to form the intermediate product **8**. Compound **8** is deprotonated by 4-dimethylaminopyridine/pyridine and the carboxylate by-product becomes the leaving group. The carboxylate by-product is protonated by 4-dimethylaminopyridine$^+$/ pyridine$^+$ and made into butyraldehyde.

2 Results and discussion

Many of the results in this section will be compared to results from Sigrid Sløgedal Løvland's Master's thesis [57]. This is due to the fact that this Master is a continuation on the work done in Løvland's Master's thesis.

2.1 Organic synthesis

2.1.1 Synthesis of 1-((1H-indol-4-yl)oxy)-3-chloropropan-2-ol (2) from 1H-indol-4-ol (1).

The product (**2**) and the epoxide (**3**) were synthesized by adding epichlorohydrin and sodium hydroxide to the starting material **1**, using 1,4-dioxane as solvent. The reaction time was 6.5 hours, which was when the starting material **1** could no longer be observed in TLC, using dichloromethane as eluent.

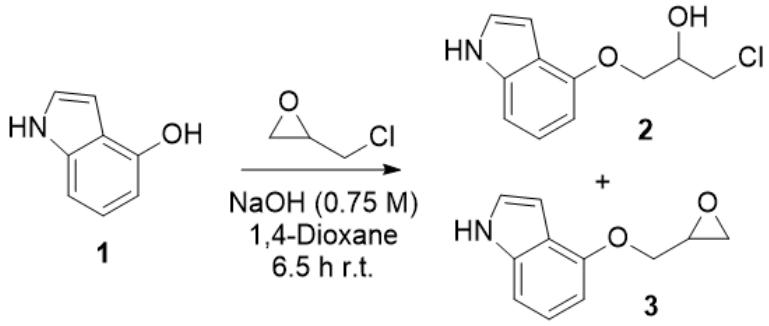

Scheme 12: Synthesis of **1** to form **2** and the epoxide **3**.

In previous research the reaction time was said to be 5 hours [57]. However, the TLC after 5 hours showed that there was still starting material **1** left in the mixture. Therefore the mixture was stirred for another 2 hours before the starting material **1** was barely visible on the TLC. Letting the mixture stir for another 2 hours lets the starting material **1** react for a longer time, but it also lets an internal reaction happen where more of the epoxide is produced. The internal reaction can be seen in Scheme 13. Seeing that the yield ended up being lower than in the previous research with a reaction time of 5 hours [57], the reaction time was reduced by 30 minutes, which ended up increasing the yield of **2**.

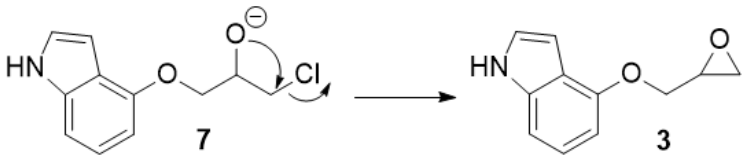

Scheme 13: Suggested mechanism for the internal reaction of **7** to form the epoxide **3**.

Since both **2** and **3** are produced, the percent yield of both individually is not determined, but instead is measured after the opening of the epoxide of **3**. After the epoxide reaction the yields are 59 % (Previous research [57]) and 76 % (Batch reaction). Comparing the two results shows the impact of increasing the reaction time to 6.5 hours.

A black precipitate of this reaction was not analyzed, because it was difficult to dissolve. Therefore the opening of the epoxide started without analyzing the product mixture of this reaction. Since the mixture could not be analyzed, it is difficult to know if there are any unidentified by-products. Analyzing this mixture might prove useful to understand the by-reactions, but it is not important for the synthesis. It should also be noted that there was a lot more precipitate for the analysis reaction than the batch reaction.

2.1.2 Opening of epoxide part of 4-(oxiran-2-ylmethoxy)-1H-indole (3) forming 1-((1H-indol-4-yl)oxy)-3-chloropropan-2-ol (2).

To convert the epoxide **3** to the desired product **2**, an opening of the epoxide group was needed. This was performed by adding lithium chloride to the mixture from the first reaction containing both compound **2** and **3** using tetrahydrofuran and acetic acid as solvent. The reaction time was 72 hours. The yield calculated over this and the last step was 76 %.

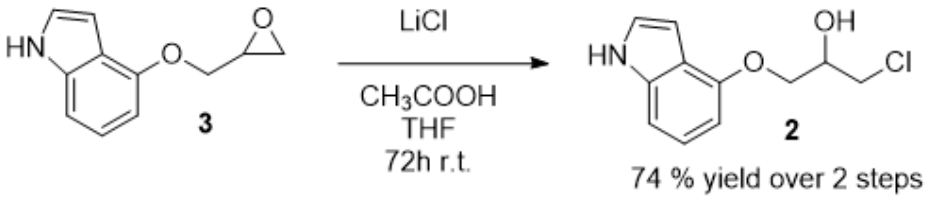

Scheme 14: Opening of epoxide **3** to form desired product **2**

The reaction time was the same as in previous research, but the yield and purity was different. The yield after the opening of epoxide was 59 % in previous research and 76

% in this thesis. A difference in yield of 17 % is substantial and therefore, in the future, this could be researched further to examine what the perfect reaction time would be. The purity based on HPLC (See Figure 47 for example of HPLC-chromatogram used to calculate purity) was 96.2 %, while it was 88.7 % in previous research. It is possible that there are impurities that are not observed in the HPLC since HPLC only shows UV-active compounds, or that an impurity could be stuck in the column.

After the reaction, flash-chromatography was performed. There were differences in how much was loss through flash column and an example of one of the analysis reactions with little loss will be used to show the difference. The amount before the flash-chromatograhy for the analysis reaction was 1.85 g and 0.92 g after, a reduction of 50.7 %. For the batch reaction it went from 4.62 g to 3.87 g with a weight loss of 14 %. The large difference might be because there was more precipitate in the analysis reaction and it might have blocked some of the product from moving through the column. For the batch reaction, flash was done slower, which lead to more reaction tubes being filled and therefore a higher percentage of the product was gathered. When choosing which reaction tubes to use and which to discard, the process was less restrictive for the batch reaction. Another possible reason for the large difference might be the sample size. This reaction was performed multiple other times as well with 1 g or less and 48 % or more was always lost through flash chromatography. This might be because losing small amounts due to mechanical errors has a larger impact on smaller amounts.

2.1.3 Synthesis the ester 1-((1H-indol-4-yl)oxy)-3-chloropropan-2-yl butyrate (4) from 1-((1H-indol-4-yl)oxy)-3-chloropropan-2-ol (2).

In order to more easily optimize the separation of compound **4** with chiral HPLC, butyric anhydride, 4-dimethylaminopyridine and pyridine was added to compound **2** with dichloromethane as solvent. This was performed to make a racemic mixture of **4**, since it would be easier to investigate by HPLC than a mixture containing more of one enantiomer. This reaction stirred for 50 hours.

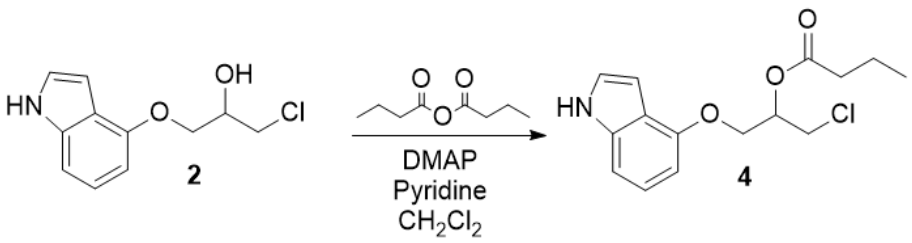

Scheme 15: Synthesis of **2** to form **4** for chiral HPLC analysis.

This reaction was performed in previous research without 4-dimethylaminopyridine and yielded 8 % of **4** with a 24 hour reaction time. The lack of 4-dimethylaminopyridine is most likely the reason for the low yield, but the low reaction time might also have had an effect. The product from this reaction was used to find the retention times of (*R*)-**4** and (*S*)-**4** and make a HPLC method for separating the two enantiomers.

2.2 Optimization of chromatographic separation of enantiomer

To calculate ee_s, ee_p and the E-value, it is required to find the amounts of the two enantiomers of both **2** and **4**. This was done using HPLC. In an attempt to improve the separation of the enantiomers of **4** a GC temperature program was also made.

2.2.1 Analysis of 1-((1H-indol-4-yl)oxy)-3-chloropropan-2-ol (2) by HPLC

To find the ee_s and the E-value, a good separation of the enantiomers of **2** is required. The starting point for making a method to separate **2** was from previous research and can be seen in Figure 48 using n-hexane:isopropanol at 80:20 ratio. The analysis time was one hour and the separation of the peaks are over 30 minutes. Therefore ratio of n-hexane and isopropanol in the range from 80 % n-hexane to 60 % with 2 % change each run, were tested to reduce the analysis time. A ratio of 60:40 between n-hexane and isopropanol resulted in an analysis time of 20 minutes with the peaks being separated by less than 5.5 minutes (See Figure 47). This method was used to calculate the ee_s of **2** seen in Figure 49. Since the peaks are still very well separated it would be possible to continue to increase the percentage of isopropanol to further reduce the analysis time, but this was not seen as necessary since the difference would be insignificant. The method that was used in this thesis to separate the enantiomers of **2** was with a chiralcel OD-H column, n-hexane:isopropanol (60:40), 1 mL/min flow. The retention times were t_R=8.0 min for (*S*)-**2**, t_R=14.9 min for (*R*)-**2**. (see Figure 47).

2.2.2 Analysis of 1-((1H-indol-4-yl)oxy)-3-chloropropan-2-yl butyrate (4) by HPLC

To find the ee_p and the E-value, a good separation of the enantiomers of **4** is required. Once again the starting point was a method from previous research [57]. Figure 10 shows the difference between the HPLC performed for this thesis and the one performed in previous research. Even though the separation needs to be better in both for baseline separation, the improvement is clear.

In order to obtain baseline separation of (*R*)-**4** and (*S*)-**4**, all ratios of n-hexane and isopropanol from 80 % to 91 % n-hexane were tested. To give an example of this, the chromatogram of the run with 85 % n-hexane is presented in Figure 9.

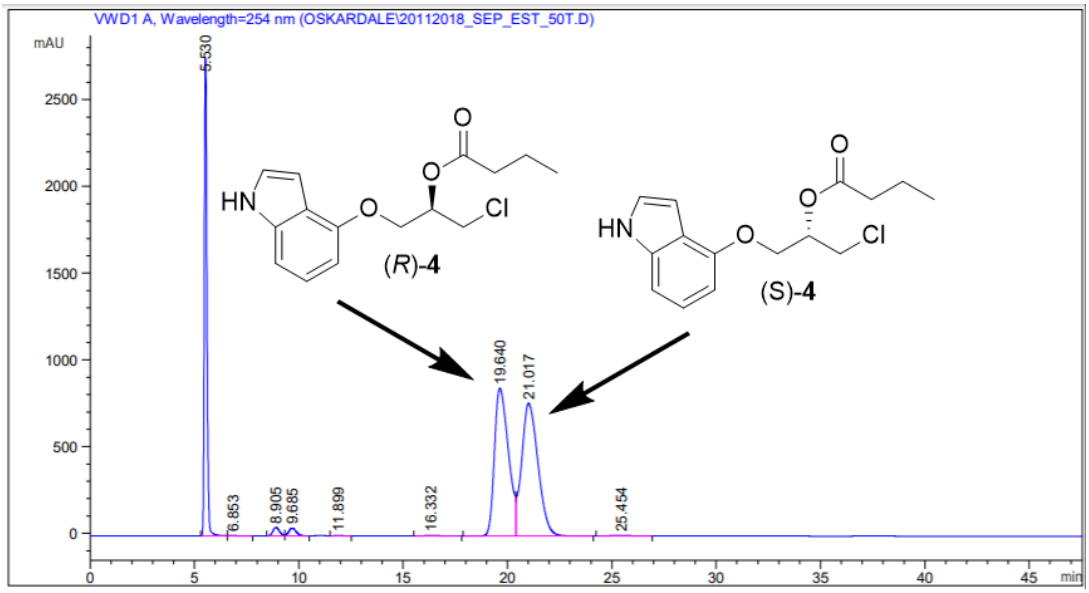

Figure 9: Chiral HPLC chromatogram showing both enantiomers of **4**. t_R=19.6 min for (*R*)-**4**, t_R=21.0 min for (*S*)-**4**. Chiralcel OD-H column, n-hexane:isopropanol (85:15), 1 mL/min flow.

The ratio 90:10 (n-hexane:isopropanol) gave the best results (See top part of Figure 10). Reducing the percentage of isopropanol more led to long analysis time. The R_s for compound **4** calculated using equation 5 is 1.08. In previous research the R_s was 0.78 for compound **4** [57]. This is a clear improvement in R_s. The fact that the peaks are even, strengthens the validity of the calculated ee_s, ee_p and E-value, which will be discussed in section 2.3.

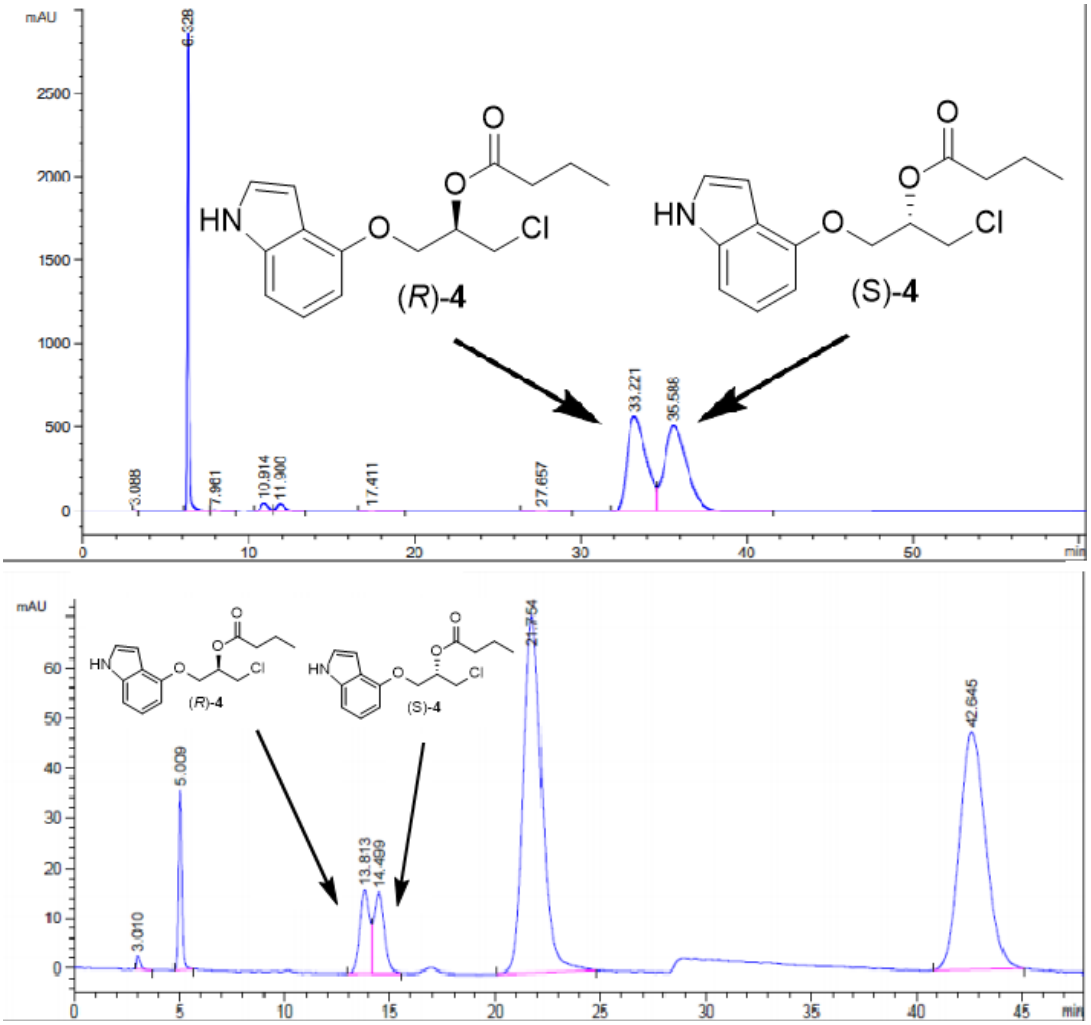

Figure 10: The upper chromatogram is the same seen in as in Figure 46, while the lower chromatogram is from previous research [57]. She used Chiralcel OD-H column and n-hexane:isopropanol (80:20), 1 mL/min flow for 27 min, then n-hexane:2-propanol (70:30)) [57]. The peaks at 13.8 min and 14.5 min are from **4**.

The method that was used in this thesis to separate the enantiomers of **4** was with a chiralcel OD-H column, n-hexane:isopropanol (90:10), 1 mL/min flow. The retention times were t_R=33.2 min for (*R*)-**4**, t_R=35.6 min for (*S*)-**4** (see Figure 46).

2.2.3 Analysis of 1-((1H-indol-4-yl)oxy)-3-chloropropan-2-yl butyrate (4) in GC

In the HPLC analysis, the R_s was 1.08. The desired R_s was 1.50 or higher and therefore GC was attempted. In the end the GC was not used due to no separation of the enantiomers of **4**, and HPLC was used. Even so, the process of finding a temperature program and trying to separate **4** will be shown in this section.

First, a sample of racemic **2**, a sample of racemic **4** and a sample containing a mixture of racemic **2** and **4** were analyzed. The chromatograms for **2** and **4** can be seen in Appendix 6.5 as Figure 51, 52 and 53. This resulted in the information that compound **4** has the lowest retention time and is a tall, narrow peak, while compound **2** was a small, broad peak with a tail. Compound **2** was included so that both compound **2** and compound **4** from the enzyme reaction could be separated in one temperature program. Since the separation of compound **4** failed and HPLC was used instead a temperature program to separate compound **2** in GC was never made. The reason both the big narrow peak before the peak of compound **2** and the smaller narrow peak after the peak of compound **2** were investigated was because both came from the sample with compound **4** and both of them could possibly be compound **4**. Even so the first peak is assumed to be compound **4** due to its size.

First a temperature program, 70-130 °C, 1°C/min, 2 min hold time, was ran and gave no indications of separation (See Figure 54). Many temperature programs were then made to manage to have a lower temperature increase at the retention time before and after compound **4** to avoid a long run time. The first successfully temperature program made used a temperature increase of 0.5 °C/min at the retention time for compound **4** and is seen in Figure 11. This also has no indication of separation.

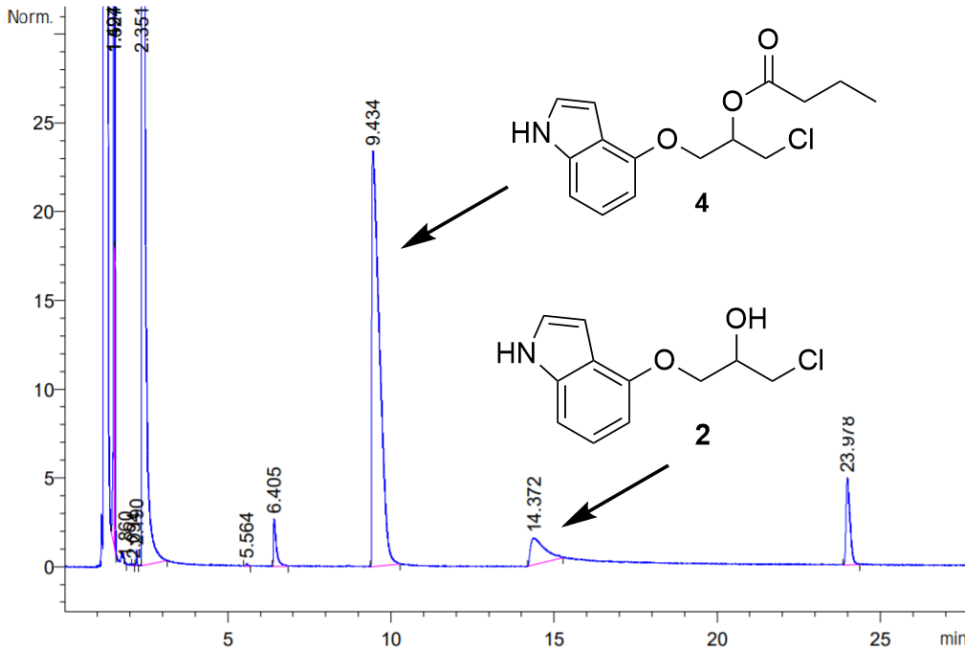

Figure 11: GC chromatogram showing compound **2** and **4**. t_R= 9.4 min for **4**. t_R= 14.4 min for **2**. The temperature program used was 70-79 °C, 3°C/min, 79-83 °C, 0.5°C/min, 83-97 °C, 3°C/min, 97-102 °C, 0.5°C/min, 2 min hold time. The column used was a Agilent column with a CP-Chirasil-Dex CB stationary phase consisting of cyclodextrin directly bonded to dimethylpolysiloxane.

Many more temperature programs were made with gradually lower temperature increases. Temperature programs with 0.4 °C/min, 0.3 °C/min, 0.2 °C/min and 0.1 °C/min were all successfully made. 0.1 °C/min would be expected to have the best separation. The temperature program used was 70-82 °C, 3°C/min, 82-84 °C, 0.1°C/min, 84-101 °C, 3°C/min, 101-103 °C, 0.1°C/min, 2 min hold time. There is still no indication of separation as can be seen in Figure 12. When the chromatogram shown in figure 12 showed no indication of a separation, it was decided that the results from HPLC would be used.

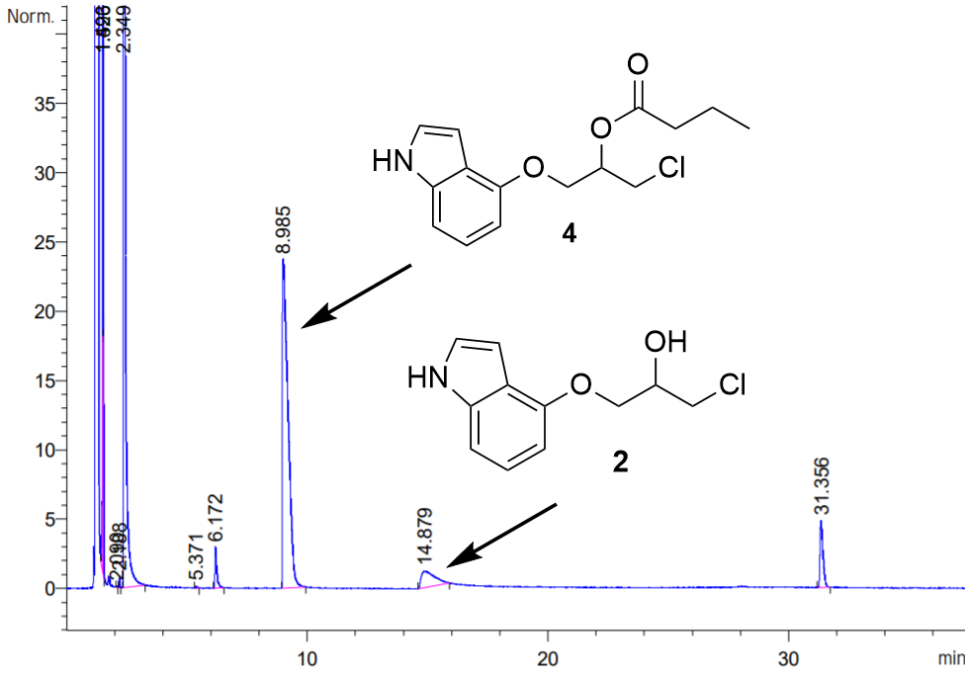

Figure 12: GC chromatogram showing compound **2** and **4**. t_R= 8.9 min for **4**. t_R= 13.2 min for **2**. 70-82 °C, 3°C/min, 82-84 °C, 0.1°C/min, 84-101 °C, 3°C/min, 101-103 °C, 0.1°C/min, 2 min hold time. The column used was a Agilent column with a CP-Chirasil-Dex CB stationary phase consisting of cyclodextrin directly bonded to dimethylpolysiloxane.

2.3 Kinetic resolutions of 1-((1H-indol-4-yl)oxy)-3-chloropropan-2-ol (2)

The kinetic resolution of **2** forming (*R*)-**2** and (*S*)-**4** was performed using the enzyme *Candida antartica* lipase B (CALB) from SyncoZymes Co, Ltd. (Shanghai, China) (Scheme 16). The reaction time when no starting material was left was around 50 hours using 1 mass-equivalent of immobilized CALB to compound **2**. 1.0055 g of starting material **2** yielded a mixture of 1.5220 g, after removing the solvent under reduced pressure. After purification with flash column it yielded 0.2832 g of ((*R*)-**2**) and 0.2163 g of ((*S*)-**4**). This gives a yield of 28.0 % for (*S*)-**2** and a combined yield of 44.4 % for both (*S*)-**2** and (*R*)-**4**.

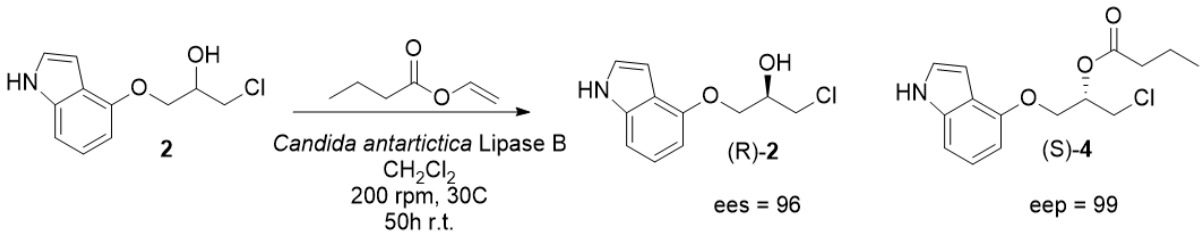

Scheme 16: The scheme shows the enzyme reaction where **2** reacted with vinyl butyrate and CALB to make (*R*)-**2** and (*S*)-**4**.

The kinetic rosolution of **2** was performed many times and the conclution was that there was no starting material left after 50 hours. In previous research 98 hours was used [57]. The difference might come from the difference in CALB and compound **2** used. In previous research 16.0 mg of compound **2** was used and 15.0 mg of CALB, while in the reaction performed as a part of this thesis used 1.0055 g of compound **2** and 1.0091 g CALB. The earlier research used a surplus of compound **2** with 7 % more of compound **2** compared to CALB. While the reactions performed as part of this thesis used a surplus of CALB compared to compound **2**. Another difference is more conservative use of molecular sieves in her thesis.

The ee_s for compound **2** was 96 %, the ee_p for compound **4** was 99 % and the E-value for the kinetic resolution was 46. The ee of 96 % for compound (*R*)-**2** is at the limit for a drug to be considered enantiopure. Even though the ee_p was good it is important to note that the calculations were done without baseline separation of compound **4** and a R_s of 1.08. This also affected the credibility of the calculated E-value of 46, but since the measuring points are on the lines the credibility of the E-value increases.

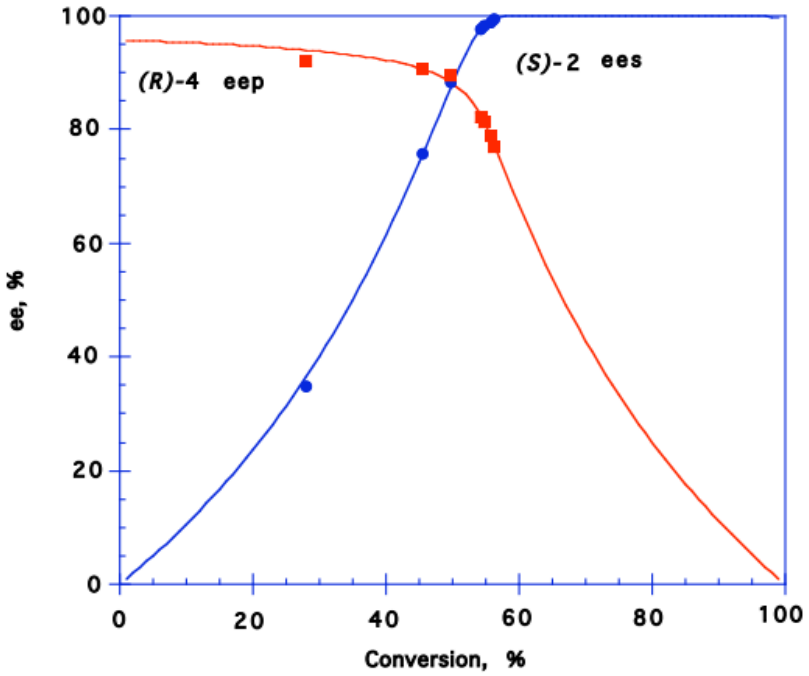

Figure 13: A graphical representation of the %ee as a function of % conversion. The blue line represents $\%ee_s$ and the red line represents $\%ee_p$. The function is calculated by EK calculator 2.1b0 PCC based on the data points seen as blue circles ($\%ee_s$) or red squares ($\%ee_p$) obtained from HPLC chromatograms in Figure 37-43. The calculated E-value was 46.

To calculate the E-value, HPLC of the enzyme reaction was used. HPLC from the product mixture of the enzyme reaction can be seen in Figure 37-43. For both compound **2** and **4** the same sample was used, but with a different program. Compound **2** used chiralcel OD-H column, n-hexane:isopropanol (60:40), 1 mL/min flow. The retention times were t_R=8.0 min for (*S*)-**2**, t_R=14.9 min for (*R*)-**2** (See Figure 47). Compound **4** used chiralcel OD-H column, n-hexane:isopropanol (90:10), 1 mL/min flow. The retention times were t_R=33.2 min for (*R*)-**4**, t_R=35.6 min for (*S*)-**4** (See Figure 46). Separating the peaks of the two enantiomers of **4** after the enzyme reaction proved difficult. Two examples of HPLC chromatograms that were used to calculate the E-value are shown in Figure 44 and 45 for the enzyme reaction after 25 and 50 hours. The HPLC method developed for calculating the ee_p and ee_s of **2** and **4** can seen in Figure 49 for compound **2** and Figure 50 for compound **4**. A GC temperature program was also developed, but ended up not being used since there was no separations of the enantiomers of compound **4**. The temperature program used was 70-82 °C, 3°C/min, 82-84 °C, 0.1°C/min, 84-101 °C, 3°C/min, 101-103 °C, 0.1°C/min, 2 min hold time. This game the retention times t_R= 8.9 min for **4** and t_R= 13.2 min for **2**.

In Morante-Zarcero *et al* it is reported that (*S*)-pindolol ((S)-**5**) was the most re-

tained in chiral HPLC out of the two enantiomers [61] of pindolol **5**. Since the spacial arrangements of (*S*)-pindolol ((S)-**5**) and (*R*)-**2** are similar, it would be expected that (*R*)-**2** would be the most retained enantiomer. In Morante-Zarcero *et al* a GC0 mm long column with a diameter of 4.6 mm was used. While Lux Cellulose-1/Sepapak-1 composed by cellulose tris-(3,5-dymethylphenylcarbamate) coated on a 5 mm silica-gel particle supplied by Phenomenex was used as the chiral stationary phase [61]. Chiral HPLC analyses performed in this thesis used a Chiralcel OD-H column of the same size and same silica-gel particle size. Since the columns used are not the same, the results can not be directly compared. Since CALB is expected to be selective towards *S*-configuration of halohydrins it would be expected that the most retained peak of compound **2** would decrease during the kinetic resolution and that the most retained peak would then be (*S*)-**2**. This observation can be seen in Figure 37-43 which suggests that the most retained peak of compound **2** is (*S*)-**2**. It is also expected that the selectivity of CALB will lead to more (*S*)-**4** than (*R*)-**4**. This observation can also be seen in Figure 37-43.

The next step includes synthesizing the enantiopure β-blocker (*S*)-pindolol ((S)-**5**) from 1-((1H-indol-4-yl)oxy)-3-chloropropan-2-ol ((*R*)-**2**).

2.4 Organic synthesis of (*S*)-pindolol ((S)-5) from 1-((1H-indol-4-yl)oxy)-3-chloropropan-2-ol ((*R*)-2)

(*S*)-pindolol ((S)-**5**) was synthesized from 1-((1H-indol-4-yl)oxy)-3-chloropropan-2-ol ((*R*)-**2**) by adding isopropylamine and stirring for 24 hours. Two methods were attempted one with and one without reflux. The method with reflux did not work and was therefore discarded.

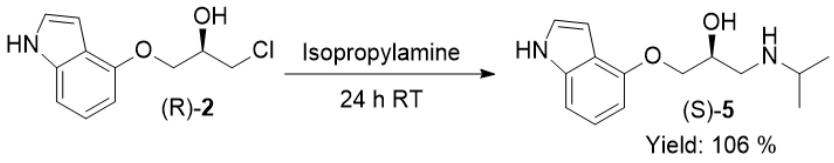

Scheme 17: Synthesis of (*R*)-**2** to produce (*S*)-Pindolol ((*S*)-**5**).

The yield of the reaction was 106 %. The impurities shown in NMR explains why the yield is over 100 %. The first reaction conditions followed was from the synthesis in Lima *et al* [60]. It was stirred under reflux for 24 hours at 42 °C, but this did not result in full conversion from TLC. Therefore another synthesis was performed based on previous research of similar compounds in our research group [62]. It was first attempted with the mixture that had already stirred for 24 hours at reflux. TLC did not show full conversion. Therefore the reaction was performed again following the same synthesis from the start

without reflux and this showed full conversion after 24 hours. This indicates that reflux is not needed for the reaction and that a reaction time of 24 hours is enough. When performing the synthesis the second time all the starting material available was used, 0.0168 g. Due to low amount of starting material (*R*)-**2**, the only purification that was performed was removing the solvent under reduced pressure. This was done to not loose any product from further purification processes. For this reaction the product mixture was evaporated at 15 mbar for 2 hours.

Lima *et al*, the same article that mentioned 24 hours of reflux, also said the product (*S*)-**5** is a white solid [60]. The product from this thesis yielded a brown-red oily liquid. This is possibly due to the impurities in the product. Seeing that the reflux reaction did not work it is difficult to say if the product from Lima *et al* is indeed the expected product (*S*)-**5**.

GC analysis of the product (*S*)-**5** is presented Appendix 6.5 as Figure 55. The concentration of the product (*S*)-**5** in sample was very low and is therefore difficult to interpret. The temperature program used was 50-200 °C with 5°C/min and 12 min hold time. The largest peak was at 35.9 min with a small peak at a slightly lower retention time. If it is assumed that the large peak is (*S*)-**5**, the smaller peak might be (*R*)-**5**. The peaks at 11.8 min and 22.2 min have low boiling points and are not determined. Considering the low concentration of (*S*)-**5** in the sample, the high predicted boiling point of 457.1 ± 35.0 °C at 760 mmHg [63] and the relatively good results from HPLC, separation of **4** by GC was not further researched.

2.5 NMR characterization of synthesis products

2.5.1 Characterization of 1-((1H-indol-4-yl)oxy)-3-chloropropan-2-ol (2)

Characterization of **2** was done using ^{1}H, ^{13}C, COSY, HMBC and HSQC NMR with $CDCl_3$ as solvent. Figure 14 shows **2** with positions numbered and table 3 shows the NMR shifts and correlations for the NMR characterization. Spectra for ^{1}H, ^{13}C and HSQC can be seen in Appendix 6.1, as Figure 25, 26 and 27 while COSY and HMBC is shown in this section as Figure 15 and 16.

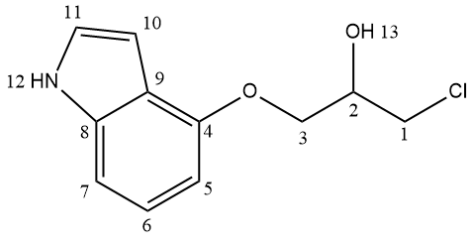

Figure 14: The structure of **2** with the protons numbered corresponding to the values in Table 3

Table 3: NMR shifts and correlations for ^{1}H, ^{13}C, COSY and HMBC NMR on compound **2**. Spectra for ^{1}H, ^{13}C and HSQC can be seen Spectra for ^{1}H, ^{13}C and HSQC can be seen in Appendix 6.1, as Figure 25, 26 and 27 while COSY and HMBC is shown in this section as Figure 15 and 16

Position	**^{1}H [ppm] (mult., int.,^{n}J [Hz])**	**^{13}C [ppm]**	**COSY [ppm]**	**HMBC [ppm]**
1	3.77 (dd, 1H, J=5.40) 3.84 (dd, 1H, J=5.58)	46.20	4.23	68.66, 70.07
2	4.23 (m, 1H)	70.07	4.29, 3.77, 3.84	68.66, 46.20
3	4.29 (m, 2H)	68.66	4.23	46.20, 70.07, 151.86
4	-	151.86	-	-
5	7.04 (d, 1H, J=8.12)	105.25	7.11	101.02
6	7.11 (m, 1H)	122.76	6.54, 7.04	99.65, 118.68, 137.39, 151.86
7	6.54 (d, 1H, J=7.56)	101.02	7.11	105.25, 123.02, 151.86
8	-	137.39	-	-
9	-	118.68	-	-
10	6.63 (s, 1H)	99.65	7.10	101.02, 122.76
11	7.10 (m, 1H)	123.02	6.63	99.65, 118.68, 137.39, 151.86
12	8.20 (s, 1H)	-	-	-
13	2.68 (d, 1H, J=5.76)	-	4.23	68.66, 46.20, 70.07

The ^{1}H spectrum (Figure 25) shows impurities at 1.67, 5.27 and 7.27. The peak at 5.27 is from dichloromethane and the peak at 7.26 is the residual peak of $CDCl_3$ [58]. The peak at 1.67 is an unknown impurity that was not characterized. The ^{13}C spectrum (Figure 26) has no unexpected peaks suggesting that the unknown impurity from the ^{1}H spectrum is a compound without carbon. The neighbouring environments of the positions

were determined through COSY and HMBC spectra (Figure 15 and 16) and the proton-carbon shifts were determined through HSQC (Figure 27). The peaks correspond with those found by Zielinska-Pisklak *et al* [64]. The spectra shown on the next page in Figure 15 and 16 are the COSY and HMBC spectra used to characterize compound **2**.

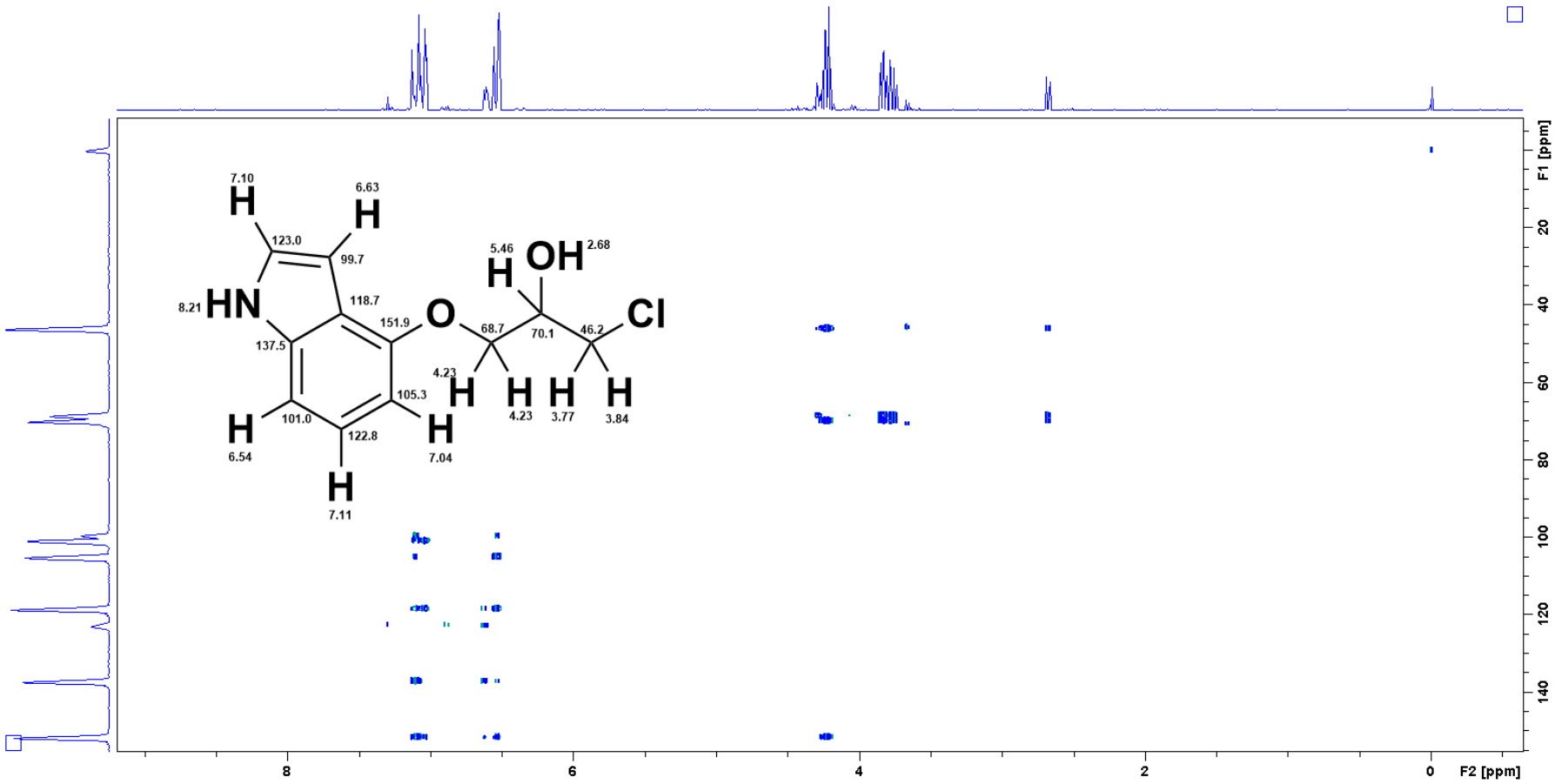

Figure 16: HMBC-NMR spectrum of **2** using a Bruker 400 MHz Avance III HD. $CDCl_3$ was used as a solvent.

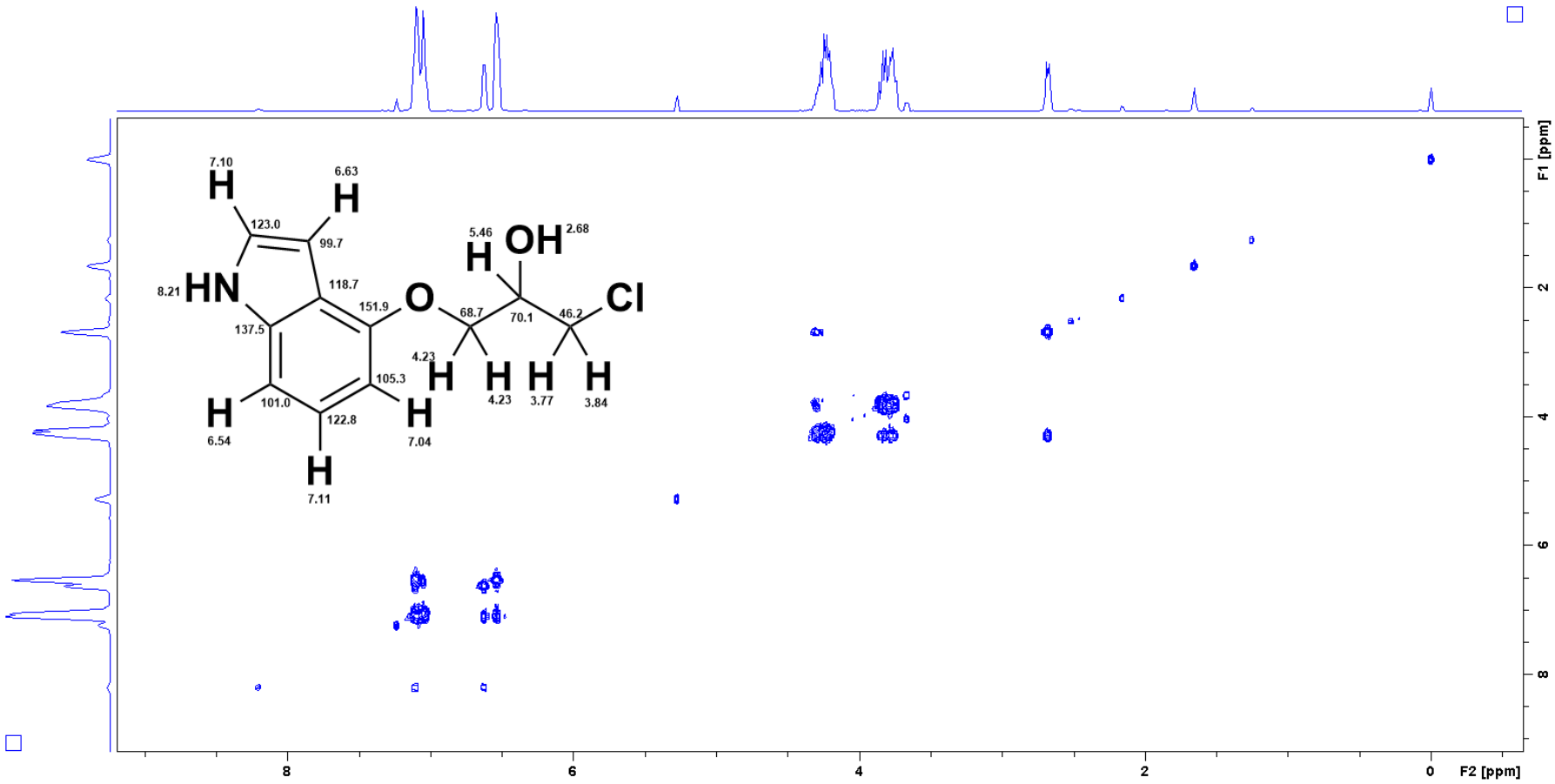

Figure 15: COSY-NMR spectrum of **2** using a Bruker 400 MHz Avance III HD. $CDCl_3$ was used as a solvent.

2.5.2 Characterization of 1-((1H-indol-4-yl)oxy)-3-chloropropan-2-yl butyrate (4)

Characterization of **4** was done using ^{1}H, ^{13}C, COSY, HMBC and HSQC NMR with $CDCl_3$ as solvent. Figure 17 shows **4** with positions numbered and table 4 shows the NMR shifts and correlations for the NMR characterization. Spectra for ^{1}H, ^{13}C and HSQC can be seen in Appendix 6.2, as Figure 28, 29 and 30 while COSY and HMBC can be seen as Figure 18 and 19 in this section.

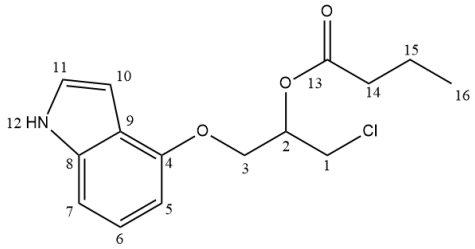

Figure 17: The structure of **4** with the protons numbered corresponding to the values in Table 4

Table 4: NMR shifts and correlations for ^{1}H, ^{13}C, COSY and HMBC NMR on compound **4**. Spectra for ^{1}H, ^{13}C and HSQC can be seen in Appendix 6.2, as Figure 28, 29 and 30 while COSY and HMBC can be seen as Figure 18 and 19 in this section.

Position	**^{1}H [ppm] (mult., int.,^{n}J [Hz])**	**^{13}C [ppm]**	**COSY [ppm]**	**HMBC [ppm]**
1	3.86 (dd, 1H, J=5.75) 3.93 (dd, 1H, J=5.51)	42.93	5.46	66.28
2	5.46 (quintet, 1H, J=10.36)	71.03	3.86, 3.93, 4.32	42.93, 66.28
3	4.32 (d, 2H, J=5.32)	66.28	5.46	42.93, 71.03
4	-	151.91	-	-
5	7.05 (m, 1H)	105.15	7.09	100.86, 118.80
6	7.09 (t, 1H, 2.28)	122.72	6.54, 7.05	100.91, 118.80, 137.37, 151.91
7	6.54 (d, 1H, J=7.48)	100.91	7.09	99.83, 105.15, 118.80, 151.91
8	-	137.37	-	-
9	-	118.80	-	-
10	6.61 (s, 1H)	99.83	6.61	118.80, 122.72, 137.37
11	7.12 (m, 1H)	122.86	6.61	99.83, 105.15, 137.37, 151.91
12	8.21 (s, 1H)	-	-	-
13	-	172.97	-	-
14	2.37 (m, 2H)	36.14	18.45	13.61, 18.45
15	1.69 (m, 2H)	18.45	13.61, 36.14	13.61, 36.14
16	0.97 (m, 3H)	13.61	18.45	18.45, 36.14

The ^{1}H spectrum (Figure 28) shows litte impurities. The only significant impurity

is the residual peak of $CDCl_3$ at 7.27. The neighbouring environments of the positions were determined through COSY and HMBC spectra (Figure 18 and 19) and the proton-carbon shifts were determined through HSQC (Figure 30). The peaks correspond with those found by *Zielinska-Pisklak et al* [64].

The spectra in Figure 18 and 19 shown on the next page are the COSY and HMBC spectra were used to characterize compound **4**.

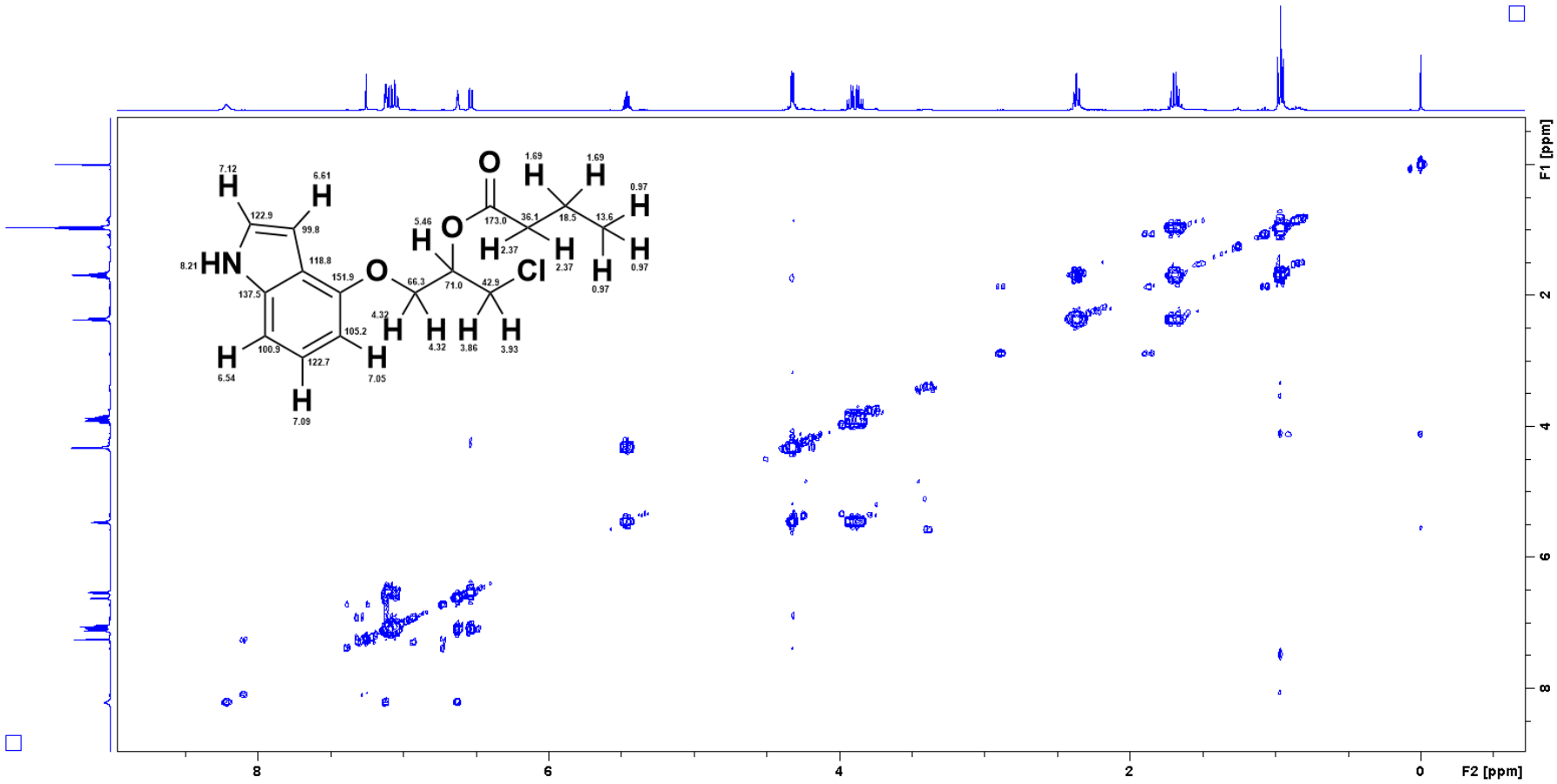

Figure 18: COSY-NMR spectrum of **4** using a Bruker 400 MHz Avance III HD. $CDCl_3$ was used as a solvent.

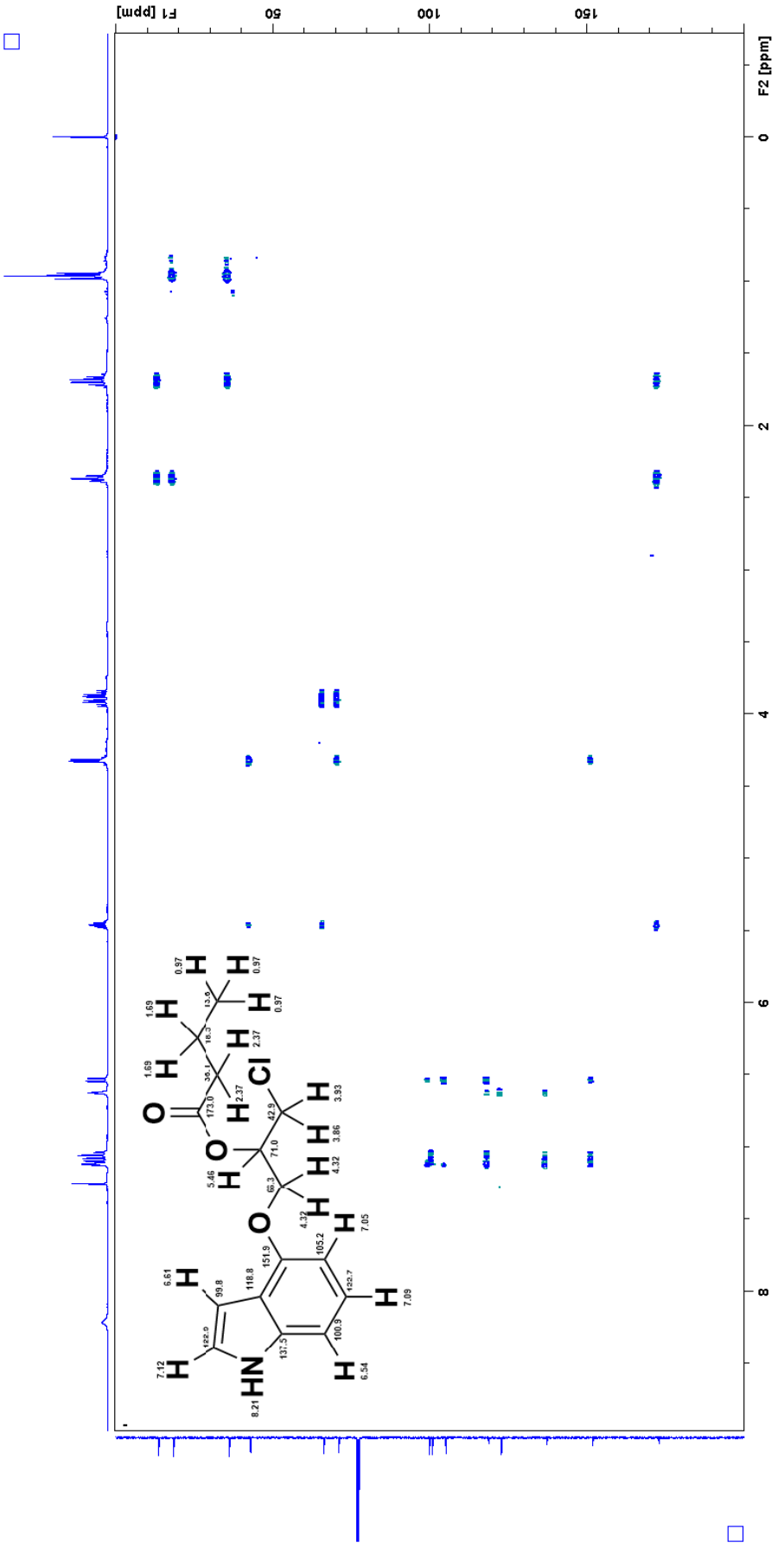

Figure 19: HMBC-NMR spectrum of **4** using a Bruker 400 MHz Avance III HD. $CDCl_3$ was used as a solvent.

2.5.3 Characterization of (*S*)-pindolol ((S)-5)

Characterization of **5** was done by ^{1}H, ^{13}C, COSY, HMBC and HSQC NMR with $CDCl_3$ as solvent, both with and without a few drops of deuterium oxide added to $CDCl_3$. The only purification performed was removing the solvent under reduced pressure. Figure 20 shows **5** with positions numbered and table 5 shows the NMR shifts and correlations for the NMR characterization. Spectra for ^{13}C and HSQC without use of deuterium oxide can be seen in Appendix 6.3, as Figure 31 and 32 while ^{1}H, COSY and HMBC can be seen as Figure 21, 23 and 24 in this section. Spectra for ^{13}C, HSQC, HMBC and COSY with the use of a few drops of deuterium oxide added to $CDCl_3$ can also be seen in Appendix 6.3 as Figure 33, 34, 35 and 36. The ^{1}H spectrum with deuterium oxide can be seen in this section as Figure 22.

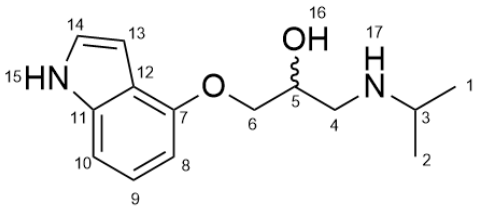

Figure 20: The structure of **5** with the protons numbered corresponding to the values in Table 5

Table 5: NMR shifts and correlations for ^{1}H, ^{13}C, COSY and HMBC NMR on compound **5**. ^{13}C and HSQC can be seen in Appendix 6.3, as Figure 31 and 32 while ^{1}H-NMR, COSY and HMBC can be seen as Figure 21, 23 and 24 in this section. The parenthesis's are uncertain values due to non-conclusive results.

Position	**^{1}H [ppm] (mult., int., ^{n}J [Hz])**	**^{13}C [ppm]**	**COSY [ppm]**	**HMBC [ppm]**
1, 2	1.16 (d, 6H, *J*=6.24)	22.35 (2C)	2.91	49.3
3	2.94 (m, 1H)	49.32	1.16	22.3, (49.1)
4	2.89 (m, 1H) 3.00 (m, 1H)	49.19	2.89, 3.00, 4.14	(49.3), 68.1, 70.6
5	4.22 (m, 1H)	68.12	2.89, 3.00, 4.14	49.1, 70.6, (152.3)
6	4.14 (m, 2H)	70.55	4.22	49.1, 68.1, (152.3)
7	-	152.26	-	-
8	6.52 (d, 1H, *J*=7.48)	100.81	7.08	104.9, 118.7, 152.3
9	7.08 (t, 1H, *J*=7.64)	122.73	6.52	100.8, (118.7), 137.4, 152.3
10	7.03 (d, 1H, *J*=8.12)	104.87	(6.52)	100.8, 118.7
11	-	137.35	-	-
12	-	118.71	-	-
13	6.64 (d, 1H, *J*=2.96)	99.77	7.12, (8.39)	(118.7), 122.8, (137.4)
14	7.12 (d, 1H, *J*=3.72)	122.81	6.64, (8.39)	(99.8), (118,7), 137.4, (152.3)
15	8.39 (d, 1H)	-	6.64, 7.12	-
16	(1.95) (d, 1H)	-	(4.22)	-
17	(1.25) (d, 1H)	-	-	-

The ^{1}H spectrum is Figure 21. This spectrum was diffiult to integrate in a way that accounted for all the protons, most likely due to the broad singlet peak at 3.1 ppm and impurities stacking with the product at 1.16. In order to removed the acetic protons, a few drops of deuterium oxide was added to $CDCl_3$ for deuterium to replace the hydrogen responsible for these impurities. This this ^{1}H spectrum is seen in Figure 22.

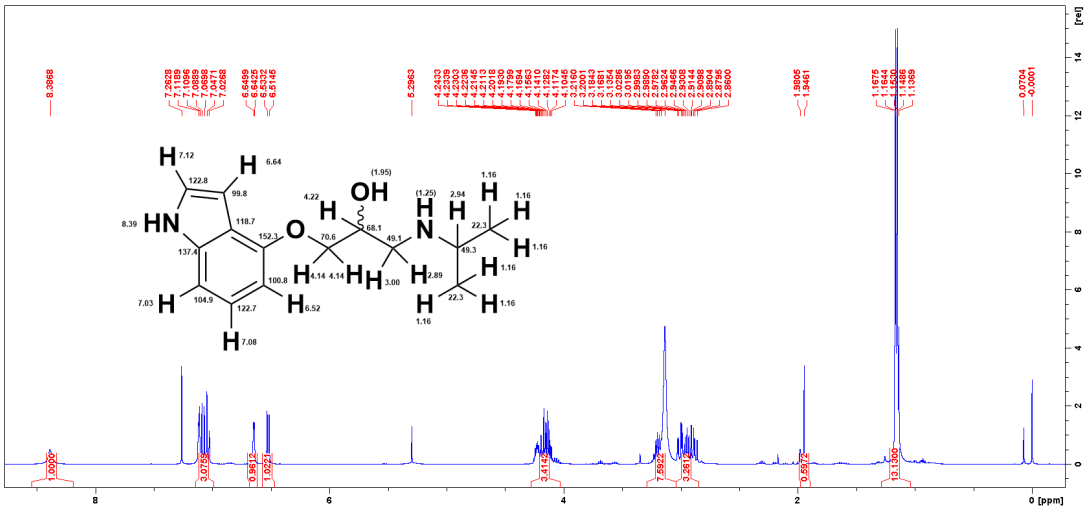

Figure 21: The ^{1}H-NMR spectrum of **5** using a Bruker 400 MHz Avance III HD. $CDCl_3$ was used as a solvent.

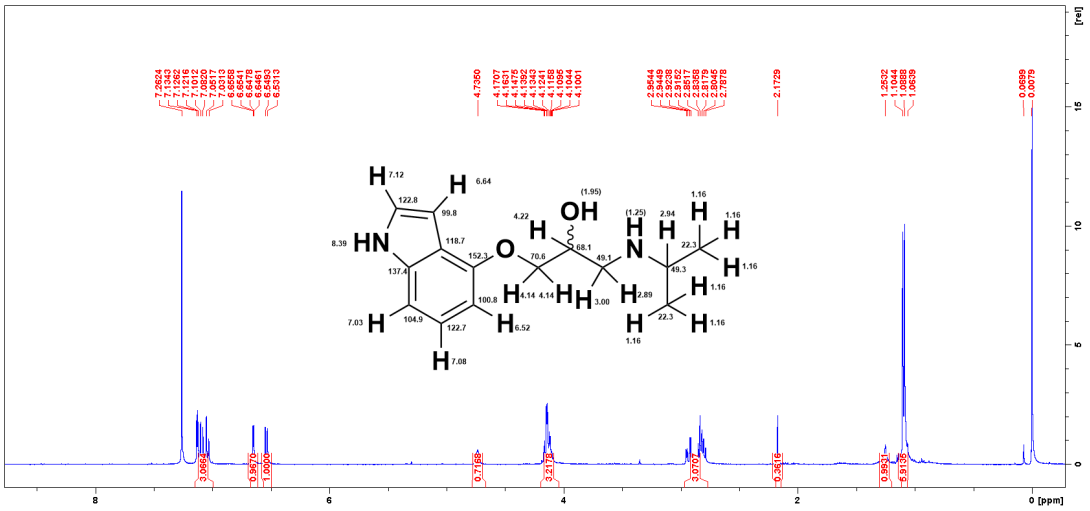

Figure 22: The ^{1}H-NMR spectrum of **5** using a Bruker 400 MHz Avance III HD. $CDCl_3$ was used as a solvent with a few drops of deuterium oxide.

The addition of a few drops of deuterium oxide to $CDCl_3$ removed the broad peak at 3.14 as well as reducing the area of the peak at 1.16. This lead to easier determination the protons in (*S*)-pindolol ((S)-**5**) , except the protons in the amine groups and the alcohol group that has been replaced by deuterium. Ideally the 3D spectra from the

sample with deuterium oxide should have been used to characterize (*S*)-pindolol ((S)-**5**) further, but as can be seen from the C^{13} spectrum in Figure 33, the peaks are so small that only 11 of the 14 carbons were detected. As a result, the spectra made from the sample without deuterium oxide was used to characterize (*S*)-pindolol ((S)-**5**), with the help of the spectra from the sample with deuterium oxide where it could be used. This was not ideal since the spectra from the sample with deuterium oxide had impurities.

The impurities of the sample without a few drops of deuterium oxide will be discussed first. The most expected impurity was isopropylamine used in the reaction to synthesis (*S*)-pindolol ((S)-**5**). Isopropylamine has expected peaks at 1.07 (CH3), 1.22 (NH) and 3.10 (CH) [65]. The peak at 1.16 that had a too large area possibly includes the CH_3 and NH peaks. On the left side of the broad peak at 3.14 it is possible to see a multiplet at around 3.2 ppm, which is possibly the CH in isopropylamine. There are also smaller impurities at 7.27, 5.30, and 0.07. The peaks at 7.27 and 5.30 have already been discussed and are most likely the residual peak of $CDCl_3$ and dichloromethane [58]. The peak at 0.07 is most likely silicone grease [58]. The broad peak at 3.14 might be there because of chemical exchange, which is one possible reason for the broadening. One proton might exchange with another population of protons, for example from the isopropylamine, alcohol groups and amine groups. The integrated area could therefore represent the total, or part of, the population of acetic protons that is exchanging. This will in turn lead to difficulty finding the protons of the alcohol in position 16 and the protons of the amine in position 17 in figure 20. Even so, they were both given shifts at 1.25 (NH) and 1.95 (OH). The reason for this is that the in the ^1H spectrum with deuterium oxide there is a singlet at 1.25. Even though the expected value of the amine is at 5.52 (The expected value from ChemDraw Professional 16.0), the addition of deuterium oxide might have changed the shift. The integral fits and if compared with isopropylamine the shift is correct. A strong argument against this is that the deuterium oxide would most likely remove the peak. The reason for determining the OH group at 1.95, even though the expected value is different (5.37 is the expected value from ChemDraw Professional 16.0) is because of the COSY spectrum in Figure 23 showing a correlation to the proton with a shift of 4.22, in other words the proton on the same carbon as the OH group. The ^{13}C spectrum showed impurities at 22.81, 24.64 and 43.20. The peaks at 24.64 and 43.20 corresponds to the expected peaks of isopropylamine [66]. The peak at 22.81 is insignificant and it has not been characterized.

For the spectrum with a few drops of deuterium oxide added to $CDCl_3$ there are some additional peaks. The first one is at 1.25 and has already been discussed as potentially being the amine on position 17. The peak at 1.95 is removed which is expected if the peak is the OH on position 16. There are new peaks at 2.17 and 4.73 while the dichloromethane

and the amine peak of the proton in position 15 is removed as well as the broad peak at 3.14 and the multiplet at around 3.2. The impurity at 2.17 is acetone while the signal at 4.73 is the residual peak of deuterium oxide [58]. The broad peak at 3.14 most likely consisted of OH or NH groups that were replaced with OD or ND and are therefore no longer in the spectrum. The only impurity that has not been discussed is the impurity overlapping the product at 1.16. This is expected to be from the CH_3 groups of isopropylamine and the protons should not interchange with deuterium. The reason for the removal of this impurity is most likely that it was dissolved in the deuterium oxide instead of the $CDCl_3$. This can also explain why some of the other peaks were removed with the addition of deuterium oxide. There are no visible impurities in the ^{13}C spectrum, but that can be because many of the carbons are not visible.

The neighbouring environments of the carbons were determined through COSY and HMBC spectra (Figure 23 and 24) and the proton-carbon shifts were determined through HSQC (Figure 32). Comparing the shifts from ChemDraw Professional 16.0 with the shift found in this thesis they are very similar. The shifts of the alcohol group and amine groups do not fit, but have already been discussed.

The spectra shown on the next page in Figure 23 and 24 are the COSY and HMBC spectra were used to characterize compound **5**.

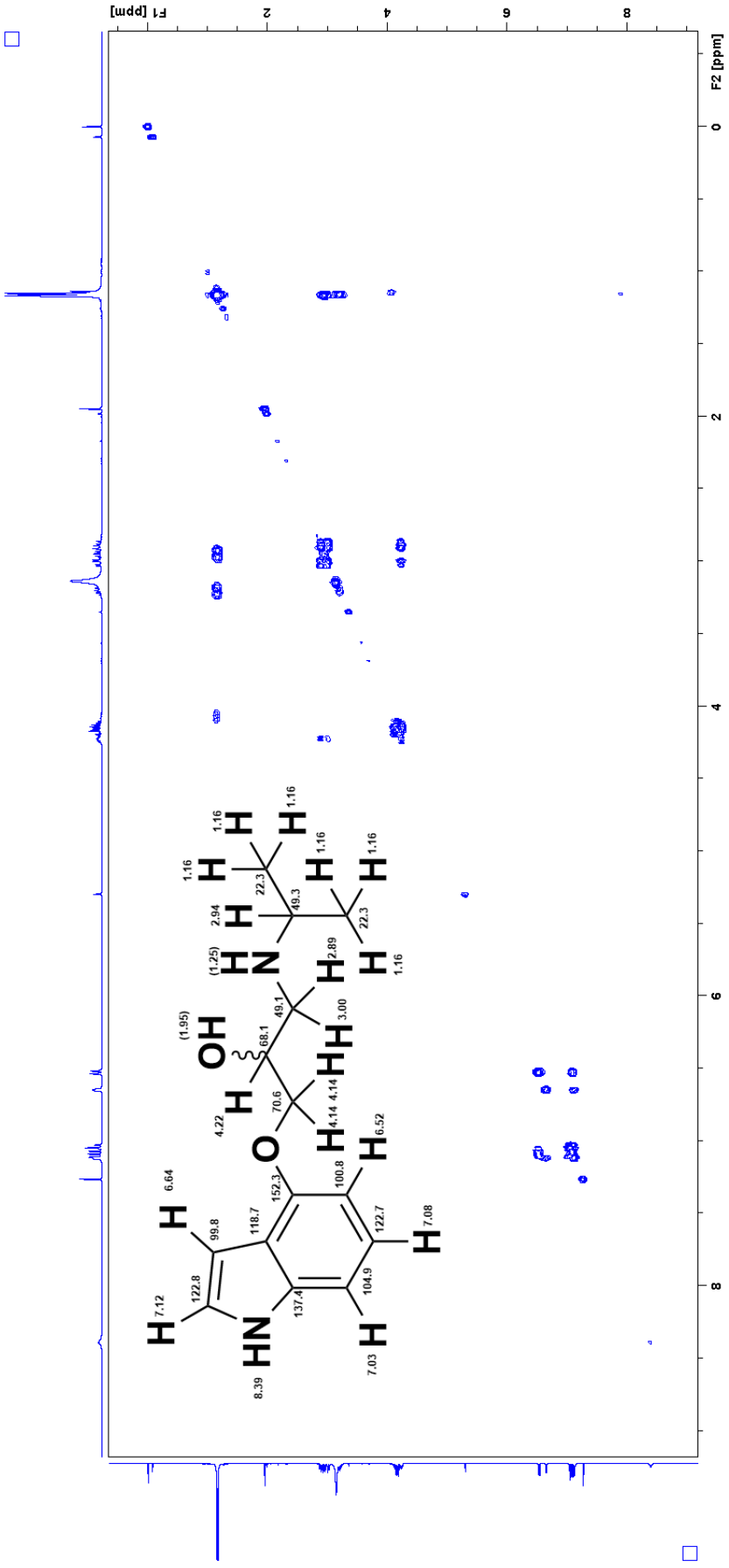

Figure 23: COSY-NMR spectrum of (*S*)-**5** using a Bruker 400 MHz Avance III HD. $CDCl_3$ was used as a solvent.

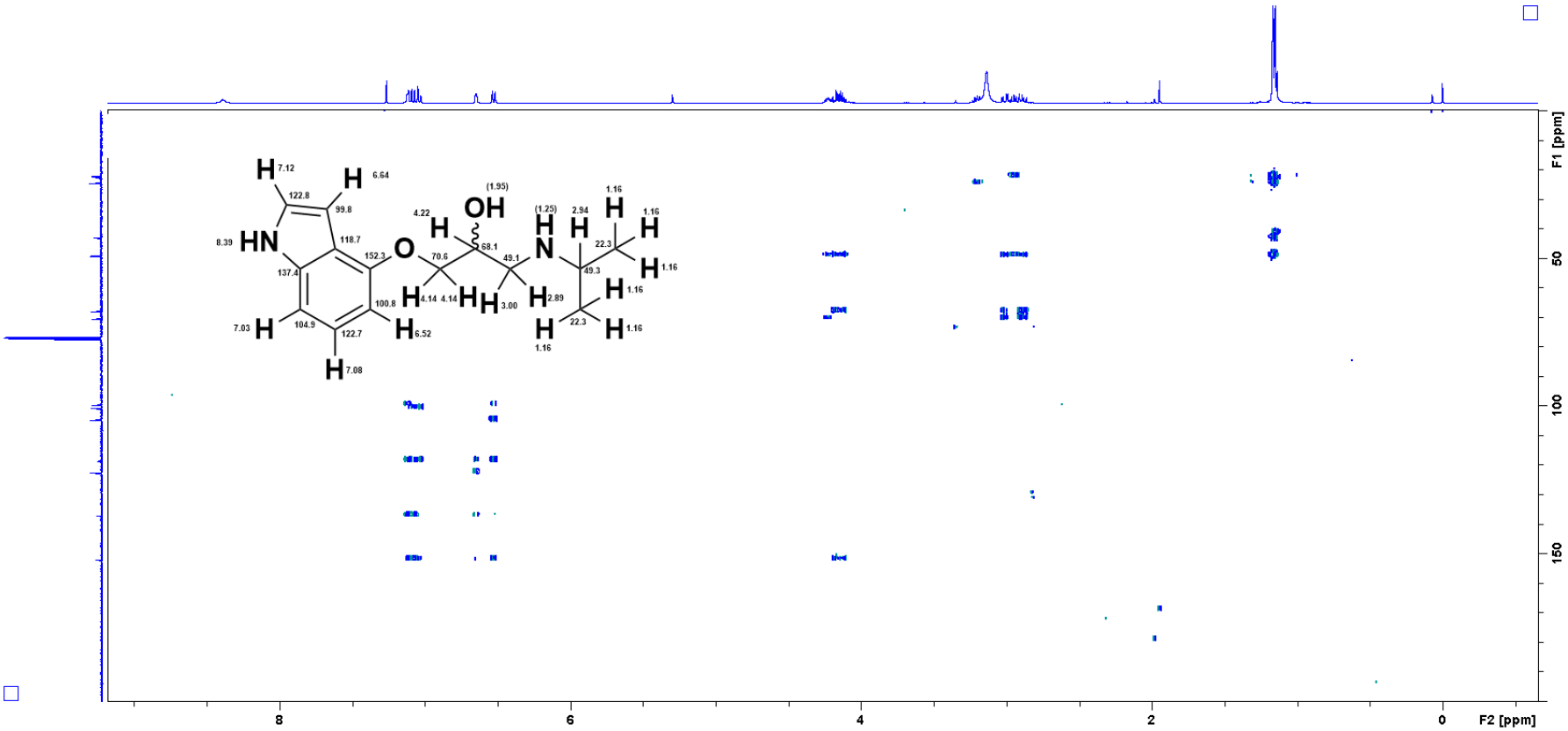

Figure 24: HMBC-NMR spectrum of (*S*)-**5** using a Bruker 400 MHz Avance III HD. $CDCl_3$ was used as a solvent.

3 Experimental section

3.1 Important reagents

3.1.1 1H-Indol-4-ol (1) as starting material

The starting material 1H-indol-4-ol (**1**) as well as all other solvents and chemicals were bought at Sigma-Aldrich-Merck group (Oslo, Norway) for the use in this project. Dry dichloromethane was stored in flasks containing molecular sieves. It was acquired from a solvent purifier, MBraun MB-SPS-800, München, Germany. Additional solvents were stored in flasks containing molecular sieves (4Å).

The enzyme used was *Candida antarctica* Lipase B (CALB) (activity 10000 PLU/g, lot20170315) as a catalyst and it was immobilized on high hydrophobic macroporous resin, produced in fermentation with genetically modified *Pichia pastoris*. It was a gift from SyncoZymes Co, Ltd. (Shanghai, China).

The molecular sieves used were 4 Å and activated at 1000 °C for 24 hours.

3.2 Chromatography

3.2.1 TLC

In TLC analyses Merck silica 60 F254 plates were used and UV at $\lambda = 254$ nm was used for detection.

3.2.2 Flash chromatography

The flash chromatography was performed with silica gel (pore size 60 Å, 200-400 mesh particle size). CH_2Cl_2 was used as eluent and the size of the columns varied.

3.2.3 HPLC

The chiral HPLC apparatus used was an Agilent HPLC 1100 system. It had a manual injector (Rheodyne 77245i/Agilent 10 μL loop) and the wavelength detector was set to 254 nm. The column was a Chrialcel OD-H columm (Diacel, Chiral Technologies Europe, 250 mm $\times$ 4.6 mm ID, 5 μm particle size). The methods used for separation was either 20%isopropan/80%n-n-hexane; 1mL/min, 10 μL injections when 1-((1H-indol-4-yl)oxy)-3-chloropropan-2-ol (**2**) was present or 10%isopropan/90%n-n-hexane; 1mL/min, 10 μL when only 1-((1H-indol-4-yl)oxy)-3-chloropropan-2-yl butyrate (**4**) was analyzed.

3.2.4 GC

The GC apparatus used was a Agilent 7890B with FID detector. The column used a CP-Chirasil-Dex CB stationary phase consisting of cyclodextrin directly bonded to dimethylpolysiloxane. The carrying gas was Helium and the samples were dissolved in EtAc. The colum had a flow of 2 mL/min, an injection volume of 1 μL and the split ratio was 30:1. The FID temperature was 250 °C and the injector temperature was 220 °C.

3.3 Polarimeter

The polarimeter used was Anton Paar MCP 5100 system with a MCP Software 4.00. The wavelength measured was 579 nm, the sample cell was 1.0 mL, 50 mm path length and 5 mm internal diameter with Cat.- No. of 104133. The samples were dissolved in methanol at RT.

3.4 NMR

The NMR analyses were done using a Bruker 400 MHz Avance III HD (Bruker, Rheinstetten, Germany), equipped with SampleCase and a 5-mm SmartProbe z-gradient probe.

3.5 Software

All molecular structures were drawn using ChemDraw Proffessional 16.0 whoch was also used to find molecular weight of some compounds. Culculations of E-values were performed using E&K calculator 2.1b0 PCC [67]. All NMR spectra were processed using Bruker's TopSpin^{TM}.

3.6 Synthesis

The sythesis in 3.6.1, 3.6.2 and 3.6.4 were performed as described by Løvland [57], 3.6.3 was performed as described by Jacobsen [68] and 3.6.5 was performed as described by Lund [62].

3.6.1 Synthesis of 1-((1H-Indol-4-yl)oxy)-3-chloropropan-2-ol (2) from 1H-indol-4-ol (1).

1H-Indol-4-ol (**1**) (3.00 g, 22.56 mmol) was dissolved in 1,4-dioxane (18 mL), it was mixed with NaOH (0.98 g, 24.50 mmol) dissolved in H_2O (10 mL) and (±)-epichlorohydrin (18 mL, 229.80 mmol) was added. The mixture was stirred at room temperature until 1H-Indol-4-ol (**1**) (CH_2Cl_2, R_f=0.20) was no longer observed in TLC (6.5 hours). The mixture was extracted with CH_2Cl_2 (250 mL) and washed with EtOAc (150 mL*3) and H_2O (150 mL*3). The organic phase was dried over anhydrous $MgSO_4$ and the solvent was removed under reduced pressure. This yielded a mixture of 4-(oxiran-2-ylmethoxy)-1H-indole (**3**) and 1-((1H-indol-4-yl)oxy)-3-chloropropan-2-ol (**2**). Spectroscopic data for the product **2**: ^{1}-H NMR (400 MHz, $CDCl_3$), δ_H: 2.68 (d, 1H, J=5.76, OH), 3.77 (dd, 1H, J=5.40, CH_2), 3.84 (dd, 1H, J=5.58, CH_2), 4.23 (m, 1H, CH), 4.29 (m, 2H, CH_2), 6.54 (d, 1H, J=7.56, =CH), 6.63 (s, 1H, =CH), 7.04 (d, 1H, J=8.12, =CH), 7.10 (m, 1H, N-CH=), 7.11 (m, 1H, =CH), 8.20 (s, 1H, =NH). ^{1}3C NMR (400 MHz, $CDCl_3$), δ_C: 46.20 (CH_2), 68.66 (CH_2), 70.07 (HO-CH), 99.65 (=CH), 101.02 (=CH), 105.25 (=CH), 118.68 (=C=), 122.76 (=CH), 123.02 (N-CH=), 137.39 (=C=), 151.86 (=C=). See Table 3 (Page 29).

3.6.2 Opening of epoxide part of 4-(oxiran-2-ylmethoxy)-1H-indole (3) forming 1-((1H-indol-4-yl)oxy)-3-chloropropan-2-ol (2).

The product mixture described in 3.6.1 (4.62 g) was dissolved in a mixture of AcOH (14 mL, 244.55 mmol) and THF (77.5 mL) and LiCl (2.11 g, 49.77 mmol) was added. The mixture was stirred for 70 h and the pH was adjusted to 7 by adding $NaCO_3$. The mixture was extracted with CH_2Cl_2 (250 mL) and washed with brine (130 mL*3). The organic phase was dried over anhydrous $MgSO_4$ and the solvent was removed under reduced pressure. This mixture was purified by flash chromatography using CH_2Cl_2 as eluent. This yielded 1-((1H-indol-4-yl)oxy)-3-chloropropan-2-ol (**2**) (3.87 g, 17.15 mmol). Spectroscopic data for the product **2**: ^{1}-H NMR (400 MHz, $CDCl_3$), δ_H: 2.68 (d, 1H, J=5.76, OH), 3.77 (dd, 1H, J=5.40, CH_2), 3.84 (dd, 1H, J=5.58, CH_2), 4.23 (m, 1H, CH), 4.29 (m, 2H, CH_2), 6.54 (d, 1H, J=7.56, =CH), 6.63 (s, 1H, =CH), 7.04 (d, 1H, J=8.12, =CH), 7.10 (m, 1H, N-CH=), 7.11 (m, 1H, =CH), 8.20 (s, 1H, =NH). ^{1}3C NMR

(400 MHz, $CDCl_3$), δ_C: 46.20 (CH_2), 68.66 (CH_2), 70.07 (HO-CH), 99.65 (=CH), 101.02 (=CH), 105.25 (=CH), 118.68 (=C=), 122.76 (=CH), 123.02 (N-CH=), 137.39 (=C=), 151.86 (=C=). See Table 3 (Page 29).

HPLC analysis of **2** was performed (t_R for (*S*)-**2** was 8.0 min, t_R for (*R*)-**2** was 14.5 min, n-hexane:isopropanol (70:30), 1 mL/min flow). See appendix (Figure 47, page XXX).

3.6.3 Synthesis of the ester 1-((1H-indol-4-yl)oxy)-3-chloropropan-2-yl butyrate (4) from 1-((1H-indol-4-yl)oxy)-3-chloropropan-2-ol (2).

1-((1H-Indol-4-yl)oxy)-3-chloropropan-2-ol (**2**) (0.52 g, 2.30 mmol), butyric anhydride (0.51 g, 3.22 mmol), DMAP (4-Dimethylaminopyridine) (0.25 g, 2.04 mmol) and pyridine (0.42 g, 5.31 mmol) was added to CH_2Cl_2 (16 mL). The mixture was stirred for 50 h, at RT. The mixture was extracted with CH_2Cl_2 (100 mL) and washed with brine (60 mL*3). The organic phase was dried over anhydrous $MgSO_4$ and the solvent was removed under reduced pressure. After flash chromatography using CH_2Cl_2 as eluent, it yielded 1-((1H-indol-4-yl)oxy)-3-chloropropan-2-yl butyrate (**4**) (0.79 g, 2.68 mmol). Spectroscopic data for the product **4**: ^{1}-H NMR (400 MHz, $CDCl_3$), δ_H: 0.97(m, 3H, CH_3), 1.69(m, 2H, CH_2), 2.36(m, 2H, CH_2),3.84 (dd, 1H, *J*=5.75, CH_2), 3.91 (dd, 1H, *J*=5.51, CH_2), 4.31 (d, 2H, *J*=5.32, CH_2), 5.45 (quintet, 2H, *J*=10.36, =C-O), 6.52 (d, 1H, *J*=7.48, =CH), 6.61 (s, 1H, =CH), 7.02 (d, 1H, *J*=8.12, =CH), 7.07 (m, 1H, =CH), 7.09 (m, 1H, N-CH=), 8.62 (s, 1H, =NH). ^{1}3C NMR (400 MHz, $CDCl_3$), δ_C: 13.61 (CH_3), 18.34 (CH_2), 36.14 (CH_2), 42.92 (CH_2), 66.634 (CH_2), 71.10 (O-CH), 99.62 (=CH), 100.86 (=CH), 105.28 (=CH), 118.80 (=C=), 122.59 (=CH), 123.01 (N-CH=), 137.47 (=C=), 151.90 (=C=), 173.04 (C=O). See Table 4 (Page 33).

HPLC analysis of **4** was performed (t_R for (*S*)-**4** was 35.6 min, t_R for (*R*)-**4** was 33.2 min, n-hexane:isopropanol (90:10), 1 mL/min flow). See appendix (Figure 46, page XIX) .

3.6.4 Kinetic resolution of 1-((1H-indol-4-yl)oxy)-3-chloropropan-2-ol (2).

1-Chloro-3-(1H-indol-4-yloxy)-propan-2-ol (1.01 g, 4.46 mmol) was dissolved in CH_2Cl_2 (185 mL) and lumps (100 lumps) of molecular sieves were added. Vinyl butyrate (3.75 mL, 29.54 mmol) and immobilized CALB (1.01 g) was added. The mixture added to a reaction tube and placed in a orbital shaker at 30°C and 200 rpm. Samples (150 μL) were collected regularly for HPLC analysis. The batch reaction yielded 1.6220 g after removing the solvent under reduced pressure. This was purified by flash using CH_2Cl_2 as eluent yielding 0.2832 g (1.25 mmol) (*S*)-**2** and 0.2163 g (0.73 mmol) (*R*)-**4**. This gives

a yield of 28.03 % for (*S*)-**2** and a combined yield of 44.39 % for both (*S*)-**2** and (*R*)-**4**. The ee_s was 96 %, the ee_p was 99 % and the E-value was 46. The specific rotation of ((*R*)-**2**) was $[\alpha_{379}^{20}]$=-10.4° (MeOH, c=1.00g/100cm^3) and $[\alpha_{379}^{20}]$= 5.8° for ((*R*)-**4**) (MeOH, c=1.00g/100cm^3). Spectroscopic data for the product **2**: ^{1}-H NMR (400 MHz, $CDCl_3$), δ_H: 2.68 (d, 1H, *J*=5.76, OH), 3.77 (dd, 1H, *J*=5.40, CH_2), 3.84 (dd, 1H, *J*=5.58, CH_2), 4.23 (m, 1H, CH), 4.29 (m, 2H, CH_2), 6.54 (d, 1H, *J*=7.56, =CH), 6.63 (s, 1H, =CH), 7.04 (d, 1H, *J*=8.12, =CH), 7.10 (m, 1H, N-CH=), 7.11 (m, 1H, =CH), 8.20 (s, 1H, =NH). ^{1}-H NMR (400 MHz, $CDCl_3$), δ_C: 46.20 (CH_2), 68.66 (CH_2), 70.07 (HO-CH), 99.65 (=CH), 101.02 (=CH), 105.25 (=CH), 118.68 (=C=), 122.76 (=CH), 123.02 (N-CH=), 137.39 (=C=), 151.86 (=C=). See Table 3. Spectroscopic data for the product **4**: ^{1}-H NMR (400 MHz, $CDCl_3$), δ_H: 0.97(m, 3H, CH_3), 1.69(m, 2H, CH_2), 2.36(m, 2H, CH_2),3.84 (dd, 1H, *J*=5.75, CH_2), 3.91 (dd, 1H, *J*=5.51, CH_2), 4.31 (d, 2H, *J*=5.32, CH_2), 5.45 (quintet, 2H, *J*=10.36, =C-O), 6.52 (d, 1H, *J*=7.48, =CH), 6.61 (s, 1H, =CH), 7.02 (d, 1H, *J*=8.12, =CH), 7.07 (m, 1H, =CH), 7.09 (m, 1H, N-CH=), 8.62 (s, 1H, =NH). ^{1}3C NMR (400 MHz, $CDCl_3$), δ_C: 13.61 (CH_3), 18.34 (CH_2), 36.14 (CH_2), 42.92 (CH_2), 66.634 (CH_2), 71.10 (O-CH), 99.62 (=CH), 100.86 (=CH), 105.28 (=CH), 118.80 (=C=), 122.59 (=CH), 123.01 (N-CH=), 137.47 (=C=), 151.90 (=C=), 173.04 (C=O). See Table 4 (page 33).

HPLC analysis of the mixture was performed (t_R for (*R*)-**4** was 14.2 min, t_R for (*S*)-**4** was 15.0 min, t_R for (*S*)-**2** was 22.6 min, t_R for (*R*)-**2** was 51.9 min, n-hexane:isopropanol (80:20), 1 mL/min flow)). See appendix (40). HPLC analysis of the mixture with only (**4**) in the chromatogram was performed ((t_R for (*R*)-**4** was 34.0 min, t_R for (*S*)-**4** was 36.3 min, n-hexane:isopropanol (90:10), 1 mL/min flow). See appendix (Figure 46, page XIX).

3.6.5 Addition of isopropylamine to synthesize (*S*)-pindolol (*S*)-5 from (*R*)-1-((1H-indol-4-yl)oxy)-3-chloropropan-2-ol ((*R*)-2).

(*R*)-1-((1H-indol-4-yl)oxy)-3-chloropropan-2-ol ((*R*)-**2**) (0.0168 g, 0.0744 mmol) was mixed with water (0.600 mL) and isopropylamine (2.000 mL). The mixture was stired for 24 hours. This yielded (*S*)-pindolol ((S)-**5**) (0.0195 g) with some impurities and therefore the % yield and mmol is not stated. Spectroscopic data for the product **5**:^{1}-H NMR (400 MHz, $CDCl_3$), δ_H: 1.16(d, 6H, *J*=6.24, $2CH_3$), 1.25(s, 1H, OH), 1.95(s, H, , =NH), 2.89(m, 1H, CH_2), 2.94(m, 1H, CH), 3.00 (m, 1H, CH_2), 4.14 (m, 2H, CH_2), 4.22 (m, 1H0, CH), 6.52 (d, 1H, *J*=7.48, =CH), 6.64 (d, 1H, *J*=2.96, =CH), 7.03 (d, 1H, *J*=8.12, =CH), 7.08 (t, 1H, *J*=7.64, =CH), 7.12 (d, 1H, *J*=3.72, =CH), 8.39 (s, 1H, =NH). ^{1}3C NMR (400 MHz, $CDCl_3$), δ_C: 22.35 ($2CH_3$), 49.19 (CH_2), 49.32 (CH), 68.12 (CH), 70.55 (CH_2), 99.77 (=CH), 100.81 (=CH), 104.87 (=CH), 118.71 (=C=), 122.73 (=CH), 122.81

(=CH), 137.35 (=CH=), 152.26 (=C=). See Table 5 (Page 37).

4 Conclusion

In this thesis compound (*S*)-**5** was synthesized by first synthesizing **2** and **3** from **1** in a two-step reaction. (*R*)-**2** and (*S*)-**4** was then synthesized from **2** using the enzyme CALB in a kinetic resolution. Finally, (*S*)-**5** was synthesized from (*R*)-**2**. To find ee_p, ee_s and the E-value, methods to separate the enantiomers of **2** and **4** were made. A full NMR characterization of compound **2**, **4** and **5** was also performed.

The two-step reaction to synthesize **2** had a yield of 76 %. Through comparison of earlier attempts of this synthesis it was concluded that a reaction time between 5 and 7 hours was ideal for the reaction shown in Scheme 12. This is to balance between having as much reaction time as possible without letting the epoxide (**3**) become too dominant. The purity of **2** was found by HPLC to be 96.2 %. Doing the flash column with a slow flowrate also increased the yield. The kinetic resolution of **2** yielded (*R*)-**2** and (*S*)-**4**. The ee_s of (*R*)-**2** was 96 % and the ee_p of (*S*)-**4** was 99 % while the E-value for the reaction was 46. After purification with flash column it yielded 0.2832 g of ((*R*)-**2**) and 0.2163 g of ((*S*)-**4**). This gives a yield of 28.03 % for (*R*)-**2** and a combined yield of 44.39 % for both (*S*)-**2** and (*R*)-**4**. Even though the values were calculated with a R_s og 1.08, they are a strong indicator of the enantioselectivity of CALB. The specific rotation of ((*R*)-**2**) was $[\alpha_{379}^{20}]$=-10.4° (MeOH, c=1.00g/100cm^3) and $[\alpha_{379}^{20}]$= 5.8° for ((*R*)-**4**) (MeOH, c=1.00g/100cm^3). The synthesis of (*S*)-**5** was performed with a yield of 106 %. Since there are impurities shown in NMR the yield can not be properly determined. In this thesis the reaction was first attempted with reflux, but TLC showed (*R*)-**2** left and therefore it was concluded that the reaction should be performed at RT. The small amount of starting material, 0.0168 g, lead to little purification which lead to difficulties in calculating yield and characterizing the compound. The synthesis to make racemic **4** for analysis of **4** was also performed. The synthesis of **4** worked as expected, yielding racemic **4**.

To analyze the enantiomers of **2** and **4**, HPLC was used. A method for separating (*R*)-**2** and (*S*)-**2** was made which separated the two enantiomers in a 18 min method with 5.5 min separating the peaks. Separating (*R*)-**4** and (*R*)-**4** proved difficult and many attempts were made. The best method gave a R_s of 1.08. This was an improvement from similar earlier work [57] with an R_s of 0.78. Due to not managing to separate the peaks, GC was also used to try to separate the enantiomers of **4**. After many methods being attempted, with as low temperature increase as 0.1 °C/min, there were no indications of separating the enantiomers and subsequently the results from HPLC were used. The ee_s and ee_p values were 96 % and 99 %, respectively, while the E-value was 46. The ee of compound (*R*)-**2** is 96 %, which is the limit for a drug to be considered enantiopure.

Even though the ee_p was improved it is important to note that the calculations were done without baseline separation of compound **4** and a R_s of 1.08.

5 Future work

To improve the separation of (*S*)-**4** and (*R*)-**4**, through either GC or HPLC, in order to improve baseline separation, several mobile phases should be tested. For HPLC, new mobile phases should be used since no combinations of n-hexane and 2-propanol gave baseline separation. For GC the results are so indecisive that it would be recommended to make a new temperature program from scratch.

References

[1] *FDA's policy statement for the development of new stereoisomeric drugs.* Chirality **1992**, *4*, 338.

[2] Anastas, P. T.; Warner, J. C. *Green Chemistry: Theory and Practice*, Oxford University Press, **1998**).

[3] Hughes, G.; Lewis, J.C. *Introduction: Biocatalysis in Industry.* Chem. Rev., **2018**, *118 (1)*, pp 1–3.

[4] Lin, G.-Q.; You, Q.-D.; Cheng, J.-F., Chiral *Drugs: Chemistry and Biological Action.* Wiley: Hoboken, J.N, **2011**, 323-347

[5] Kim JH.; Scialli AR, *Thalidomide: the tragedy of birth defects and the effective treatment of disease.*. Toxicol Sci. **2012**, *125(2)*, 613.

[6] Blaschke, G.; Kraft, H. P.; Fickentscher, K.; Kohler, F., *Chromatographic separation of racemic thalidomide and teratogenic activity of its enantiomers (author's transl). Arzneimittel-Forschung* **1979**, *29 (10)*, 1640-2

[7] Teo, S.; Colburn, W.; Tracewell, W.; Kook, K.; Stirling, D.; Jaworsky, M.; Scheffler, M.; Thomas, S.; Laskin, O., *Clinical Pharmacokinetics of Thalidomide. Clin. Pharmacokin.* **2004**, *43 (5)*, 311-327.

[8] Echizen, H.; Manz, M.; Eichelbaum, M.*Electrophysiologic effects of dextro- and levo-Verapamil on sinus node and AV node function in humans.* J Cardiovasc Pharmacol. **1988**; *12(5)*:543-6.

[9] Satoh, K.; Yanagisawa, T.; Taira, N. *Coronary vasodilator and cardiac effects of optical isomers of Verapamil in the dog.* J Cardiovasc Pharmacol. **1980**; *2(3)*, 309-18.

[10] Nguyen, L.A.; He, H.; Pham-Huy, C., *Chiral Drugs: An Overview*Chiral Drugs: An Overview, **2006**, *2(2)*, 85–100.

[11] Wong, G. W.; Boyda, H. N.; Wright, J. M. *Blood pressure lowering efficacy of partial agonist beta blocker monotherapy for primary hypertension.* Cochrane Database Syst Rev. 11. **2014**

[12] Blier P, Bergeron R (1998). "The use of pindolol to potentiate antidepressant medication". J Clin Psychiatry. 59 Suppl 5: 16–23, discussion 24–5. PMID 9635544.

Celada P, Bortolozzi A, Artigas F (2013). "Serotonin 5-HT1A receptors as targets for agents to treat psychiatric disorders: rationale and current status of research". CNS Drugs. 27 (9): 703–16.

[13] Liu Y, Zhou X, Zhu D, Chen J, Qin B, Zhang Y, Wang X, Yang D, Meng H, Luo Q, Xie P. *Is pindolol augmentation effective in depressed patients resistant to selective serotonin reuptake inhibitors? A systematic review and meta-analysis.* Hum Psychopharmacol. **2015**, *30 (3)*: 132–42.

[14] Landau, E. R.; Achilladelis, B.; Scriabine, A. *Discovery and Development of Major Drugs. Chapter 2 in Pharmaceutical Innovation: Revolutionizing Human Health* . Chemical Heritage Foundation, **1999**.

[15] Golightly, L.K., *Pindolol: a review of its pharmacology, pharmacokinetics, clinical uses, and adverse effects.* Pharmacotherapy. , **1982**, *2*, 134-47.

[16] Koch-Weser, J.; Frishman, W. H., *Pindolol: A New β-Adrenoceptor Antagonist with Partial Agonist Activity.* N. Engl. J. Med. **1983**, *308 (16)*, 940-944.

[17] Gibson, A. J.; Raphael, A. B., *Understanding beta-blockers.* Nursing, **2014**, *44 (6)*, 55-59

[18] Anderson, J., *Beta-Blockers. Card. Electrophysiol.* Rev. **2000**, *4 (3)*, 301-308.

[19] Picture from `http://www.e-safe-anaesthesia.org/sessions/15_05/d/ELFH_Session/561/tab_788.html`

[20] Fox, S. I., *Human Physiology.* McGraw-Hill: New York, **2011**.

[21] Pasteur, L.C.R. *Mémoire de L. Pasteur sur la fermentation de l'acide tartrique.* Seances Acad. Sci **1958**, *46*, 615

[22] Gal, J., *The Discovery of Biological Enantioselectivity: Louis Pasteur and the Fermentation of Tartaric Acid, 1857—A Review and Analysis 150 Yr Later*, Chirality, **2008**, *20*, 5-19.

[23] Bommarius, A. S.; Riebel, B. R.,; `Biocatalysis`, Wiley-VCH: Weinheim, Germany, **2004**.

[24] Faber, K., *Biotransformations in Organic Chemistry: A Textbook.* Springer: Berlin, **2011**.

[25] Keith, J. M.; Larrow, J. F.; Jacobsen, E. N. *Practical Considerations in Kinetic Resolution Reactions". Adv. Synth. Catal.* **2001**, *343*: 5–26.

[26] Keith, J. M.; Larrow, J. F.; Jacobsen, E. N., *Practical Considerations in Kinetic Resolution Reactions*, Adv. Synth. Catal., **2001** *343*, 5–26.

[27] T. Anthonsen, *Basic Biotechnology - Synthesis of Chemicals using Enzymes*, , Cambridge University Press, **2001**.

[28] Melissa Hill, Laura Lan, Andrew Jilwan, *The "Ping-Pong" Mechanism*, LibreTexts, **2019**

[29] Anthonsen, T.; Jongejan,J. A., *Lipases Part B: Enzyme Characterization and Utilization*, Methods in Enzymology, Academic Press, **1997**, 473-495.

[30] H. W. Anthonsen, B. H. Ho, T. Anthonsen, *Tetrahedron: Asymmetry*, **1996**, *7*, 2633-2638.

[31] Reusch, W. *Resolution of Racemates*, IOCD, **2013**

[32] Monsan, P.; Combes, D., *Effect of Water Activity on Enzyme Action and Stability* , Ann. N. Y. Acad. Sci. **2006**, *434(1)*, 048 - 060

[33] Wescott,C. R.; Klibanov, A. M., *J. Am. Chem. Soc.*, **1993**, *115*, 1629-1631

[34] Laane, C.; Boeren, S.; Vos, K.; Veeger, C., *Biotechnol. Bioeng.*, **1987**, *30*, 81-87

[35] Krishna, S. H.; Persson, M.;Bornscheuer, U. T., *Tetrahedron: Asymmetry* **2002**, *13*, 2693-2696.

[36] Jacobsen, E. E.; Anthonsen, T., *Can. J. Chem.*, **2002**, *80*, 577-581

[37] Cong Li, H. Z.; Tan, T.; Feng, W., *J. Biol. Chem.*, **2010**, 28434-28441.

[38] Jacobsen,E. E.; Hoff, B. H.; Anthonsen, T., *Chirality*, **2000**, *12*, 654-659.

[39] Lima, G. V.; Da Silva, M. R.; de Sousa Fonseca, T.; de Lima, L. B.; de Oliveira, M.D. C. F.; de Lemos, T. L. G.; Zampieri, D.; Dos Santos, J. C. S.; Rios, N. S.; Gonçalves, L. R. B.; Molinari, F.; de Mattos, M. C., *Chemoenzymatic synthesis of (S)-Pindolol using lipases.* Appl. Catal. A, General **2017**, *546*, 7-14.

[40] Castro, A. M. d.; Carniel, A., *A novel process for poly(ethylene terephthalate) depolymerization via enzyme-catalyzed glycolysis.* Biochem. Eng. J. **2017**, *124*, 64-68.

[41] Sun, S.; Hu, B., *A novel method for the synthesis of glyceryl monocaffeate by the enzymatic transesterification and kinetic analysis.* Food Chem. **2017**, *214*, 192-198.

[42] Meyer, J.; Horst, A. E. W.; Steinhagen, M.; Holtmann, D.; Ansorge-Schumacher, M.B.; Kraume, M.; Drews, A., *A continuous single organic phase process for the lipase catalyzed synthesis of peroxy acids increases productivity.* Eng. Life Sci. **2017**, *17 (7)*, 759.

[43] Jaeger, K.E.; Reetz, M. T., *Microbial lipases form versatile tools for biotechnology.* Trends Biotechnol. **1998**, *16 (9)*, 396-403.

[44] Qian, Z.; Horton, J.R.; Cheng, X.;Lutz, S., *Structural redesign of lipase B from Candida antarctica by circular permutation and incremental truncation*, J. Mol. Biol., **2009**, *393(1)*, 191–201.

[45] Uppenberg, J.; Hansen, M. T.; Patkar, S.; Jones, T., *Structure*, **1994**, *2*, 293-308.

[46] Martinelle, M.; Holmquist, M.; Hult, K., *BBA - Lipid Lipid Met.* **1995**, *1258*, 272-276.

[47] Derawi, D. *Enzymatic glycerolysis of methyl laurate utilizing Candida antarctica lipase b*, Universiti Kebangsaan Malaysia, **2016**, *20*, 1366.

[48] Tipton, K., *Translocases (EC 7): A new EC Class.* Enzyme Nomenclature News, **2018**.

[49] Boyce, S; Tipton, F. K., *Enzyme Classification and Nomenclature*, Nature Encyclopedia of Life Sciences **2001**.

[50] Pandeeti Emmanuel VijayPaulVeeraiahSangeethaRouthu GyanaDeepika, *Chapter 9 - Emerging Trends in the Industrial Production of Chemical Products by Microorganisms*, Acedemic press, **2019**

[51] Barkovich, M., *High Performance Liquid Chromatography*, Chemistry Libretext, **2019**.

[52] Thet, K.; Woo, N., *Gas Chromatography*, CHEMISTRY LIBRETEXTS, **2019**.

[53] Grob, K, *Carrier Gases for GC.* Restek Advantage, Restek Corporation. **2016**.

[54] Austli, G. B. *Synthesis of Enantiopure -Blocker (S)-Practolol by Lipase Catalysis.* Master's Thesis, Norwegian University of Science and Technology, **2018**

[55] Bøckmann, P. *Synthesis of enantiopure -blocker (S)-metoprolol and derivatives by lipase catalysis.* Master's thesis, Norwegian University of Science and Technology, **2016**.

[56] Lund, I. T. *Mekanistiske studier i kjemo-enzymatisk syntese av enantiomert rene byggestener for betablokkeren Atenolol.* Master's thesis, Norwegian University of Science and Technology, **2015**, 58.

[57] Løvland, S. S. *Synthesis of building blocks for (S)-pindolol and vitamin K_2 by use of lipase catalysis* Master's Thesis, Norwegian University of Science and Technology, **2018**

[58] ¨ Gregory, R. F.; Alexander, J. M. M.; Nathaniel, H. S.; Hugo, E. G.; Abraham, N.; Brian, M. S.; John, E. B.; Karen, I. G., *NMR Chemical Shifts of Trace Impurities: Common Laboratory Solvents, Organics, and Gases in Deuterated Solvents Relevant to the Organometallic Chemist*, Organometallics **2010**, *29*, 2176–2179.

[59] *Compound Summary for CID 7798 Butyric Anhydride*, PubChem Open chemistry database, **2018**

[60] G. V. Lima *et al*, *Chemoenzymatic synthesis of (S)-Pindolol using lipases*, CATALYSIS, **2017**, *7-14*,

[61] Morante-Zarcero, S.; Sierra, I., *Simultaneous enantiomeric determination of propranolol, metoprolol, pindolol, and atenolol in natural waters by HPLC on newpolysaccharide-based stationary phase using a highly selective molecularly imprinted polymer extraction.* Chirality. **2012**, *24 (10)*, 860-866

[62] Lund, T.L.; *Mekanistiske studier i kjemi-enzymatisk syntese av enantiomert rene byggestener for betablokkeren Atenolol*, **2015**.

[63] *Pindolol*, Chemspider, Predicted data generated using the ACD/Labs Percepta Platform - PhysChem Module

[64] Zielinska-Pisklak, M.; Pisklak, D.; Wawer, I.; Zielinska-Pisklak, M., *1H and 13C NMR characteristics of Delta *b-blockers.* Magn. Reson. Chem. **2011**, *49 (5)*, 284-290.

[65] *Isopropylamine(75-31-0)1HNMR*, WinChembase, **2017**

[66] *Isopropylamine(75-31-0)13CNMR*, WinChembase, **2017**

[67] Anthonsen, H. W.; Hoff, B. H.; Anthonsen T. *Calculation of Enantiomer Ratio and Equilibrium Constants in Biocatalytic Ping-Pong Bi-Bi Resolutions.* Tetrahedron: Assymetry **1996**, *7 (9)*, 2633-2638

[68] Jacobsen; E.E. *Rasematoppløsning av derivater av 1,2-dioler katalysert av Candida antartica lipase B* Master's Thesis, Norwegian University of Science and Technology, **1999**, 116.

6 Appendix

6.1 NMR of 1-((1H-indol-4-yl)oxy)-3-chloropropan-2-ol (2)

6.1.1 ^{1}H-NMR spectrum for 1-((1H-indol-4-yl)oxy)-3-chloropropan-2-ol (2)

^{1}H-NMR spectrum of **2** showing its structure with corresponding shifts for ^{1}H and ^{13}C.

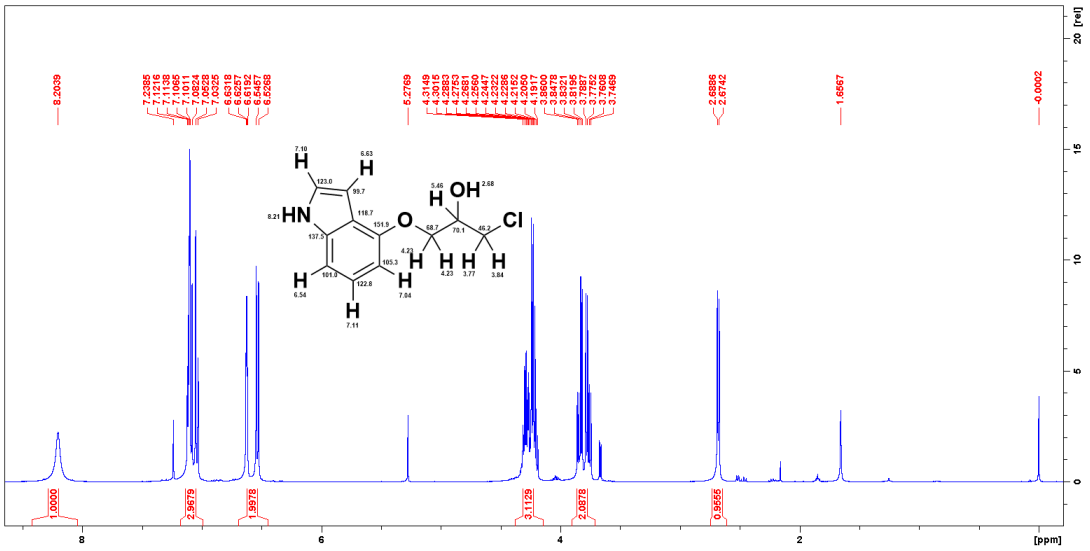

Figure 25: ^{1}H-NMR spectrum of 1-((1H-indol-4-yl)oxy)-3-chloropropan-2-ol (**2**) using a Bruker 400 MHz Avance III HD. $CDCl_3$ was used as a solvent.

6.1.2 ^{13}C-NMR spectrum for 1-((1H-indol-4-yl)oxy)-3-chloropropan-2-ol (2)

^{13}C-NMR spectrum of **2** showing its structure with corresponding shifts for ^{1}H and ^{13}C.

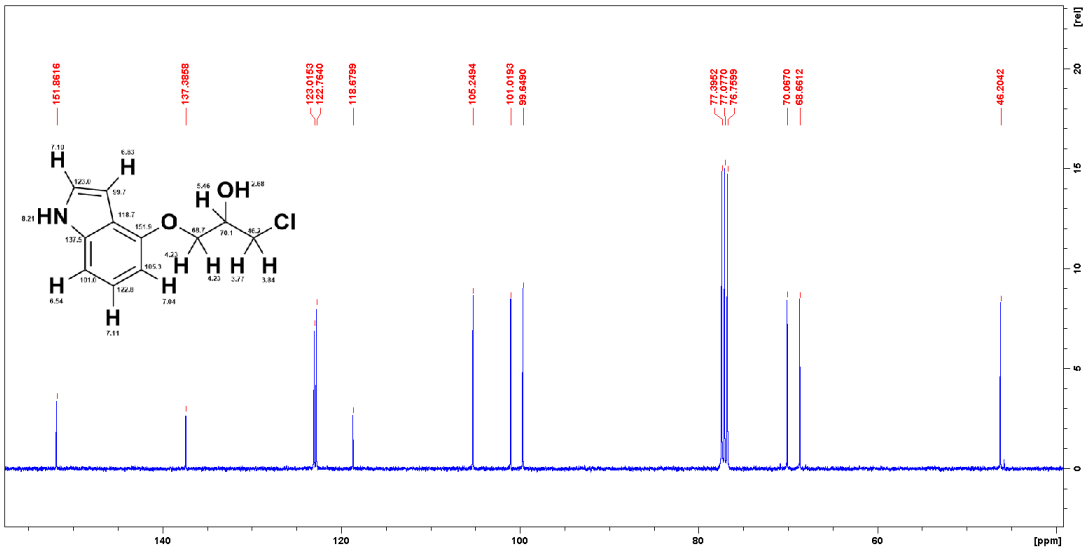

Figure 26: ^{13}C-NMR spectrum of **2** using a Bruker 400 MHz Avance III HD. $CDCl_3$ was used as a solvent.

6.1.3 HSQC-NMR spectrum for 1-((1H-indol-4-yl)oxy)-3-chloropropan-2-ol (2)

HSQC-NMR spectrum of **2** showing its structure with corresponding shifts for ^{1}H and ^{13}C.

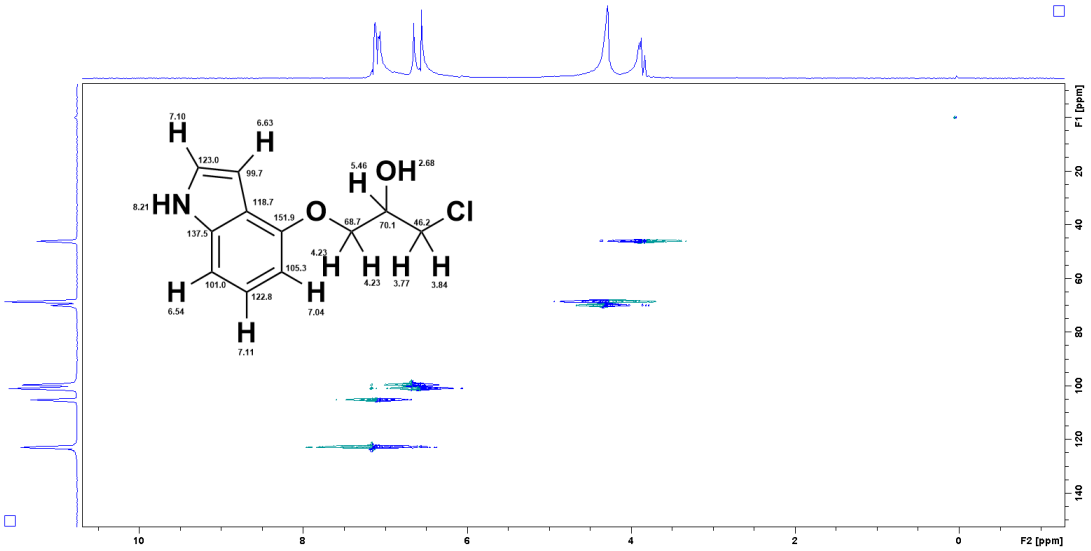

Figure 27: HSQC-NMR spectrum of **2** using a Bruker 400 MHz Avance III HD. $CDCl_3$ was used as a solvent.

6.2 NMR of 1-((1H-indol-4-yl)oxy)-3-chloropropan-2-yl butyrate (4)

6.2.1 ^{1}H-NMR spectrum for 1-((1H-indol-4-yl)oxy)-3-chloropropan-2-yl butyrate (4)

^{1}H-NMR spectrum of **4** showing its structure with corresponding shifts for ^{1}H and ^{13}C.

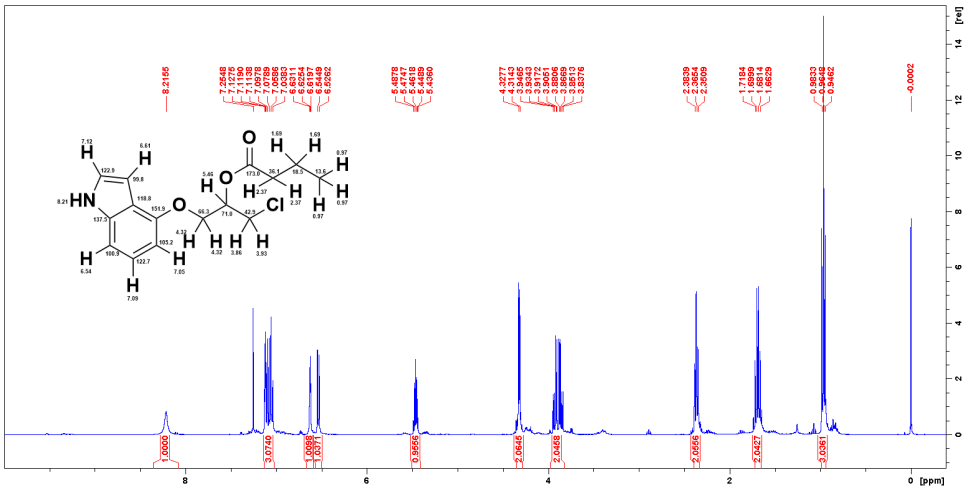

Figure 28: ^{1}H-NMR spectrum of 1-((1H-indol-4-yl)oxy)-3-chloropropan-2-yl butyrate (**4**) using a Bruker 400 MHz Avance III HD. $CDCl_3$ was used as a solvent.

6.2.2 ^{13}C spectrum for 1-((1H-indol-4-yl)oxy)-3-chloropropan-2-yl butyrate (4)

^{13}C-NMR spectrum of **4** showing its structure with corresponding shifts for ^{1}H and ^{13}C.

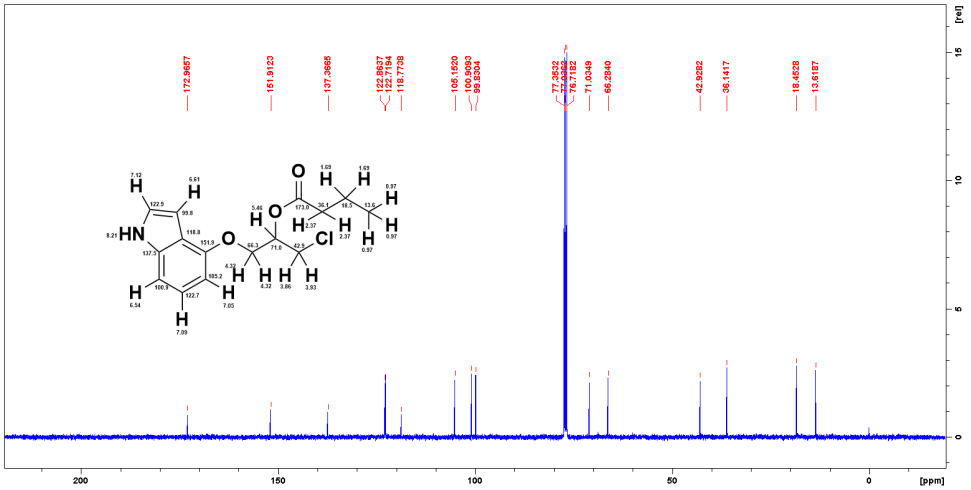

Figure 29: ^{13}C-NMR spectrum of **4** using a Bruker 400 MHz Avance III HD. $CDCl_3$ was used as a solvent.

6.2.3 HSQC-NMR spectrum for 1-((1H-indol-4-yl)oxy)-3-chloropropan-2-yl butyrate (4)

HSQC-NMR spectrum of **4** showing its structure with corresponding shifts for ^{1}H and ^{13}C.

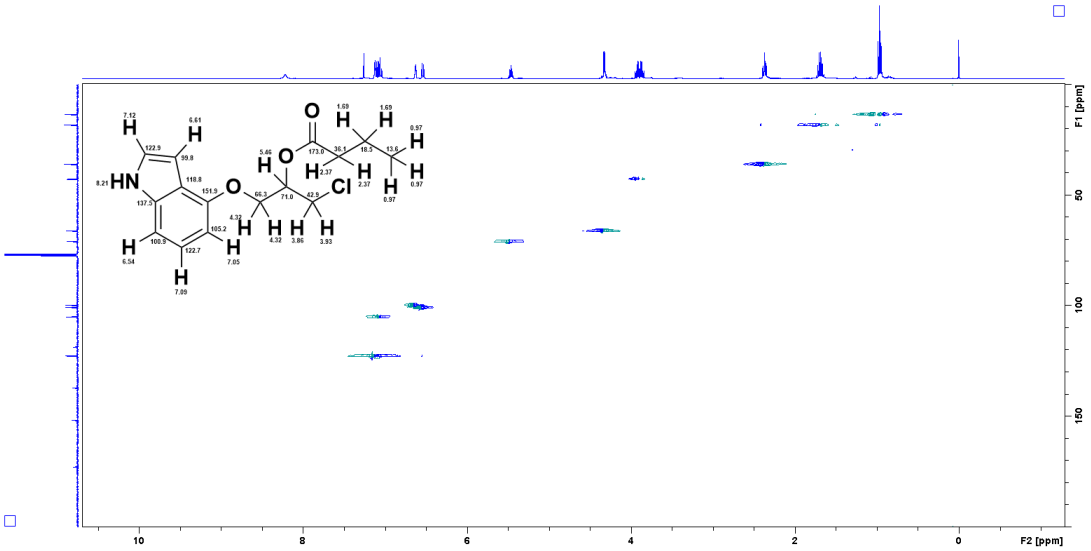

Figure 30: HSQC-NMR spectrum of **4** using a Bruker 400 MHz Avance III HD. $CDCl_3$ was used as a solvent.

6.3 NMR of (*S*)-pindolol ((S)-5) with and without deuterium oxide added to $CDCl_3$

For the characterization of (*S*)-pindolol ((S)-**5**) spectra with and without deuterium oxide added to $CDCl_3$ were used. This was because of peaks hindering the characterization unless a few drops of deuterium oxide was added to $CDCl_3$. The spectra without deuterium oxide were used and the corresponding shifts you see are from the spectra without deuterium oxide except for the amine protons with a shift of 1.25 in parenthesis.

6.3.1 ^{13}C spectrum for (*S*)-pindolol ((S)-5)

^{13}C-NMR spectrum of **5** showing its structure with corresponding shifts for ^{1}H and ^{13}C.

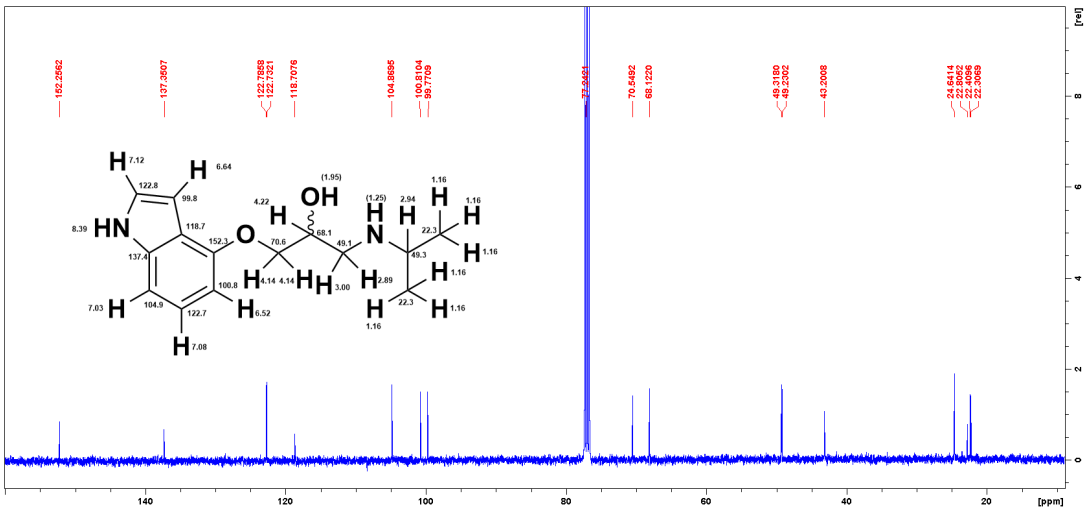

Figure 31: ^{13}C-NMR spectrum of **5** using a Bruker 400 MHz Avance III HD. $CDCl_3$ was used as a solvent.

6.3.2 HSQC-NMR spectrum for (*S*)-pindolol ((S)-5)

HSQC-NMR spectrum of **5** showing its structure with corresponding shifts for ^{1}H and ^{13}C.

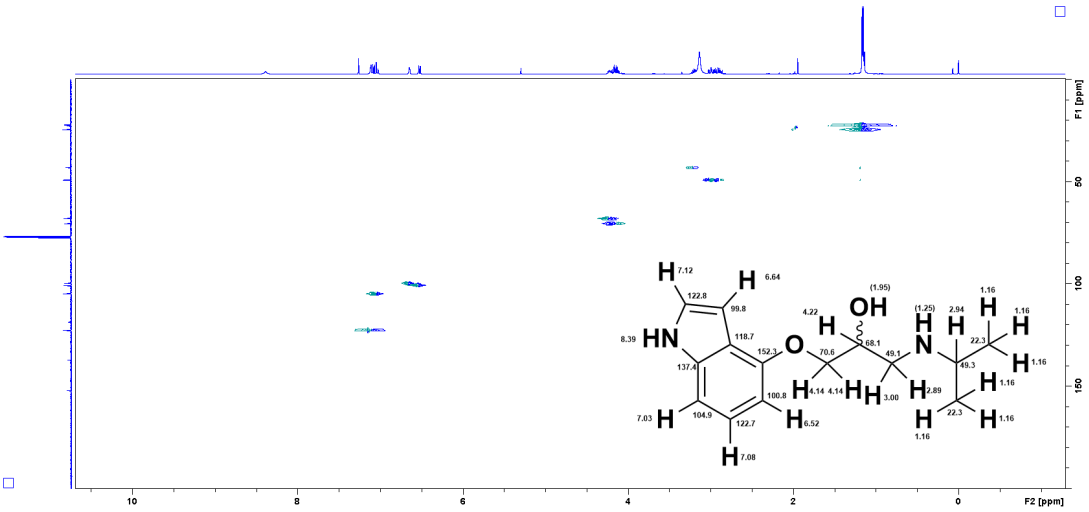

Figure 32: HSQC-NMR spectrum of **5** using a Bruker 400 MHz Avance III HD. $CDCl_3$ was used as a solvent.

6.3.3 ^{13}C spectrum for (*S*)-pindolol ((S)-5) with a few drops of deuterium oxide added to $CDCl_3$

^{13}C-NMR spectrum of **5** with a few drops of deuterium oxide added to $CDCl_3$ showing its structure with corresponding shifts for ^{1}H and ^{13}C.

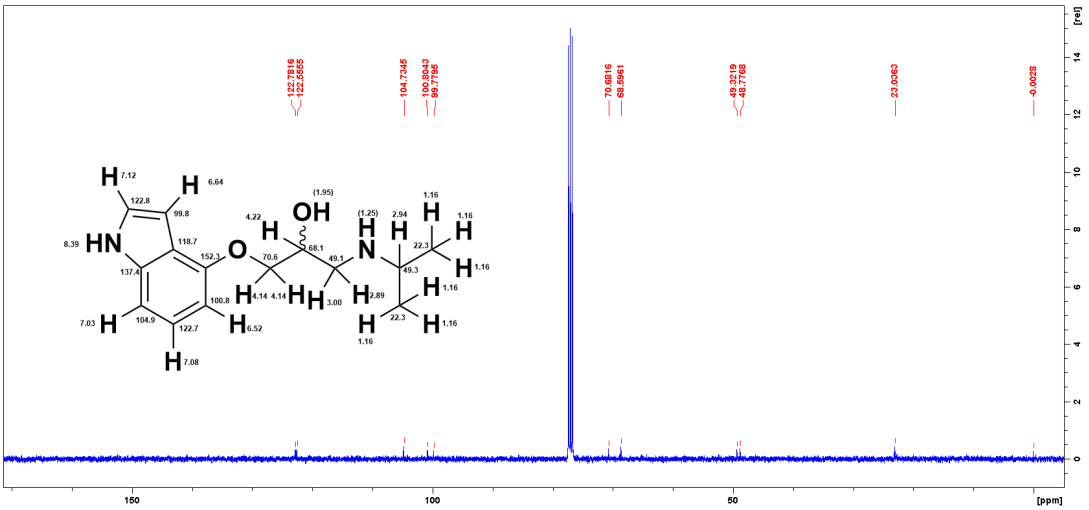

Figure 33: ^{13}C-NMR spectrum of **5** using a Bruker 400 MHz Avance III HD. $CDCl_3$ was used as a solvent with a few drops of deuterium oxide.

6.3.4 HSQC-NMR spectrum for (*S*)-pindolol ((S)-5) with a few drops of deuterium oxide added to $CDCl_3$

HSQC-NMR spectrum of **5** with a few drops of deuterium oxide added to $CDCl_3$ showing its structure with corresponding shifts for ^{1}H and ^{13}C.

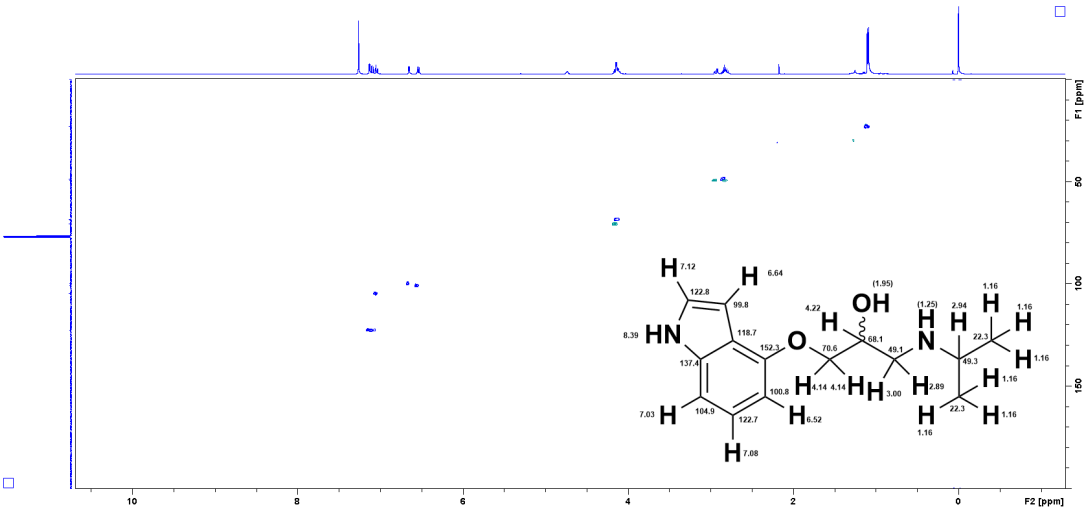

Figure 34: HSQC-NMR spectrum of **5** using a Bruker 400 MHz Avance III HD. $CDCl_3$ was used as a solvent with a few drops of deuterium oxide.

6.3.5 HMBC-NMR spectrum for (*S*)-pindolol ((S)-5) with a few drops of deuterium oxide added to $CDCl_3$

HMBC-NMR spectrum of **5** with a few drops of deuterium oxide added to $CDCl_3$ showing its structure with corresponding shifts for ^{1}H and ^{13}C.

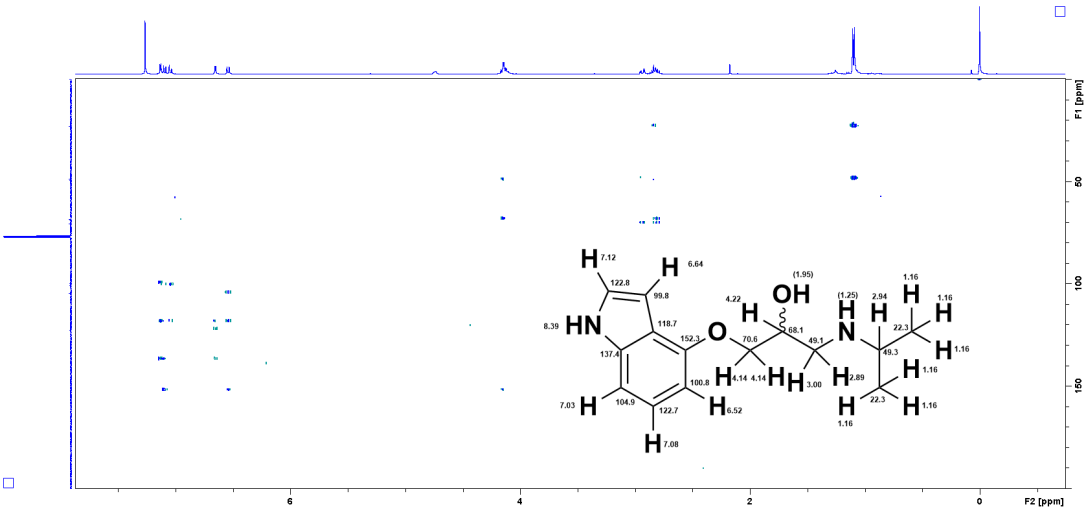

Figure 35: HMBC-NMR spectrum of **5** using a Bruker 400 MHz Avance III HD. $CDCl_3$ was used as a solvent with a few drops of deuterium oxide.

6.3.6 COSY-NMR spectrum for (*S*)-pindolol ((S)-5) with a few drops of deuterium oxide added to $CDCl_3$

COSY-NMR spectrum of **5** with a few drops of deuterium oxide added to $CDCl_3$ showing its structure with corresponding shifts for ^{1}H and ^{13}C.

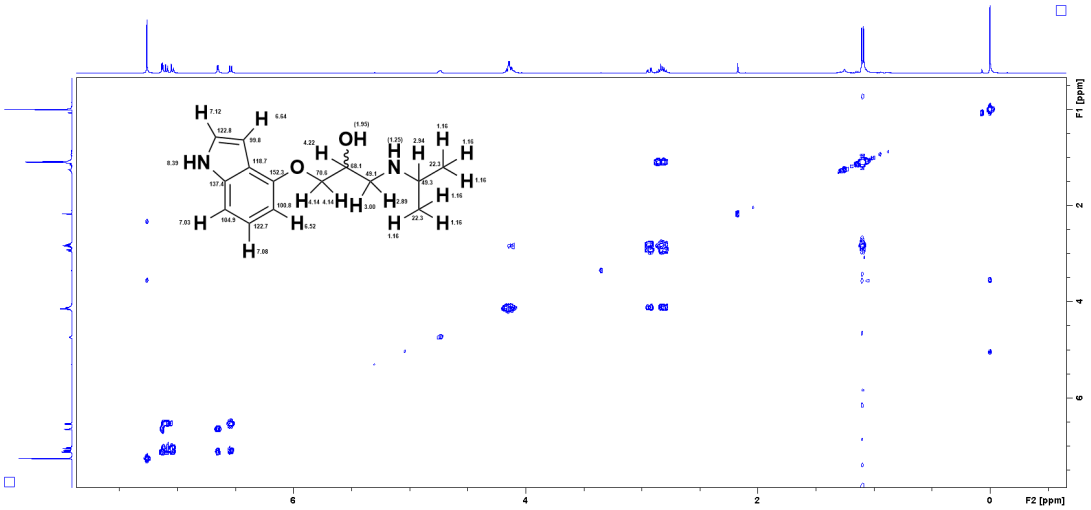

Figure 36: COSY-NMR spectrum of **5** using a Bruker 400 MHz Avance III HD. $CDCl_3$ was used as a solvent with a few drops of deuterium oxide.

6.4 HPLC analysis of enzyme catalyzed kinetic resolution

6.4.1 Chromatogram of enzyme reaction after 9 hours showing enatiomers of 1-((1H-indol-4-yl)oxy)-3-chloropropan-2-ol (2) and 1-((1H-indol-4-yl)oxy)-3-chloropropan-2-yl butyrate (4)

The Chiral HPLC chromatogram showing both enantiomers of **2** and **4**. The sample was taken 9 hours after the enzyme reaction with CALB started. Under the chromatogram is a table showing the data for all the peaks. The best method used for separating (*R*)-**2** and (*S*)-**2** was n-hexane:isopropanol (60:40). The best method used for separating (*R*)-**4** and (*S*)-**4** was n-hexane:isopropanol (90:10) and gave a R_s of 1.08.

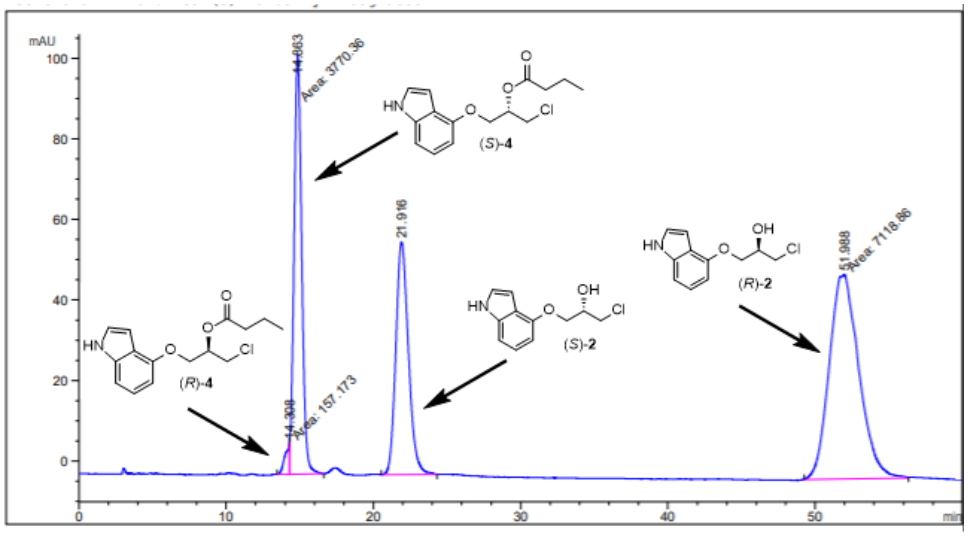


```
=====================================================================
                        Area Percent Report
=====================================================================

Sorted By             :      Signal
Multiplier:                   :      1.0000
Dilution:                     :      1.0000
Use Multiplier & Dilution Factor with ISTDs


Signal 1: VWD1 A, Wavelength=254 nm

Peak RetTime Type  Width     Area      Height     Area
  #   [min]        [min]  mAU   *s    [mAU   ]      %
----|-------|----|-------|----------|----------|--------|
   1  14.308 MF    0.3297  157.17279    7.94443   1.0856
   2  14.863 FM    0.6044 3770.36230  103.97175  26.0429
   3  21.916 BB    0.9003 3431.13306   57.71453  23.6997
   4  51.988 MM    2.3365 7118.85938   50.78061  49.1718

Totals :                  1.44775e4   220.41132
```

Figure 37: Chiral HPLC chromatogram showing both enantiomers of **2** and **4**, 9 hours into the enzyme reaction. t_R=52.0 min for (*R*)-**2**, t_R=21.9 min for (*S*)-**2**, t_R=14.3 min for (*R*)-**4**, t_R=14.9 min for (*S*)-**4**. Chiralcel OD-H column, n-hexane:isopropanol (80:20), 1 mL/min flow.

6.4.2 Chromatogram of enzyme reaction after 21 hours showing enatiomers of 1-((1H-indol-4-yl)oxy)-3-chloropropan-2-ol (2) and 1-((1H-indol-4-yl)oxy)-3-chloropropan-2-yl butyrate (4)

The Chiral HPLC chromatogram showing both enantiomers of **2** and **4**. The sample was taken 21 hours after the enzyme reaction with CALB started. Under the chromatogram is a table showing the data for all the peaks. The best method used for separating (*R*)-**2** and (*S*)-**2** was n-hexane:isopropanol (60:40). The best method used for separating (*R*)-**4** and (*S*)-**4** was n-hexane:isopropanol (90:10) and gave a R_s of 1.08.

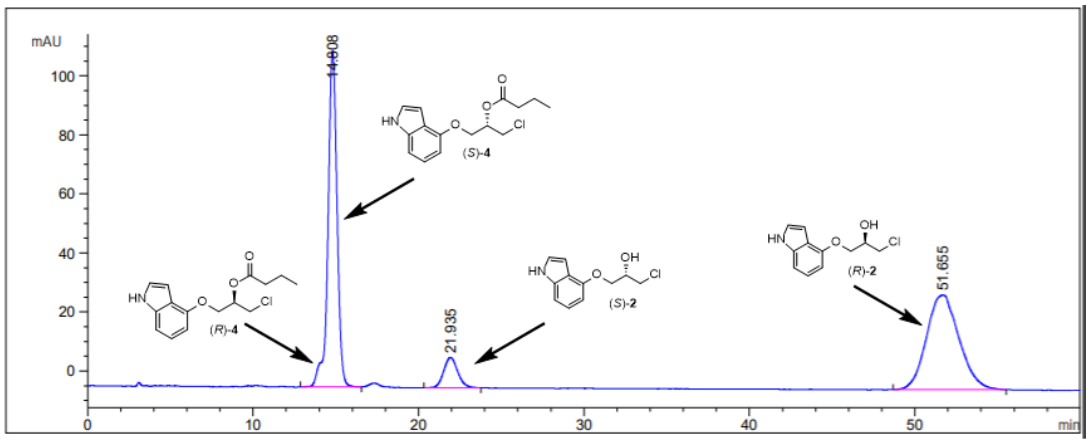


```
=====================================================================
                      Area Percent Report
=====================================================================

Sorted By             :      Signal
Multiplier:                   :      1.0000
Dilution:                     :      1.0000
Use Multiplier & Dilution Factor with ISTDs


Signal 1: VWD1 A, Wavelength=254 nm

Peak RetTime Type  Width     Area      Height     Area
  #   [min]        [min]  mAU   *s    [mAU   ]      %
----|-------|----|-------|----------|----------|--------|
   1  14.808 BB    0.5803 4329.84131  113.91475  46.4385
   2  21.935 BB    0.8502  607.25952   10.31027   6.5130
   3  51.655 BB    1.6603 4386.71680   32.03187  47.0485

Totals :                  9323.81763  156.25689
```

Figure 38: Chiral HPLC chromatogram showing both enantiomers of **2** and **4**, 21 hours into the enzyme reaction. t_R=51.7 min for (*R*)-**2**, t_R=21.9 min for (*S*)-**2**, t_R=14.4 min for (*R*)-**4**, t_R=14.8 min for (*S*)-**4**. Chiralcel OD-H column, n-hexane:isopropanol (80:20), 1 mL/min flow.

6.4.3 Chromatogram of enzyme reaction after 25 hours showing enatiomers of 1-((1H-indol-4-yl)oxy)-3-chloropropan-2-ol (2) and 1-((1H-indol-4-yl)oxy)-3-chloropropan-2-yl butyrate (4)

The Chiral HPLC chromatogram showing both enantiomers of **2** and **4**. The sample was taken 25 hours after the enzyme reaction with CALB started. Under the chromatogram is a table showing the data for all the peaks. The best method used for separating (*R*)-**2** and (*S*)-**2** was n-hexane:isopropanol (60:40). The best method used for separating (*R*)-**4** and (*S*)-**4** was n-hexane:isopropanol (90:10) and gave a R_s of 1.08.

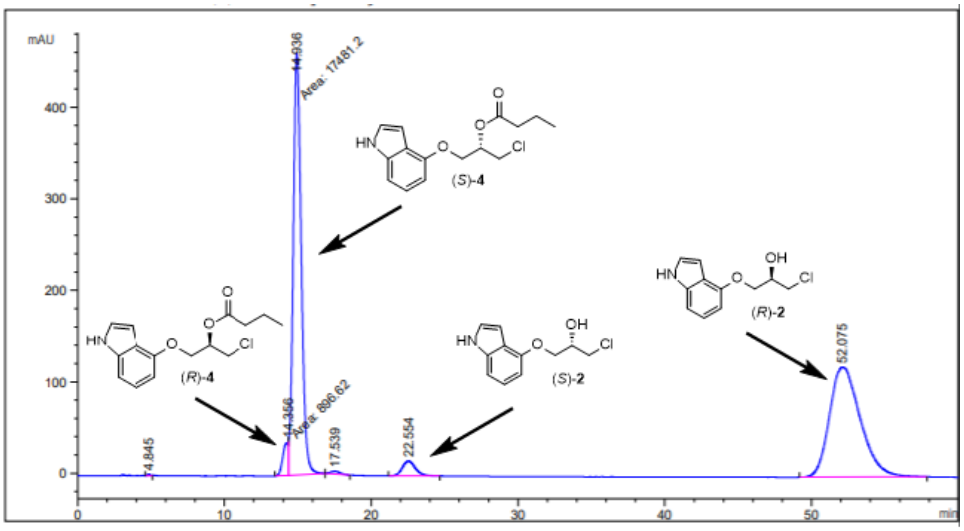


```
=====================================================================
                    Area Percent Report
=====================================================================

Sorted By             :      Signal
Multiplier:                   :      1.0000
Dilution:                     :      1.0000
Use Multiplier & Dilution Factor with ISTDs


Signal 1: VWD1 A, Wavelength=254 nm

Peak RetTime Type  Width     Area      Height     Area
  #   [min]        [min]  mAU   *s    [mAU   ]      %
----|-------|----|-------|----------|----------|--------|
   1   4.845 VV    0.1566   20.18870    1.86848   0.0544
   2  14.356 MF    0.4033  896.62018   37.04958   2.4170
   3  14.936 FM    0.6332 1.74812e4   460.15964  47.1231
   4  17.539 BB    0.5968  132.02632    3.03228   0.3559
   5  22.554 BB    0.9485 1019.53180   16.38924   2.7483
   6  52.075 BB    1.8855 1.75473e4   120.17603  47.3013

Totals :                  3.70969e4   638.67523
```

Figure 39: Chiral HPLC chromatogram showing both enantiomers of **2** and **4**, 25 hours into the enzyme reaction. t_R=52.1 min for (*R*)-**2**, t_R=22.6 min for (*S*)-**2**, t_R=14.4 min for (*R*)-**4**, t_R=14.9 min for (*S*)-**4**. Chiralcel OD-H column, n-hexane:isopropanol (80:20), 1 mL/min flow.

6.4.4 Chromatogram of enzyme reaction after 50 hours showing enatiomers of 1-((1H-indol-4-yl)oxy)-3-chloropropan-2-ol (2) and 1-((1H-indol-4-yl)oxy)-3-chloropropan-2-yl butyrate (4)

The Chiral HPLC chromatogram showing both enantiomers of **2** and **4**. The sample was taken 50 hours after the enzyme reaction with CALB started. Under the chromatogram is a table showing the data for all the peaks. The best method used for separating (*R*)-**2** and (*S*)-**2** was n-hexane:isopropanol (60:40). The best method used for separating (*R*)-**4** and (*S*)-**4** was n-hexane:isopropanol (90:10) and gave a R_s of 1.08.

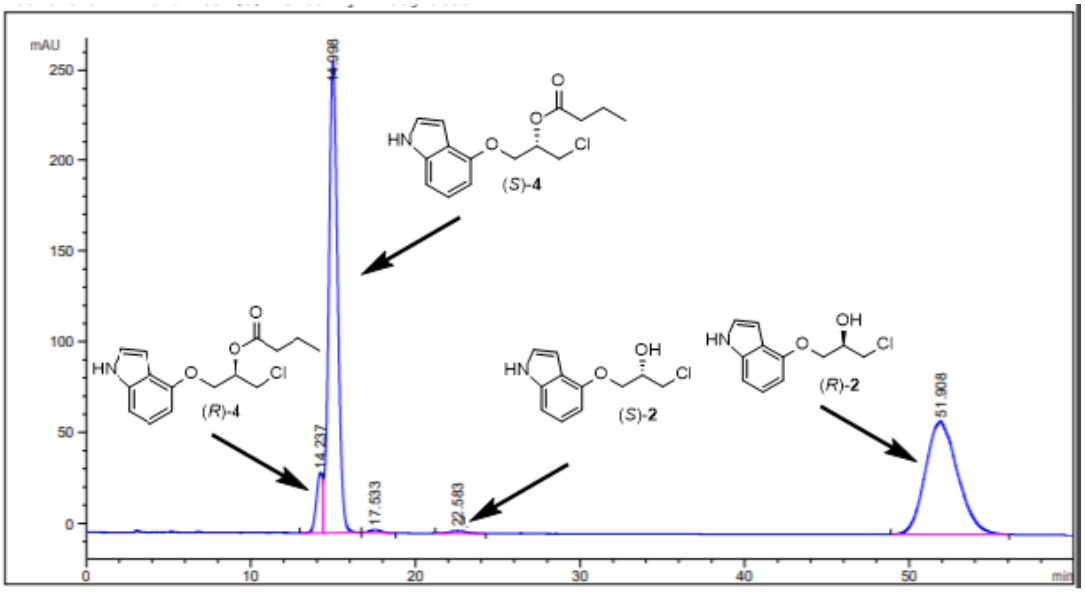

Area Percent Report

Sorted By : Signal
Multiplier: : 1.0000
Dilution: : 1.0000
Use Multiplier & Dilution Factor with ISTDs

Signal 1: VWD1 A, Wavelength=254 nm

Peak #	RetTime [min]	Type	Width [min]	Area mAU *s	Height [mAU]	Area %
1	14.237	BV	0.4093	886.82019	33.18827	4.6202
2	14.998	VB	0.5738	9674.50293	260.08206	50.4032
3	17.533	BB	0.6196	77.80814	1.72450	0.4054
4	22.583	MM	1.0383	76.66011	1.23050	0.3994
5	51.908	BB	1.6416	8478.44531	62.47109	44.1718
Totals :				1.91942e4	358.69641	

Figure 40: Chiral HPLC chromatogram showing both enantiomers of **2** and **4**, 50 hours into the enzyme reaction. t_R=51.9 min for (*R*)-**2**, t_R=22.6 min for (*S*)-**2**, t_R=14.2 min for (*R*)-**4**, t_R=15.0 min for (*S*)-**4**. Chiralcel OD-H column, n-hexane:isopropanol (80:20), 1 mL/min flow.

6.4.5 Chromatogram of enzyme reaction after 76 hours showing enatiomers of 1-((1H-indol-4-yl)oxy)-3-chloropropan-2-ol (2) and 1-((1H-indol-4-yl)oxy)-3-chloropropan-2-yl butyrate (4)

The Chiral HPLC chromatogram showing both enantiomers of **2** and **4**. The sample was taken 76 hours after the enzyme reaction with CALB started. Under the chromatogram is a table showing the data for all the peaks. The best method used for separating (*R*)-**2** and (*S*)-**2** was n-hexane:isopropanol (60:40). The best method used for separating (*R*)-**4** and (*S*)-**4** was n-hexane:isopropanol (90:10) and gave a R_s of 1.08.

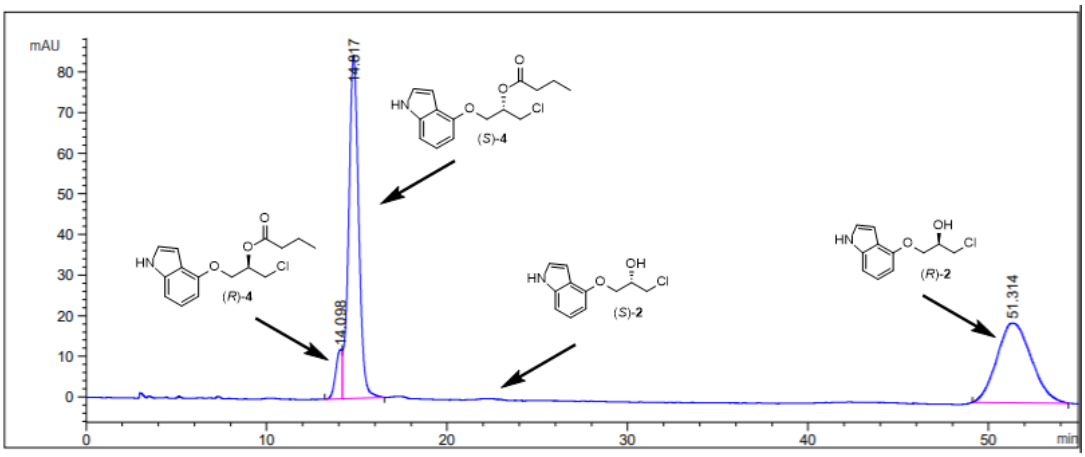


```
=====================================================================
                    Area Percent Report
=====================================================================

Sorted By             :      Signal
Multiplier:                   :      1.0000
Dilution:                     :      1.0000
Use Multiplier & Dilution Factor with ISTDs


Signal 1: VWD1 A, Wavelength=254 nm

Peak RetTime Type  Width     Area      Height     Area
  #   [min]        [min]  mAU   *s    [mAU   ]      %
----|-------|----|-------|----------|----------|--------|
   1  14.098 BV    0.3677  288.10577   12.11475   4.6865
   2  14.817 VB    0.5913 3269.12354   84.47409  53.1770
   3  51.314 BB    1.5838 2590.40039   19.54929  42.1366

Totals :                  6147.62970  116.13813
```

Figure 41: Chiral HPLC chromatogram showing both enantiomers of **2** and **4**, 76 hours into the enzyme reaction. t_R=51.3 min for (*R*)-**2**, t_R=22.5 min for (*S*)-**2**, t_R=14.1 min for (*R*)-**4**, t_R=14.8 min for (*S*)-**4**. Chiralcel OD-H column, n-hexane:isopropanol (80:20), 1 mL/min flow.

6.4.6 Chromatogram of enzyme reaction after 99 hours showing enatiomers of 1-((1H-indol-4-yl)oxy)-3-chloropropan-2-ol (2) and 1-((1H-indol-4-yl)oxy)-3-chloropropan-2-yl butyrate (4)

The Chiral HPLC chromatogram showing both enantiomers of **2** and **4**. The sample was taken 99 hours after the enzyme reaction with CALB started. Under the chromatogram is a table showing the data for all the peaks. The best method used for separating (*R*)-**2** and (*S*)-**2** was n-hexane:isopropanol (60:40). The best method used for separating (*R*)-**4** and (*S*)-**4** was n-hexane:isopropanol (90:10) and gave a R_s of 1.08.

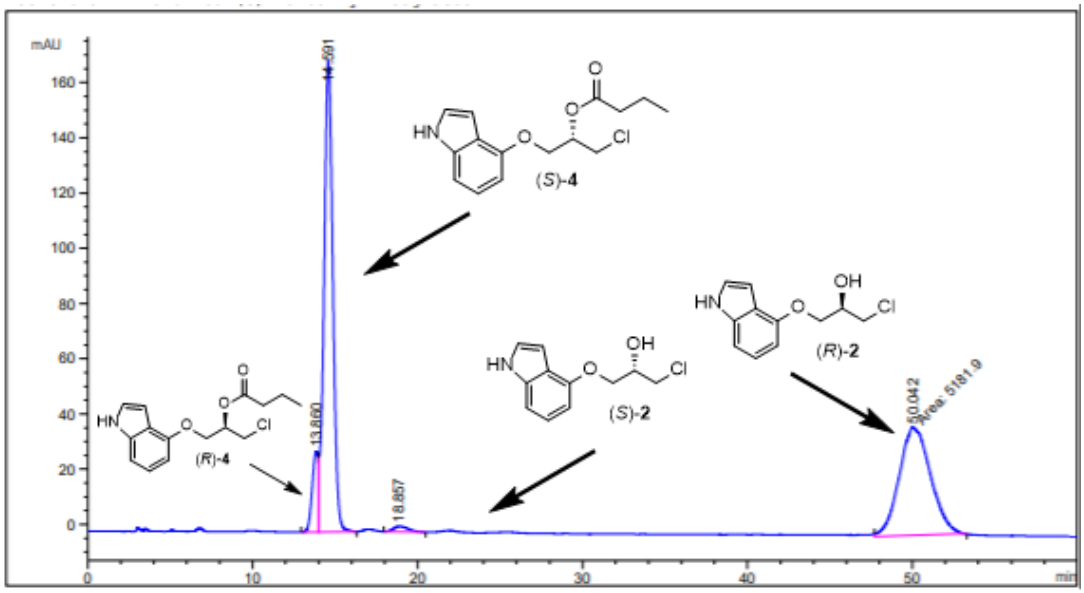

Area Percent Report

Sorted By : Signal
Multiplier: : 1.0000
Dilution: : 1.0000
Use Multiplier & Dilution Factor with ISTDs

Signal 1: VWD1 A, Wavelength=254 nm

Peak #	RetTime [min]	Type	Width [min]	Area mAU *s	Height [mAU]	Area %
1	13.860	BV	0.3908	748.17554	29.18126	6.0236
2	14.591	VB	0.5709	6370.60596	170.67906	51.2898
3	18.857	BB	0.7332	120.12781	1.95018	0.9671
4	50.042	MM	2.1999	5181.89648	39.25871	41.7195
Totals :				1.24208e4	241.06921	

Figure 42: Chiral HPLC chromatogram showing both enantiomers of **2** and **4**, 99 hours into the enzyme reaction. t_R=50.0 min for (*R*)-**2**, t_R is not there for (*S*)-**2**, t_R=13.9 min for (*R*)-**4**, t_R=14.5 min for (*S*)-**4**. Chiralcel OD-H column, n-hexane:isopropanol (80:20), 1 mL/min flow.

6.4.7 Chromatogram of enzyme reaction after 122 hours showing enatiomers of 1-((1H-indol-4-yl)oxy)-3-chloropropan-2-ol (2) and 1-((1H-indol-4-yl)oxy)-3-chloropropan-2-yl butyrate (4)

The Chiral HPLC chromatogram showing both enantiomers of **2** and **4**. The sample was taken 122 hours after the enzyme reaction with CALB started. Under the chromatogram is a table showing the data for all the peaks. The best method used for separating (*R*)-**2** and (*S*)-**2** was n-hexane:isopropanol (60:40). The best method used for separating (*R*)-**4** and (*S*)-**4** was n-hexane:isopropanol (90:10) and gave a R_s of 1.08.

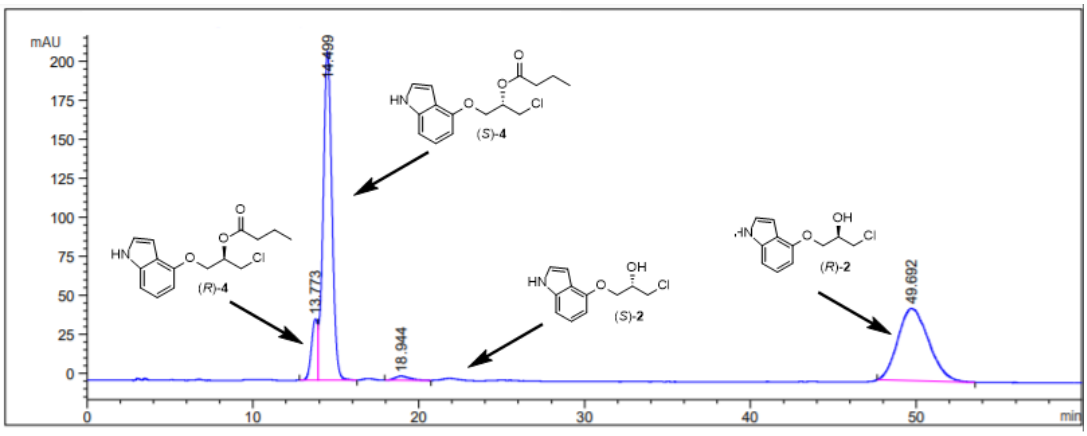


```
=====================================================================
                      Area Percent Report
=====================================================================

Sorted By             :      Signal
Multiplier:                   :      1.0000
Dilution:                     :      1.0000
Use Multiplier & Dilution Factor with ISTDs


Signal 1: VWD1 A, Wavelength=254 nm

Peak RetTime Type  Width     Area      Height     Area
  #   [min]        [min]  mAU   *s   [mAU   ]      %
----|-------|----|-------|----------|----------|--------|
   1  13.773 BV    0.3948 1016.70874   39.32351   6.7950
   2  14.499 VB    0.5683 7822.73193  210.80241  52.2821
   3  18.944 BB    0.8201  167.07570    2.64977   1.1166
   4  49.692 BB    1.7112 5956.01660   46.18904  39.8062

Totals :                  1.49625e4   298.96473
```

Figure 43: Chiral HPLC chromatogram showing both enantiomers of **2** and **4**, 122 hours into the enzyme reaction. t_R=49.7 min for (*R*)-**2**, t_R is not there for (*S*)-**2**, t_R=13.8 min for (*R*)-**4**, t_R=14.5 min for (*S*)-**4**. Chiralcel OD-H column, n-hexane:isopropanol (80:20), 1 mL/min flow.

6.4.8 Chromatogram of enzyme reaction after 25 hours showing only enantiomers of 1-((1H-indol-4-yl)oxy)-3-chloropropan-2-yl butyrate (4)

The Chiral HPLC chromatogram showing both enantiomers of **4**. The sample was taken 25 hours after the enzyme reaction with CALB started. The same sample as in section 5.4.3 with different mobile phase ratios. Under the chromatogram is a table showing the data for all the peaks. The best method used for separating (*R*)-**4** and (*S*)-**4** was n-hexane:isopropanol (90:10) and gave a R_s of 1.08.

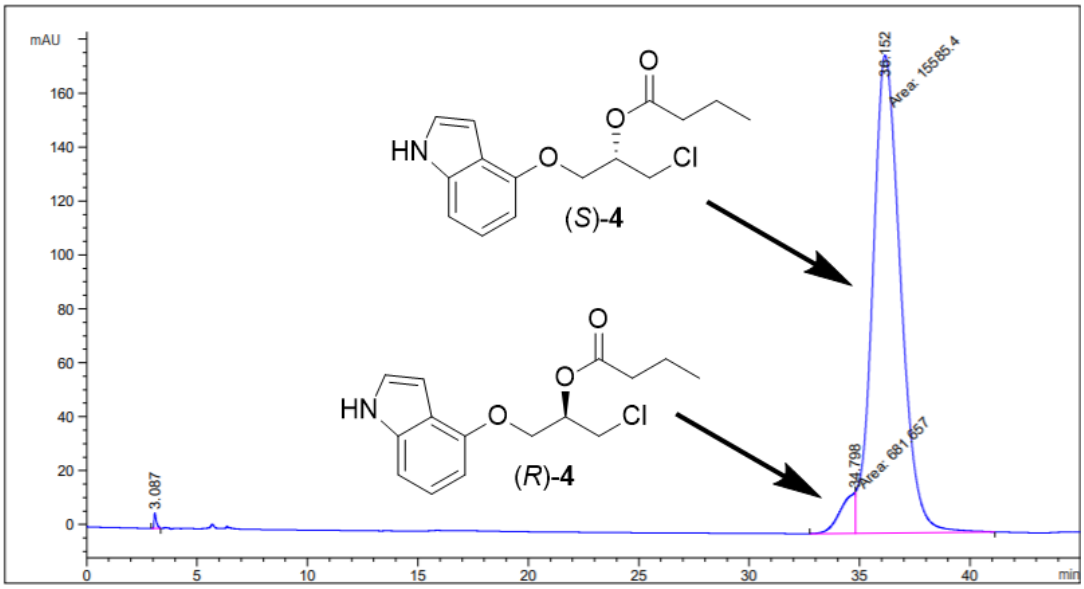


```
=====================================================================
                        Area Percent Report
=====================================================================

Sorted By             :      Signal
Multiplier:                   :      1.0000
Dilution:                     :      1.0000
Use Multiplier & Dilution Factor with ISTDs


Signal 1: VWD1 A, Wavelength=254 nm

Peak RetTime Type  Width     Area      Height     Area
  #   [min]        [min]  mAU   *s    [mAU   ]      %
----|-------|----|-------|----------|----------|--------|
   1   3.087 BB    0.1090   40.88786    5.65910   0.2507
   2  34.798 MF    0.7430  681.65680   15.29137   4.1799
   3  36.152 FM    1.4667 1.55854e4   177.09827  95.5694

Totals :                  1.63079e4   198.04874
```

Figure 44: Chiral HPLC chromatogram showing both enantiomers of **4**, 25 hours into the enzyme reaction. t_R=34.8 min for (*R*)-**4**, t_R=36.2 min for (*S*)-**4**. Chiralcel OD-H column, n-hexane:isopropanol (90:10), 1 mL/min flow.

6.4.9 Chromatogram of enzyme reaction after 50 hours showing only enantiomers of 1-((1H-indol-4-yl)oxy)-3-chloropropan-2-yl butyrate (4)

The Chiral HPLC chromatogram showing both enantiomers of **4**. The sample was taken 50 hours after the enzyme reaction with CALB started. The same sample as in section 5.3.4, with different mobile phase ratios. Under the chromatogram is a table showing the data for all the peaks. The best method used for separating (*R*)-**4** and (*S*)-**4** was n-hexane:isopropanol (90:10) and gave a R_s of 1.08.

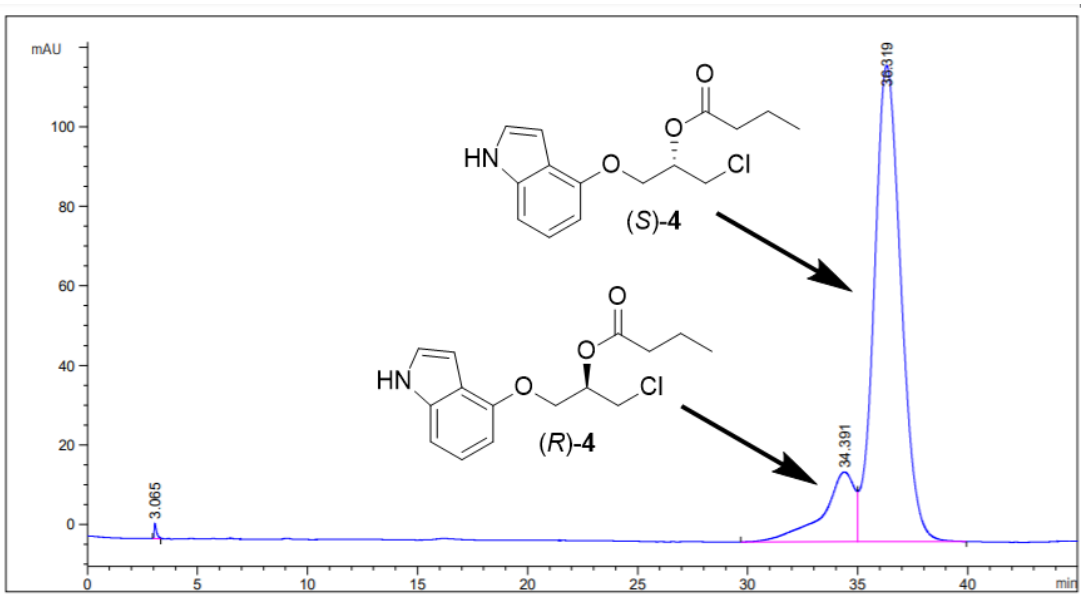


```
=====================================================================
                      Area Percent Report
=====================================================================

Sorted By             :      Signal
Multiplier:                   :      1.0000
Dilution:                     :      1.0000
Use Multiplier & Dilution Factor with ISTDs


Signal 1: VWD1 A, Wavelength=254 nm

Peak RetTime Type  Width     Area      Height     Area
  #   [min]        [min]  mAU   *s    [mAU   ]      %
----|-------|----|-------|----------|----------|--------|
   1   3.065 BB    0.1000   28.26996    3.85895   0.2365
   2  34.391 BV    1.3878 1764.53564   17.56000  14.7638
   3  36.319 VB    1.3332 1.01590e4   119.76627  84.9997

 Totals :                 1.19518e4   141.18523
```

Figure 45: Chiral HPLC chromatogram showing both enantiomers of **4**, 50 hours into the enzyme reaction. t_R=34.4 min for (*R*)-**4**, t_R=36.3 min for (*S*)-**4**. Chiralcel OD-H column, n-hexane:isopropanol (90:10), 1 mL/min flow.

6.4.10 Chromatogram of 1-((1H-indol-4-yl)oxy)-3-chloropropan-2-yl butyrate (4) with 90:10 ratio between n-hexane and isopropanol

The Chiral HPLC chromatogram showning both enantiomers of **4** as a racemic mixture made from **2**. This was done to better separate the peaks. Under the chromatogram is a table showing the data for all the peaks. The best method used for separating (*R*)-**4** and (*S*)-**4** was n-hexane:isopropanol (90:10) and gave a R_s of 1.08.

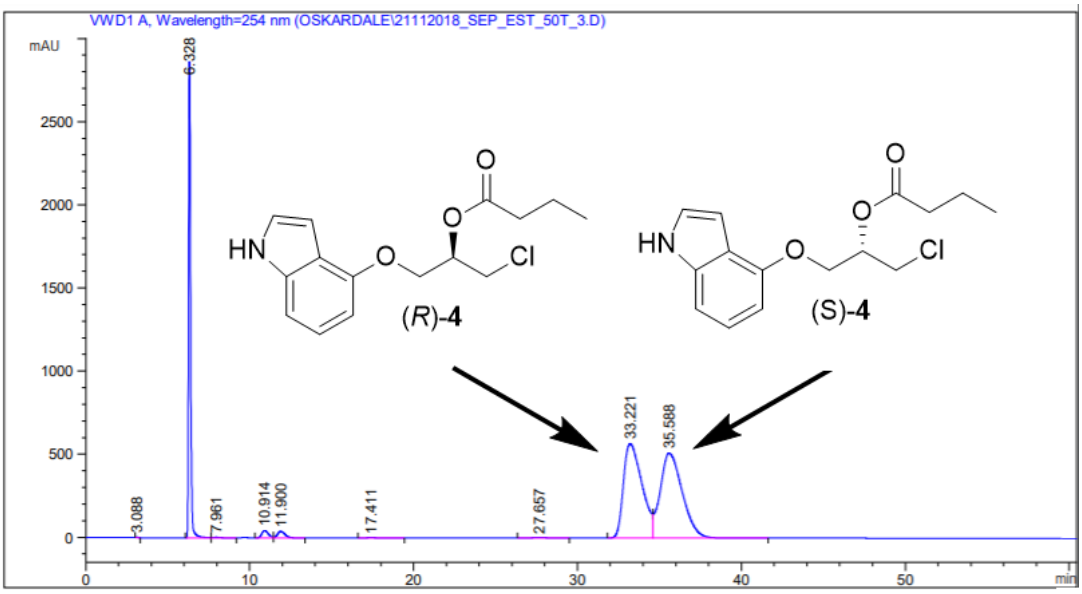


```
================================================================================
                          Area Percent Report
================================================================================

Sorted By             :      Signal
Multiplier:                   :      1.0000
Dilution:                     :      1.0000
Use Multiplier & Dilution Factor with ISTDs


Signal 1: VWD1 A, Wavelength=254 nm

Peak RetTime Type  Width     Area      Height     Area
  #   [min]        [min]  mAU   *s    [mAU   ]      %
----|-------|----|-------|----------|----------|--------|
   1   3.088 BB    0.1106   32.22479    4.45411   0.0268
   2   6.328 BV    0.1343 2.47616e4  2865.51074  20.5936
   3   7.961 VB    0.4157  103.77206    3.59172   0.0863
   4  10.914 BV    0.4246 1209.85364   44.13988   1.0062
   5  11.900 VB    0.4798 1247.48962   39.58311   1.0375
   6  17.411 BB    0.6039   94.46683    2.22791   0.0786
   7  27.657 BB    0.8466  227.22568    3.27792   0.1890
   8  33.221 BV    1.1501 4.47616e4   566.71844  37.2270
   9  35.588 VB    1.4312 4.78013e4   510.71066  39.7550

Totals :                  1.20240e5  4040.21450
```

Figure 46: Chiral HPLC chromatogram showing both enantiomers of **4**. t_R=33.2 min for (*R*)-**4**, t_R=35.6 min for (*S*)-**4**. Chiralcel OD-H column, n-hexane:isopropanol (90:10), 1 mL/min flow.

6.4.11 Chromatogram of 1-((1H-indol-4-yl)oxy)-3-chloropropan-2-ol (2) with 60:40 ratio between n-hexane and isopropanol

The Chiral HPLC chromatogram showning both enantiomers of **2**. Under the chromatogram is a table showing the data for all the peaks. The best method used for separating (*R*)-**2** and (*S*)-**2** was n-hexane:isopropanol (60:40).

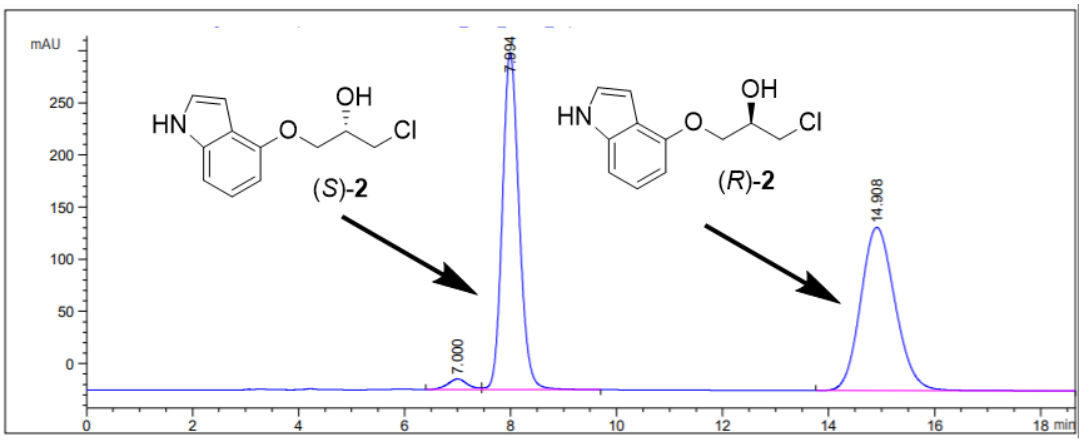


```
=====================================================================
                    Area Percent Report
=====================================================================

Sorted By             :      Signal
Multiplier:                   :      1.0000
Dilution:                     :      1.0000
Use Multiplier & Dilution Factor with ISTDs


Signal 1: VWD1 A, Wavelength=254 nm

Peak RetTime Type  Width     Area      Height     Area
  #   [min]        [min]  mAU   *s    [mAU   ]      %
----|-------|----|-------|----------|----------|--------|
   1   7.000 VV    0.3932  271.35992   10.30375   1.8782
   2   7.994 VB    0.3392 7099.15430  323.21384  49.1352
   3  14.908 BBA   0.7008 7077.69824  156.52959  48.9867

Totals :                 1.44482e4   490.04717
```

Figure 47: Chiral HPLC chromatogram showing both enantiomers of **2**. t_R=8.0 min for (*S*)-**2**, t_R=14.9 min for (*R*)-**2**. Chiralcel OD-H column, n-hexane:isopropanol (60:40), 1 mL/min flow.

6.4.12 Chromatogram of 1-((1H-indol-4-yl)oxy)-3-chloropropan-2-ol (2) with 80:20 ratio between n-hexane and isopropanol

The Chiral HPLC chromatogram showning both enantiomers of **2**. Under the chromatogram is a table showing the data for all the peaks.The best method used for separating (*R*)-**2** and (*S*)-**2** was n-hexane:isopropanol (80:20).

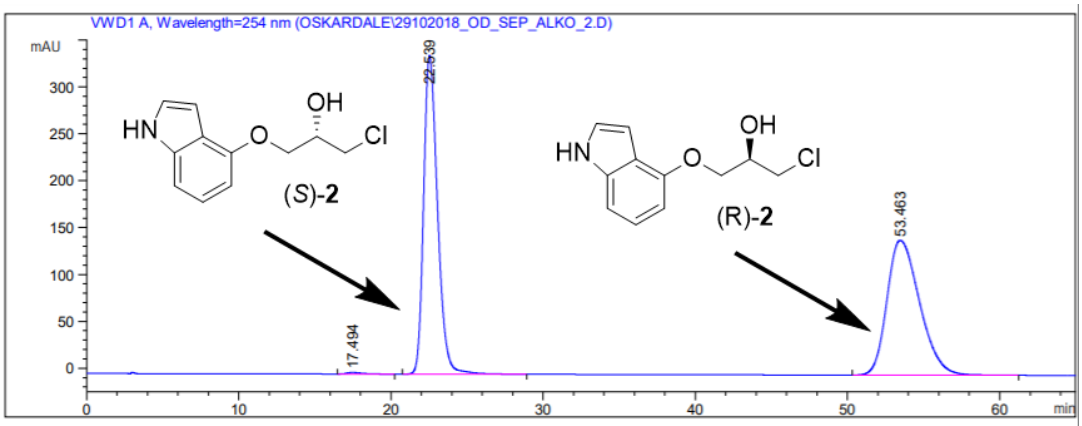


```
=====================================================================
                      Area Percent Report
=====================================================================

Sorted By             :      Signal
Multiplier:                   :      1.0000
Dilution:                     :      1.0000
Use Multiplier & Dilution Factor with ISTDs


Signal 1: VWD1 A, Wavelength=254 nm

Peak RetTime Type  Width     Area      Height     Area
  #   [min]        [min]  mAU   *s    [mAU   ]      %
----|-------|----|-------|----------|----------|--------|
   1  17.494 BB    0.8615  122.77483    1.72686   0.2845
   2  22.539 BB    0.9775 2.15719e4   340.00549  49.9861
   3  53.463 BB    2.2412 2.14611e4   143.86723  49.7294

Totals :                 4.31557e4   485.59958
```

Figure 48: Chiral HPLC chromatogram showing both enantiomers of **2**. t_R=22.5 min for (*S*)-**2**, t_R=53.5 min for (*R*)-**2**. Chiralcel OD-H column, n-hexane:isopropanol (80:20), 1 mL/min flow.

6.4.13 Chromatogram of 1-((1H-indol-4-yl)oxy)-3-chloropropan-2-ol (2) with 60:40 ratio between n-hexane and isopropanol

The Chiral HPLC chromatogram showning both enantiomers of **2**. Under the chromatogram is a table showing the data for all the peaks. The best method used for separating (*R*)-**2** and (*S*)-**2** was n-hexane:isopropanol (60:40).

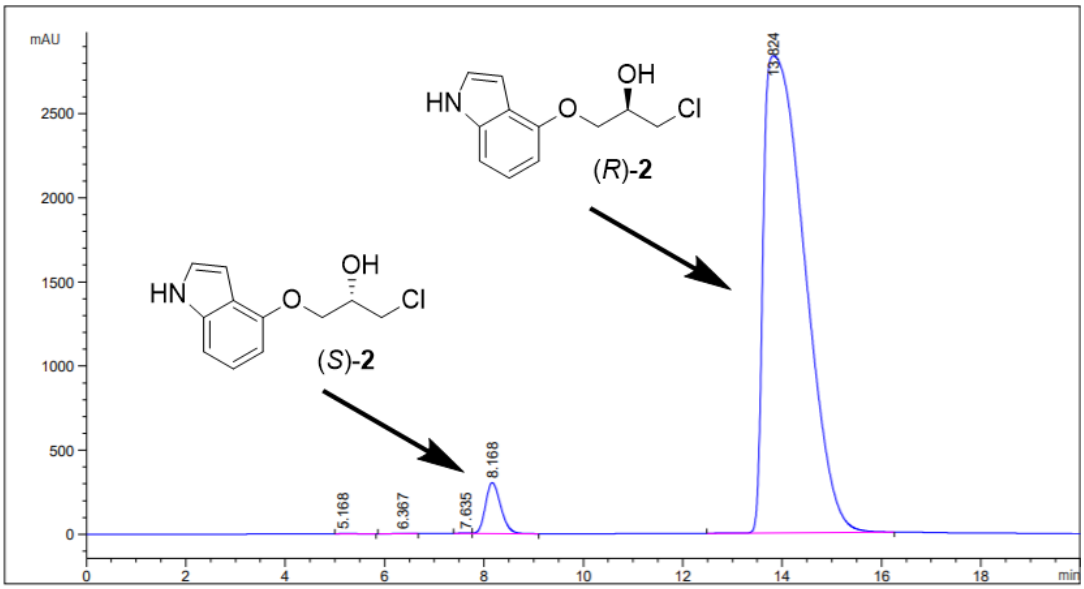


```
=====================================================================
                    Area Percent Report
=====================================================================

Sorted By             :      Signal
Multiplier:                   :      1.0000
Dilution:                     :      1.0000
Use Multiplier & Dilution Factor with ISTDs


Signal 1: VWD1 A, Wavelength=254 nm

Peak RetTime Type  Width     Area      Height     Area
  #   [min]        [min]  mAU   *s   [mAU   ]      %
----|-------|----|-------|----------|----------|--------|
   1   5.168 VB    0.3438   70.80617    3.14938   0.0420
   2   6.367 BV    0.3600   51.77530    2.07185   0.0307
   3   7.635 VV    0.2255   57.22117    3.92288   0.0339
   4   8.168 VB    0.3302 6460.19287  303.12344   3.8303
   5  13.824 BB    0.9098 1.62019e5  2835.21973  96.0631

Totals :                  1.68659e5  3147.48728
```

Figure 49: Chiral HPLC chromatogram showing both enantiomers of **2**. t_R=8.2 min for (*S*)-**2**, t_R=13.8 min for (*R*)-**2**. Chiralcel OD-H column, n-hexane:isopropanol (60:40), 1 mL/min flow.

6.4.14 Chromatogram of 1-((1H-indol-4-yl)oxy)-3-chloropropan-2-yl butyrate (4) with 90:10 ratio between n-hexane and isopropanol

The Chiral HPLC chromatogram showning both enantiomers of **4**. Under the chromatogram is a table showing the data for all the peaks. The best method used for separating (*R*)-**4** and (*S*)-**4** was n-hexane:isopropanol (90:10) and gave a R_s of 1.08.

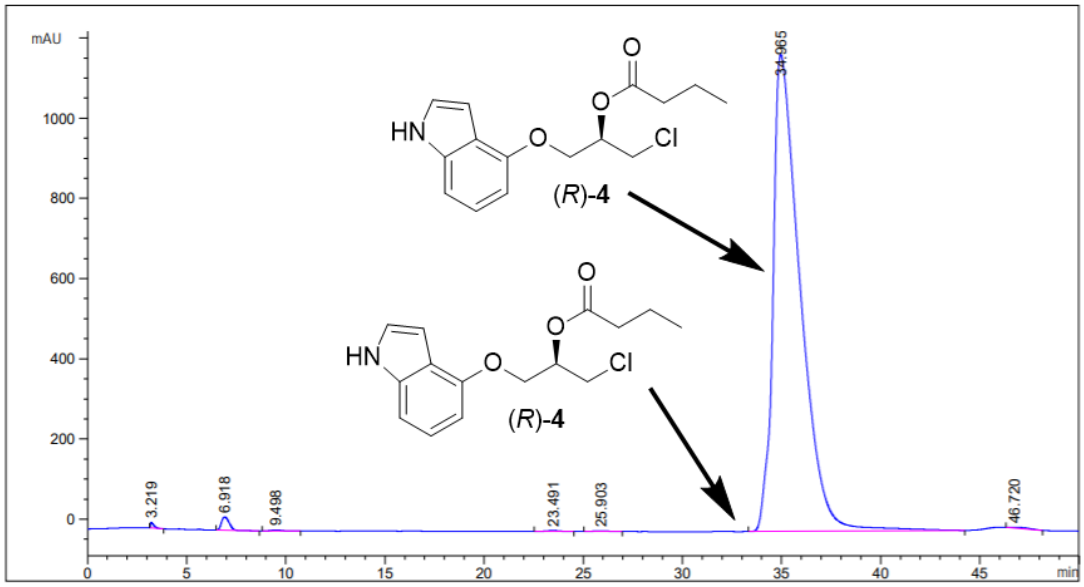


```
=====================================================================
                    Area Percent Report
=====================================================================

Sorted By             :      Signal
Multiplier:                   :      1.0000
Dilution:                     :      1.0000
Use Multiplier & Dilution Factor with ISTDs


Signal 1: VWD1 A, Wavelength=254 nm

Peak RetTime Type  Width     Area      Height     Area
  #   [min]        [min]  mAU   *s   [mAU   ]      %
----|-------|----|-------|----------|----------|--------|
   1   3.219 BB    0.1704  158.27606   14.24984   0.1377
   2   6.918 BB    0.4443  916.86395   33.52037   0.7976
   3   9.498 BB    0.5367  104.35294    2.90710   0.0908
   4  23.491 BB    0.6542   94.79767    2.05106   0.0825
   5  25.903 BB    0.6456   89.05264    1.85144   0.0775
   6  34.965 BB    1.4307 1.13424e5  1188.59338  98.6725
   7  46.720 BBA   0.9940  162.61855    1.96028   0.1415

Totals :                  1.14949e5  1245.13347
```

Figure 50: Chiral HPLC chromatogram showing both enantiomers of **4**. t_R= Not observable for (*R*)-**4**, t_R= 35.0 min for (*S*)-**4**. Chiralcel OD-H column, n-hexane:isopropanol (90:10), 1 mL/min flow.

6.5 GC

6.5.1 Chromatogram of 1-((1H-indol-4-yl)oxy)-3-chloropropan-2-ol (2) from 50 to 200 °C, 10°C/min

The GC chromatogram for compound **2**. The temperature program used was 50-200 °C, 10°C/min, 2 min hold time.

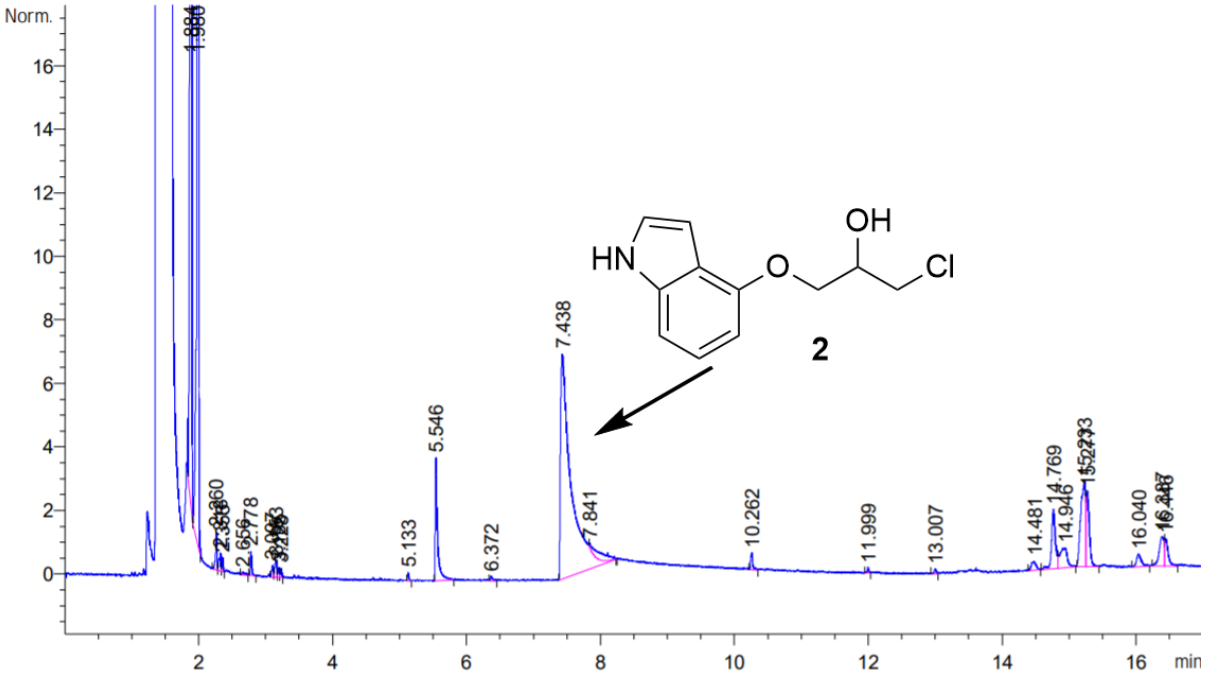

Figure 51: GC chromatogram showing compound **2**. t_R= 7.4 min for **2**. The temperature program used was 50-200 °C, 10°C/min, 2 min hold time. The column used was a Agilent column with a CP-Chirasil-Dex CB stationary phase consisting of cyclodextrin directly bonded to dimethylpolysiloxane.

6.5.2 Chromatogram of 1-((1H-indol-4-yl)oxy)-3-chloropropan-2-yl butyrate (4) from 50 to 200 °C, 10°C/min

The GC chromatogram for compound **4**. The temperature program used was 50-200 °C, 10°C/min, 2 min hold time.

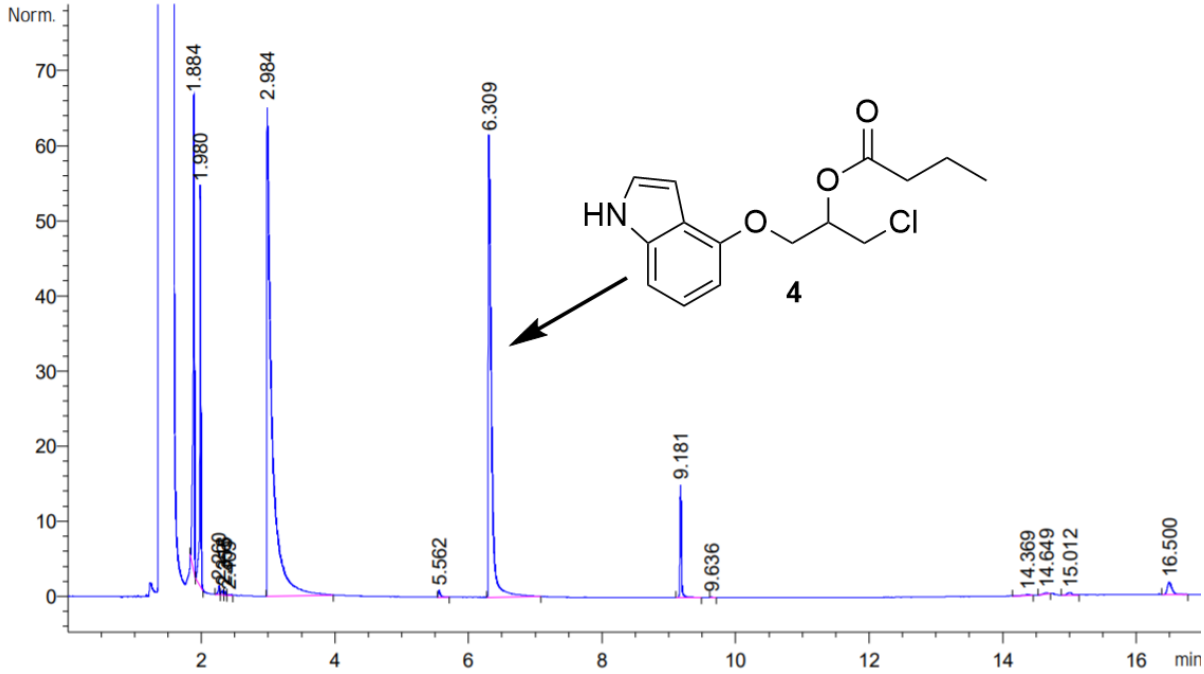

Figure 52: GC chromatogram showing compound **4**. t_R= 6.3 min for **4**. The temperature program used was 50-200 °C, 10°C/min, 2 min hold time. The column used was a Agilent column with a CP-Chirasil-Dex CB stationary phase consisting of cyclodextrin directly bonded to dimethylpolysiloxane.

6.5.3 Chromatogram of 1-((1H-indol-4-yl)oxy)-3-chloropropan-2-yl butyrate (4) and 1-((1H-indol-4-yl)oxy)-3-chloropropan-2-ol (2) from 50 to 200 °C, 10°C/min

The GC chromatogram for compound **2** and **4**. The temperature program used was 50-200 °C, 10°C/min, 2 min hold time.

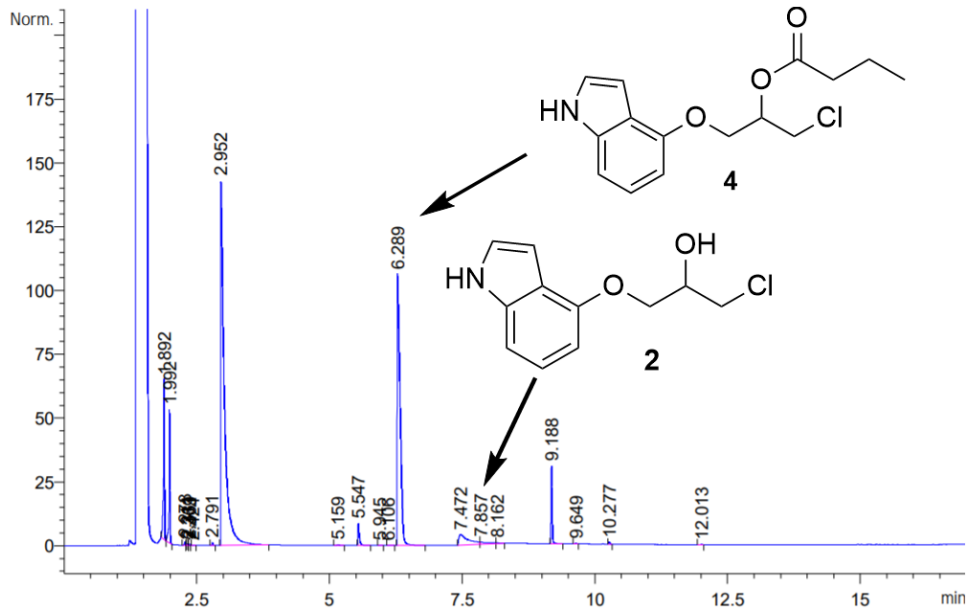

Figure 53: GC chromatogram showing compound **2** and **4**. t_R= 6.3 min for **4**. t_R= 7.5 min for **2**. The temperature program used was 50-200 °C, 10°C/min, 2 min hold time . The column used was a Agilent column with a CP-Chirasil-Dex CB stationary phase consisting of cyclodextrin directly bonded to dimethylpolysiloxane.

6.5.4 Chromatogram of 1-((1H-indol-4-yl)oxy)-3-chloropropan-2-ol (2) and 1-((1H-indol-4-yl)oxy)-3-chloropropan-2-yl butyrate (4) from 70 to 130 °C, 1.0°C/min

The GC chromatogram for compound **2** and **4**. The temperature program used was 70-130, 1.0°C/min, 2 min hold time. The goal was to separate the peaks at 11.2 and 29.8 min .

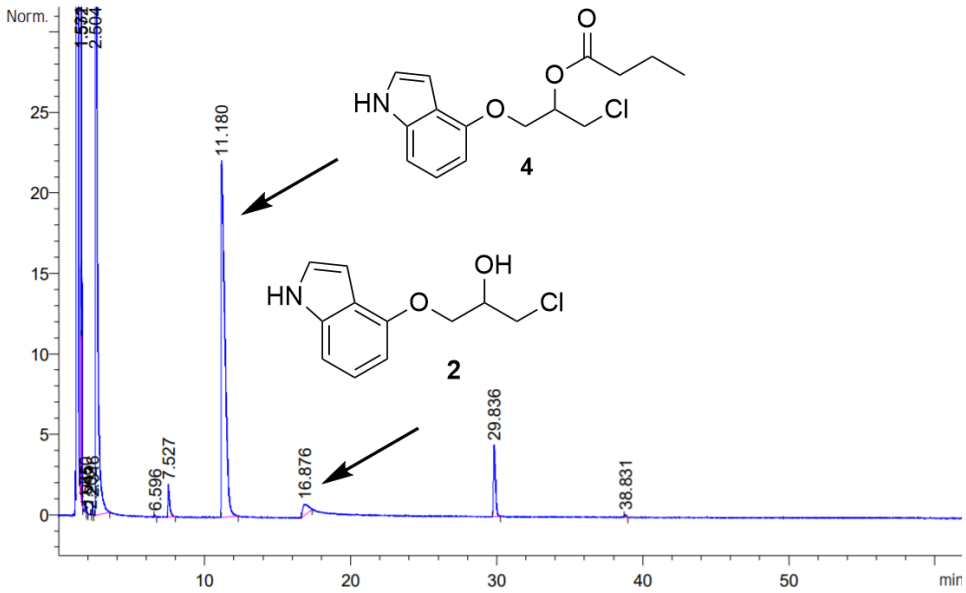

Figure 54: GC chromatogram showing compound **2** and **4**. t_R= 11.2 min for **4**. t_R= 16.9 min for **2**. The temperature program used was 70-130 °C, 1°C/min, 2 min hold time . The column used was a Agilent column with a CP-Chirasil-Dex CB stationary phase consisting of cyclodextrin directly bonded to dimethylpolysiloxane.

6.5.5 Chromatogram of (*S*)-pindolol ((*S*)-5) from 50 to 200 °C, 10°C/min

The GC chromatogram for compound **5**. The temperature program used was 50-200 5°C/min, 12 min hold time. This was a sample of (*S*)-**5** with very low concentration due to little sample. Therefore non of the peaks were characterized as (*S*)-**5**.

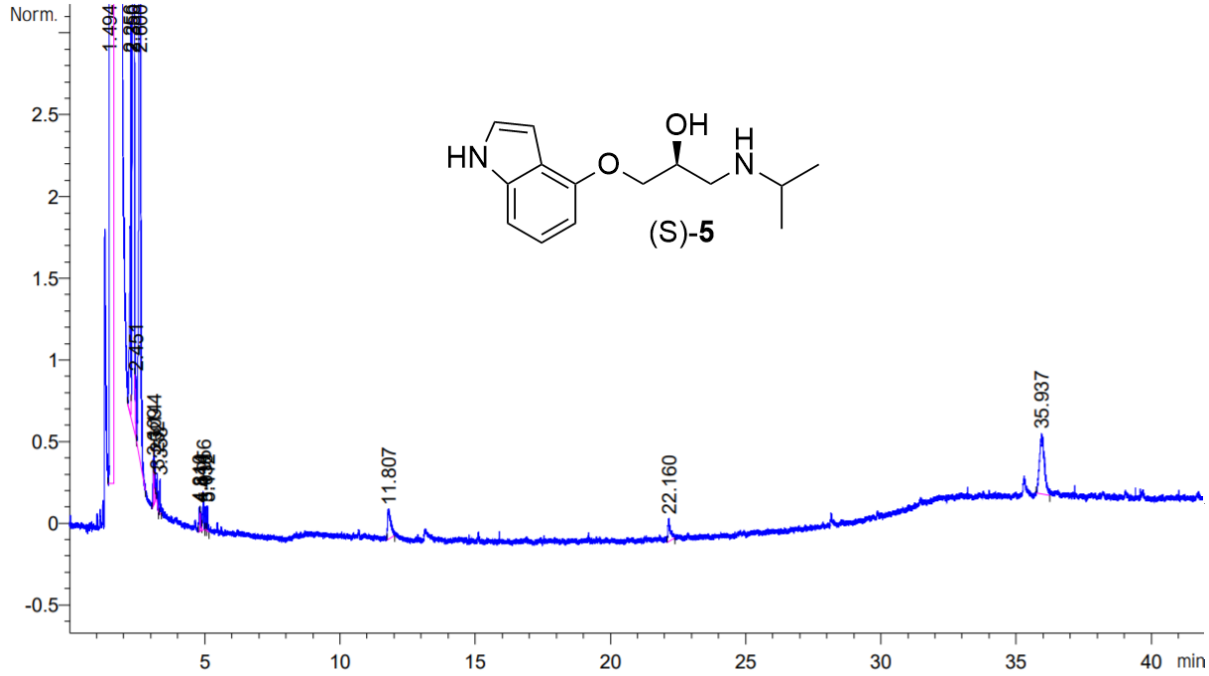

Figure 55: GC chromatogram showing compound (*S*)-**5**. The temperature program used was 50-200 5°C/min, 12 min hold time. The column used was a Agilent column with a CP-Chirasil-Dex CB stationary phase consisting of cyclodextrin directly bonded to dimethylpolysiloxane.